PHYSICS TODAY

March 2020 • volume 73, number 3

A publication of the American Institute of Physics

MULTISCALE MODELING BEYOND EQUILIBRIUM

What caused Australia's bushfires?

Discrepant Hubble constants

The emergence of magnetic skyrmions

PHYSICS TODAY

March 2020 | volume 73 number 3

FEATURES

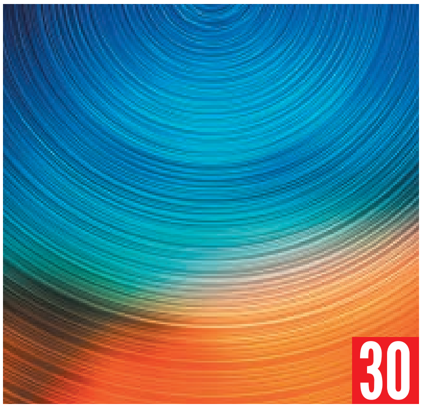

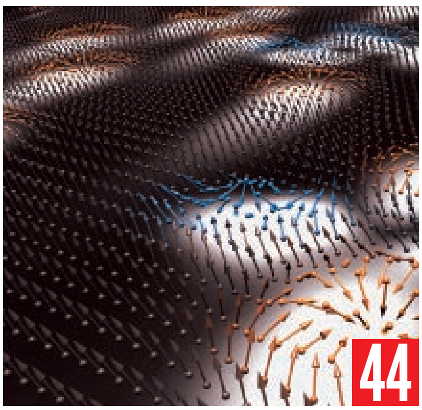

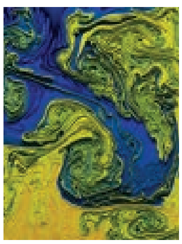

ON THE COVER: Computational modeling connects dynamics on a hierarchy of length and time scales. In this computational fluid dynamics simulation, artist and scientist–programmer Mark J. Stock turns initially banded colors into intricate system-scale flows by simply and repeatedly exchanging the properties of individual adjacent pixels. To read about how physics-based multiscale models capture the unique and counterintuitive behaviors of polymeric liquids and solids, see the article by Jay Schieber and Markus Hütter on **page 36**. (Detail from *CF126_480*, 2020, courtesy of Mark J. Stock.)

Recently on PHYSICS TODAY ONLINE

www.physicstoday.org

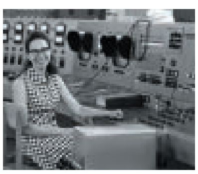

AIP ESVA

▶ Gloria Lubkin

One of the most influential staff members in Physics Today's 72-year history, former editor-in-chief Gloria Lubkin died in January at age 86. A collection of remembrances details the sizable impact she had on the magazine and on the physical sciences and science-writing communities.

physicstoday.org/Mar2020a

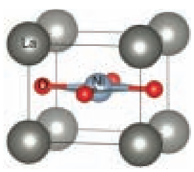

PHYS. REV. X, CC BY 4.0

▶ Nickel intrigue

A November 2019 Search and Discovery story detailed a newly discovered nickel oxide superconductor. Researchers have now determined that the material has surprisingly similar electronic properties to the cuprate superconductors and could help expose the long-sought mechanism underlying their behavior.

physicstoday.org/Mar2020b

NASA

▶ *Hubble* telescope

Next month is the 30th anniversary of the launch of the *Hubble Space Telescope*. For an upcoming story, Physics Today wants to hear from readers: Which *Hubble* images, measurements, and discoveries stand out most to you? Let us know at pteditors@aip.org or on Facebook or Twitter.

physicstoday.org/Mar2020c

Physics Today (ISSN 0031-9228, coden PHTOAD) volume 73, number 3. Published monthly by the American Institute of Physics, 1305 Walt Whitman Rd, Suite 300, Melville, NY 11747-4300. Periodicals postage paid at Huntington Station, NY, and at additional mailing offices. POSTMASTER: Send address changes to Physics Today, American Institute of Physics, 1305 Walt Whitman Rd, Suite 300, Melville, NY 11747-4300. Views expressed in Physics Today and on its website are those of the authors and not necessarily those of AIP or any of its member societies.

PHYSICS TODAY

www.physicstoday.org

DEPARTMENTS

The American Institute of Physics is a federation of scientific societies in the physical sciences, representing scientists, engineers, educators, and students. AIP offers authoritative information, services, and expertise in physics education and student programs, science communication, government relations, career services, statistical research in physics employment and education, industrial outreach, and history of the physical sciences. AIP publishes PHYSICS TODAY and is also home to the Society of Physics Students and to the Niels Bohr Library and Archives. AIP owns AIP Publishing, a scholarly publisher in the physical and related sciences.

SUBSCRIPTION QUESTIONS? +1 800 344-6902 | +1 516 576-2270 | **ptsubs@aip.org**

Address
American Center for Physics
One Physics Ellipse
College Park, MD 20740-3842
+1 301 209-3100
pteditors@aip.org

PhysicsToday **@physicstoday**

Cubic millimeters and inches

Charles Day

One rainy day this past summer, my wife, Jan, and I looked out of our kitchen window and noticed our neighbor's backyard was flooding. "How much water do you think is there?" she asked.

I estimated the backyard was 6 meters wide and 6 meters long. About 3 centimeters of water covered its bricked surface. Before I had finished my mental calculation of 1080 liters, Jan offered an eyeball estimate, "more than 200 gallons."

If either of us had tried to calculate an answer in imperial units, we would have estimated the yard's dimensions in feet and then converted to area in square inches. The final conversion to gallons entails remembering (or looking up) that there are 231 cubic inches in a US gallon. Whereas the metric calculation involves multiplying three numbers, the imperial one involves multiplying five numbers and dividing by a sixth.

The ease of scaling up in length and of converting length to area and volume was built into the metric system by its French founders, among them Joseph Louis Lagrange and Pierre Simon Laplace. Despite that advantage, the UK resisted—and the US continues to resist—mandating metric. Early proponents of metric in the UK included James Clerk Maxwell and William Thomson, known later as Lord Kelvin. James Joule's discovery in the 1840s that mechanical energy is equivalent to heat was one motivating factor. In 1875 Maxwell, Kelvin, and their colleagues proposed a new system of units, based on the centimeter, gram, and second. It included a new unit for energy, the erg (1 g·cm^2/s^2), and a new unit for force, the dyne (1 g·cm/s^2).

The British physicists and their allies eventually scored a partial victory. In 1896 Parliament passed an act that legalized—but didn't mandate—the use of the metric system for all purposes.

To this day, proponents of the imperial system point to its appealing basis in quotidian, human measures. An inch is roughly the length of an adult thumb's distal phalange. An acre is roughly the area of a field that a farmer driving an ox can plow in a day. The original Roman mile was the length a legionnaire covered in 1000 paces. Given that centimeters, hectares, and kilometers differ from their imperial counterparts by factors of a few or less, I don't find the human argument especially persuasive. A liter is as good as a pint for ordering beer at a bar.

Draft beer is still served in pint glasses in the UK and Ireland. (Photo by JONGLEUR100/PD-SELF.)

Some Victorian advocates of the imperial system, notably John Herschel, favored basing units on precisely engineered artifacts. Until last year, when the kilogram was redefined in terms of an arbitrarily fixed value of Planck's constant, metric units were not wholly free from reliance on artifacts. But it was the ultimate source of metric units that roused Herschel's suspicion. The meter's original definition was one ten-millionth of the distance between the North Pole and the equator as measured through Paris. Such French abstractions appalled the practical Englishman. But to Maxwell, the abstraction from nature was part of metric's appeal. As historian Simon Schaffer has noted, it reflected his belief in a divinely created, uniform universe.[1]

Did Victorian scientists practice what they preached? For an answer, I consulted the complete works of John Strutt, later known as Lord Rayleigh, on the shelves of the Niels Bohr Library and Archives at the American Institute of Physics (AIP is the publisher of PHYSICS TODAY). In "On the theory of resonance," he described and analyzed his investigations into the acoustic resonances of pipes of various sizes and shapes.[2] Curiously, he cited cubic millimeters for the pipes' volumes but inches for their lengths. Kelvin also used inches on occasion. Perhaps the two physicists found inches more convenient.

I used to think that the US should join the rest of the world and adopt the metric system. Now, in light of Kelvin's and Rayleigh's undogmatic flexibility, I no longer do—because it doesn't much matter. US manufacturers already use metric, and it seems fine to keep measuring potatoes in pounds and gasoline in gallons.

References

1. S. Schaffer, in *Victorian Science in Context*, Bernard Lightman, ed., U. Chicago Press (1997), p. 439.
2. J. W. Strutt, *Philos. Trans. R. Soc. London* **161**, 77 (1871).

PT

Commentary

Harassment protection should not be just for students

I've been teaching college-level physics to life-sciences majors for several years. I routinely experience some form of disrespect, hostility, and even aggression. Student harassment of professors is an increasingly common occurrence, yet universities, departments, and even other faculty members turn a blind eye to the problem. At least two studies have documented the issue.[1]

Most instances of harassment revolve around grades. The most common scenario is a student who pleads, insists, or demands that I change their grade or offer extra credit, or who blames me for ruining their future if I don't give in to their demands. Second are students who insist that I excuse them from, permit a make-up of, or allow an extension on a quiz, exam, or assignment. I get dozens of these emails each week, with tones escalating to rudeness and threats of aggression. Clearly, accommodation should be made in some instances, but "It's Mother's Day" and "I have to babysit my mom's dog" are not legitimate excuses.

I have been cornered and intimidated by students in my office and verbally abused in my classroom and in the hallways. I'm concerned for my safety. I have had my office broken into and have had anonymous, menacing letters left in my mailbox. Such direct personal harassment is in addition to a barrage of constant vitriolic remarks online, where I've been called a "bitch," a "slut," and worse.

I am not alone in being subjected to harassment by students. I know one professor who had tires slashed and another who had excrement mailed to their home. Harassment affects men and women, young and old, and it is underreported, particularly by untenured faculty and adjuncts. They—especially women and members of minority groups—worry that reporting harassment could jeopardize their careers. Although universities rightly have policies in place to protect students from professors, none protect professors from bullying by students.

In recent years institutions of higher learning have set policies to protect students from harassment by professors. But few protections are in place when the roles are reversed. (Photo by iStock.com/KatarzynaBialasiewicz.)

Even when the harassment doesn't escalate to malicious behavior and threats of violence, students often seem to see me as the enemy, to be thwarted or denigrated at every turn. When they don't get the grade they want, some will complain to the department chair and demand my removal.

In response to my pleas for help from the administration, I've been told that this is the culture now that Trump is our president. I've been turned away from the Title IX office and multiple other offices that theoretically should help with harassment cases. Some administrators have become defensive, as if they are expecting a legal battle. Once, when I asked for an escort from the campus patrol, I was turned away because, I was told, they "don't have the resources." Certainly, a student would have been able to get such an escort on request. Even colleagues and administrators who show concern often have little idea how or whether they should help.

I think several factors are driving the recent level of harassment. First, many students have a consumer attitude in which they feel entitled to an education. They expect their professors to give them good grades because they or their parents paid a lot of money for tuition.

Second, physics is a difficult subject that most life-sciences majors view as an irrelevant obstacle to their degree or entrance to medical school. As a result, many students approach the subject with anger and resentment. In my classes, students are challenged to focus on the process rather than getting the "right" answer. They must engage their brain, develop a genuine understanding of the topic, and learn concepts so that they can apply them effectively to different problems. Study skills such as rote memorization and passive learning may have brought success in other coursework, but they are much less effective in physics. Students need to understand that physics is hard and requires time, effort, and effective study strategies.

Third, I maintain high grading standards despite the harassment. My role is to assign students relevant and challenging tasks, guide them in their learning of new knowledge and skills, evaluate their performance, and assign grades in a manner that reflects appropriate evaluation criteria. I have a responsibility to ensure that degrees handed out by my institution attest to substantive knowledge and expertise.

I love teaching, and I'm pretty good at it. Many of my days are filled with positive experiences and feedback. But on those days when I am subjected to student hostility, I wonder why I'm doing what I'm doing and how much more I can endure. Certainly, bad teachers exist, but I'm not one of them. I believe those of us who feel most deeply the effects of harassment are the ones who care the most about teaching. I'm tired of trying so hard, in so many ways, and still losing the battle. The workload makes me miss my family. I want to spend time with them in the evenings, on weekends, and on holidays instead of grading papers or preparing lectures or worrying about student demands and complaints.

At work, I am on guard. I'm afraid to talk privately with a student in my office with the door closed. I'm afraid that every word I say or write will be recorded and used against me. I feel demoralized, disheartened, and discouraged. I've experienced anxiety, depression, exhaustion, chronic stress, and stress-related illness. I know of faculty members who have resorted to alcohol and drugs because of student harassment. Some suffer from eating disorders. And I know of at least one who has attempted suicide.

Students who harass college professors should suffer serious consequences. But there are none. Administrators, department heads, and colleagues provide very little support. That lack across academia results in a toxic culture that would be unacceptable in any other industry, as pointed out in the National Academies of Sciences, Engineering, and Medicine study on sexual harassment.[2] While academia prides itself on being at the forefront of intellectual advancement, it remains one of the most hostile and toxic work environments.

The failure of academic institutions to address student harassment of professors has implications far beyond the learning environment. Our current policies shrug at unacceptable behavior. Because many of my students are in the premedicine track, the lack of consequences means that harassers will be treating patients. That can only lead to negative, even disastrous, outcomes.

References

1. A. P. Brabec et al., *Emporia State Res. Stud.* **52**, 1 (2019); A. May, K. E. Tenzek, *Teach. Higher Educ.* **23**, 275 (2018).
2. National Academies of Sciences, Engineering, and Medicine, *Sexual Harassment of Women: Climate, Culture, and Consequences in Academic Sciences, Engineering, and Medicine*, National Academies Press (2018).

Name withheld

LETTERS

US–IAEA uranium enrichment safeguards

An important safeguards issue related to uranium enrichment plants was omitted from David Kramer's Issues and Events story, "Controversy continues to swirl around uranium enrichment contract" (PHYSICS TODAY, January 2020, page 22).

Kramer notes an assertion by Centrus president and CEO Daniel Poneman that nuclear nonproliferation policy includes a red line requiring a "strict divide between civilian and military programs and materials." Kramer observes correctly that the line has already been crossed with the production of tritium in US civil nuclear reactors.

As an office director in the Nonproliferation Bureau of the US State Department, I was involved in the interagency decision to allow that production. It was predicated on two assurances from the Department of Energy: that reactors serving that purpose would remain on the list of US facilities subject to International Atomic Energy Agency (IAEA) safeguards, and that if the facility were selected for inspection, the agency's safeguards approach would be the same as used for comparable facilities in non-nuclear-weapons states that participate in the Nuclear Non-Proliferation Treaty (NPT). Note that the US sends the IAEA a list of all US nuclear facilities, excluding those associated with activities having direct national security significance. The IAEA is permitted to apply safeguards to any facility on the list, but it need not do so.

An important nuclear nonproliferation issue is whether the Centrus facilities would be eligible for the application of IAEA safeguards under the US–IAEA voluntary offer safeguards agreement. The answer should be yes. One reason is that during the negotiation of the standard NPT safeguards agreement, Australia introduced into the record a statement, which was uncontested, that all enrichment plants in non-nuclear-weapons states would be subject to safeguards regardless of the intended end use of the product material.

Brazil's enrichment facility uses that safeguards approach even though it produces fuel for its naval reactors. The US–IAEA safeguards agreement, in turn, specifies that the IAEA "shall" follow the same procedures in the US that it uses in applying safeguards "on similar material in similar facilities in non-nuclear-weapon States."

A second point also bears on the relationship between civil nuclear and military activities. In his story, Kramer writes, "US policy stipulates that uranium used for any military purpose, including nuclear fuel, must be enriched using US-origin technology." He goes on to say that a corollary would seem to require that all US commercial reactor fuel be enriched using US nuclear technology since US military bases draw power from the grid.

While that might seem so, in the course of negotiating agreements for nuclear cooperation, the US and its partners have consented to permit transfers to be used for specified military purposes. More precisely, supplying power to military bases is excluded from the definition of military purposes. The agreement with Russia states, for example, that "military purposes shall not include provision of power for military bases drawn from any power network, production of radioisotopes to be used for medical purposes in military hospitals, and other similar purposes as may be agreed by the Parties." Provisions with the same effect are included in other US agreements for nuclear cooperation.

Michael D. Rosenthal
(m.d.rosenthal@mailaps.org)
Washington, DC

CONTACT PHYSICS TODAY

Letters and commentary are encouraged and should be sent by email to **ptletters@aip.org** (using your surname as the Subject line), or by standard mail to Letters, PHYSICS TODAY, American Center for Physics, One Physics Ellipse, College Park, MD 20740-3842. Please include your name, work affiliation, mailing address, email address, and daytime phone number on your letter and attachments. You can also contact us online at **https://contact.physicstoday.org**. We reserve the right to edit submissions.

Holes in lattices in liquids

In their feature article in the February 2019 issue of PHYSICS TODAY (page 38), Robert Evans, Daan Frenkel, and Marjolein Dijkstra quote from "About liquids," an essay in which Victor Weisskopf discusses the mysterious nature of liquids.[1]

Around 1960, when I was a graduate student at the University of Washington, the thesis project of one of my fellows was to calculate the entropy of a hole in a crystal lattice. The seemingly quixotic nature of the assignment—"A hole is a nothing. How can it have an entropy?"—led to much merry banter in our group. Today, the idea of holes in lattices is well established.

Evaporation (or sublimation) occurs when molecules on the surface of a condensed phase acquire enough energy to break free, enter the gas phase, and thus achieve unconstrained mobility. Similarly, for crystalline solids, there is a characteristic temperature—the melting temperature—at which the holes become mobile and move freely throughout the lattice. Noncrystalline solids such as rubber and plastics have a range of hole and dislocation types that reach mobility at various temperatures; they soften gradually rather than exhibiting a sharp melting point.

I find that the molecule/hole analogy provides a satisfying way to visualize the phenomenon of melting and the nature of liquids.

Reference

1. V. F. Weisskopf, *Trans. N. Y. Acad. Sci.* **38**, 202 (1977).

C. V. Berney
(cvberney@rcn.com)
Watertown, Massachusetts

Correction

February 2020, page 21—Edmund Bertschinger of MIT and Mary James of Reed College jointly cochaired the TEAM-UP task force. PT

Gravitational-lensing measurements push Hubble-constant discrepancy past 5σ

If the tension can't be attributed to systematic errors, it could be a sign of new cosmological physics.

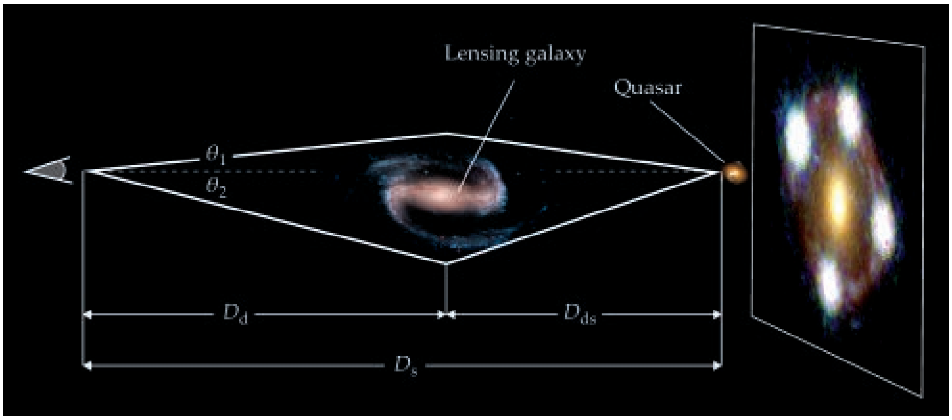

FIGURE 1. STRONG GRAVITATIONAL LENSING by a foreground galaxy can cause a quasar to appear as several distinct images. Observing the relative time delays among those images provides information about the combination of distances between Earth, the lensing galaxy, and the quasar. Given that the angles θ_1 and θ_2 are small, the difference in path lengths shown here is proportional to $D_d D_s/D_{ds}$; the difference in light travel time, which includes the effects of general relativity and the universe's expansion, is proportional to that same value. (Image by Freddie Pagani.)

Little is known about what dark matter and dark energy, the dominant components of the universe, really are. But the standard model of Big Bang cosmology, known as ΛCDM, incorporates how they outwardly behave. Dark energy, the model presumes, takes the form of a cosmological constant Λ, a constant energy density per unit volume of vacuum. Dark matter, meanwhile, is nonrelativistic (or cold; the CDM stands for "cold dark matter"), and it interacts with itself and with ordinary matter only via gravity and possibly the weak force.

With just a handful of free parameters, ΛCDM is appealing in its simplicity, and it generally agrees well with observations of the universe. But an exception is emerging in the Hubble constant H_0, the universe's present rate of expansion.

For ΛCDM to predict a value for H_0, its free parameters must be constrained—for example, by a map of the cosmic microwave background (CMB), a picture of the spatial structure of the early universe. From 2009 to 2013, the *Planck* observatory measured the CMB with great resolution and precision; its map, combined with ΛCDM, yields an H_0 of 67.4 ± 0.5 km/s/Mpc.[1] The structure of the early universe can also be inferred from the distribution of galaxies today (see the article by Will Percival, PHYSICS TODAY, December 2017, page 32); that approach gives the same prediction for H_0, albeit with wider error bars.

But H_0 can also be calculated directly from the distances to various astronomical objects and the velocities at which they're apparently receding from Earth. (See the article by Mario Livio and Adam Riess, PHYSICS TODAY, October 2013, page 41.) And direct measurements disagree with the ΛCDM value. The SH0ES (Supernova, H_0, for the Equation of State of Dark Energy) collaboration has been honing in on an H_0 measurement using so-called standard candles: type Ia supernovae and Cepheid variable stars, whose luminosities are known. The team's latest H_0 value, 74.0 ± 1.4 km/s/Mpc, differs from the ΛCDM value by 4.4 standard deviations.[2]

A difference of that magnitude, although unlikely to arise by chance alone, could still be due to some unappreciated systematic uncertainty in SH0ES's methodology. That explanation, however, is starting to look much less likely in light of new work from the H0LiCOW (H_0 Lenses in COSMOGRAIL's Wellspring) collaboration, led by Sherry Suyu, which uses gravitationally lensed quasars to independently measure H_0. In 2017 the collaboration published a first result based on three lensed quasars (reference 3; see also PHYSICS TODAY, April 2017, page 24). The current work, with key contributions by Kenneth Wong and Geoff Chen, extends the analysis to six quasars.[4] The result, 73.3 + 1.7 − 1.8 km/s/Mpc, agrees well with the SH0ES value. Combining the SH0ES and H0LiCOW measurements gives an H_0 of 73.8 ± 1.1 km/s/Mpc, which is 5.3σ different from the ΛCDM prediction.

Lensing measurements

The theoretical basis for H0LiCOW's method, called time-delay cosmography, dates back to a 1964 paper[5] by Norwegian astrophysicist Sjur Refsdal. But not until decades later did telescopes have the capability to implement it. When a quasar or other distant, luminous object lies directly in line with a massive foreground galaxy, its light can be so strongly bent that it appears to Earth-based observers as multiple images. Because the light in each image traverses a path of a different length and a different gravitational potential, as shown in figure 1, any fluctuation in the quasar's intensity shows up in the lensed images at different times.

Refsdal's insight was that measuring those time differences (which are on the order of weeks) and the images' angular deflections (on the order of arcseconds) provides crucial information about the absolute distances to the quasar and the foreground galaxy. The measurement doesn't directly yield D_d (the distance from Earth to the galaxy), D_s (the distance from Earth to the quasar), or D_{ds} (the distance from the galaxy to the quasar), but it does constrain their combination, which is enough information to calculate H_0 from the objects' known redshifts.

Earth-based telescopes suffice to resolve the lensed images and monitor their time delays. For years, the COSMOGRAIL (Cosmological Monitoring of Gravitational Lenses) collaboration has employed 1- to 2-m telescopes around the world to keep an eye on dozens of confirmed lensed quasars; some of the recorded light curves are shown in figure 2.

Measuring the time delays is just one piece of the puzzle. Another crucial ingredient in the H_0 calculation is the lensing galaxy's mass distribution, which is needed to calculate the deflection angles (which can't be directly measured, because the quasar's true position on the sky is unseen) and the gravitational effects on the light travel time for each image. The mass distribution isn't observable, but it can be modeled from the precise positions and shapes of the lensed images. An effective model requires high-resolution images from the *Hubble Space Telescope*.

It also requires some good judgement. The choice of when to stop adjusting the mass-distribution model requires a subjective assessment of how well the model agrees with the observed data. The H0LiCOW researchers worried that their decisions might be influenced, even subconsciously, by the value of H_0 they were

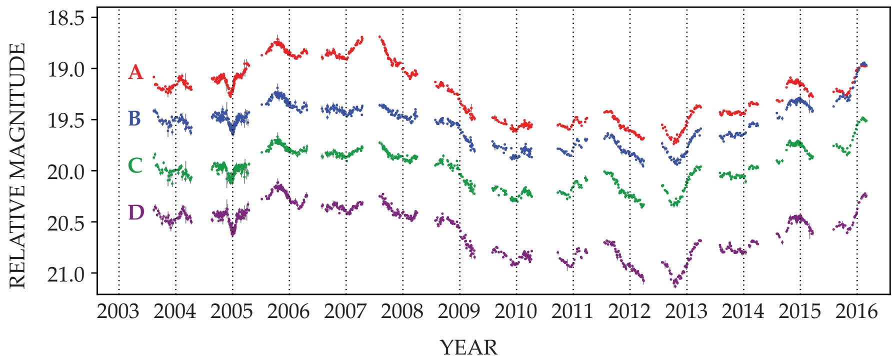

FIGURE 2. LIGHT CURVES from the four lensed images of the quasar shown in figure 1, collected over 13 years by five telescopes from the COSMOGRAIL (Cosmological Monitoring of Gravitational Lenses) collaboration. Fluctuations in the quasar's intensity appear first in images A and C, then in image B, and finally, about two weeks later, in image D. (Adapted from ref. 3.)

hoping to get. So they developed a technique of blind data analysis, whereby they could work on the model and test it against the data without ever seeing the distance or H_0 values it would yield. They agreed beforehand that once they settled on a mass distribution that looked good, there was no going back: They'd publish whatever results it yielded with no further modifications.

"Because our analysis was blind, we could have gotten any result," says Wong. "So it was a bit surprising to find that we were within 1σ of SH0ES."

Off the distance ladder

SH0ES, meanwhile, has been tackling its own challenges in precisely determining H_0. Type Ia supernovae, which are luminous enough to be seen at great distances, are extremely effective tools for measuring relative cosmic distances: Their peak luminosities are nearly all the same, so supernovae that appear dimmer must be farther away. From the slight curve in the relationship between their distances and velocities (inferred from their redshifts) came the Nobel-winning discovery that the expansion of the universe is accelerating (see PHYSICS TODAY, December 2011, page 14). That determination, however, was made without knowing the absolute distance to any of the supernovae under study, so it didn't yield a precise value of the present-day expansion rate H_0.

To convert the relative distances into absolute ones, astronomers use a hierarchy of measurements called the cosmic distance ladder (see the article by Daniel Holz, Scott Hughes, and Bernard Schutz, PHYSICS TODAY, December 2018, page 34). The distances to nearby objects, within a thousand parsecs or so, can be accurately measured using the geometric method of parallax. But supernovae of any type are rare events, and there hasn't been one close enough to Earth for many hundreds of years. Cepheid variable stars can bridge that gap. They're both numerous enough to be well represented near Earth and bright enough to be visible at the same distances as the nearest supernovae. As discovered by Henrietta Leavitt a century ago, Cepheids' luminosities are related to their pulsation periods, so their relative distances can be inferred from their apparent brightness.

SH0ES has been shoring up the links between parallax, Cepheids, and supernovae, and other groups have checked and rechecked them. But there remained the possibility that some aspect of the underlying physics—of supernova evolution, Cepheid pulsation, or the telescopes used to observe them—wasn't understood as well as astronomers thought it was.

It's important, therefore, that H0LiCOW and SH0ES get the same answer from independent methods. SH0ES's measurement has nothing to do with gravitational lensing or modeling of galaxy mass distributions, and H0LiCOW's has nothing to do with the mechanisms of Cepheids or supernovae. If SH0ES's result is marred by a systematic error, H0LiCOW's analysis would have to coincidentally include a different error of almost exactly the same magnitude and sign.

Discovery?

In high-energy physics, a signal with statistical significance of 5σ is the threshold for claiming discovery of a new particle or effect. (See, for example, PHYSICS TODAY, September 2012, page 12, and August 2019, page 14.) The statistical meaning of a 5σ result is the same in all contexts: Assuming a Gaussian distribution of measurement fluctuations, there's a 1 in 3.5 million chance that the result could arise by statistical fluctuations alone, in the absence of any underlying effect.

But cosmologists so far have been reluctant to declare that the tension in H_0 measurements must be a sign of physics beyond the ΛCDM model, in part because it's not at all clear what that physics would be. There aren't many ways the ΛCDM model could be modified that would both close the H_0 gap and maintain the model's agreement with all other measurements. Some of the possibilities theorists are exploring include dark radiation (relativistic dark particles, such as sterile neutrinos, whose wavelengths get stretched as the universe expands), non-Newtonian modifications to gravity, or a dark energy that's not constant. But there's no specific evidence, yet, of any of them, and a complete theoretical picture remains elusive.

The H0LiCOW researchers are working on adding more quasars to their analysis, with the goal of reducing their measurement uncertainty below 1%, or 0.7 km/s/Mpc. If their H_0 value remains unchanged, such a measurement would be 5σ different from the ΛCDM on its own, independent of SH0ES or any other result.

Johanna Miller

References

1. Planck collaboration, https://arxiv.org/abs/1807.06209 (2018).
2. A. G. Riess et al., *Astrophys. J.* **876**, 85 (2019).
3. V. Bonvin et al., *Mon. Not. R. Astron. Soc.* **465**, 4914 (2017).
4. K. C. Wong et al., *Mon. Not. R. Astron. Soc.* (in press).
5. S. Refsdal, *Mon. Not. R. Astron. Soc.* **128**, 307 (1964).

Rare nuclear transition provides evidence for stellar explosion mechanism

With its higher-than-expected propensity to capture electrons, neon could drive some stars' thermonuclear death.

FIGURE 1. OLIVER KIRSEBOM, KNEELING AT COMPUTER, AND COLLEAGUES designed an experiment at the University of Jyväskylä accelerator laboratory in Finland to measure how frequently radioactive fluorine-20 emitted electrons and decayed to ground-state neon-20. The photo was taken at 1444 m depth in the underground laboratory. (Image courtesy of Oliver Kirsebom.)

When the core of a massive star runs out of nuclear fuel, it collapses under its own gravity to form a neutron star or a black hole and sheds its outer layers in a supernova. (See, for example, the article by Hans Bethe, PHYSICS TODAY, September 1990, page 24.) However, for smaller stars in the 7- to 11-solar-mass range, gravitational collapse may not be the only possible route to a supernova. Those stars are abundant in our galaxy, but the final phase of their evolution is unclear. Some may undergo gravitational collapse like massive stars. But if nuclear reactions in a star's core generate sufficient energy to counter collapse, its life may also end in a thermonuclear

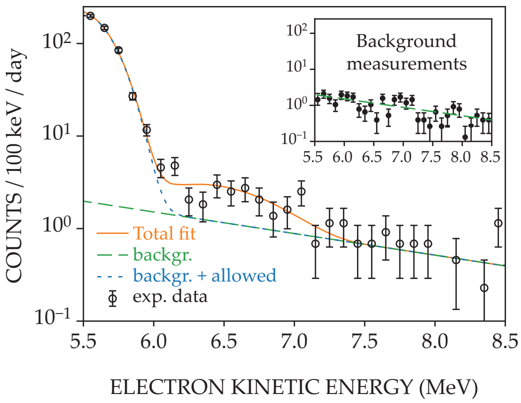

FIGURE 2. THE ENERGY SPECTRUM MEASURED DURING RADIOACTIVE DECAY of fluorine-20 to neon-20 (orange) shows the count of electrons emitted at different energies during 105 hours of decay. Below 5.4 MeV, the count exceeded that emitted by background sources (green), as predicted by simulations (blue). Between 5.4 MeV and 7 MeV, the measured count exceeded the predicted count; that difference indicated occasional occurrence of ^{20}F decay to ground state ^{20}Ne. The inset showing the background spectrum obtained without the ^{20}F beam confirms the forbidden transition's contribution to the spectrum. (Adapted from ref. 1.)

explosion that ejects some material while leaving behind a white dwarf remnant.

To understand the fate of a star, astrophysicists must delineate the nuclear reactions that occur in its core after the main fuel-burning cycle ends. At that point, stars in the range of 7–11 solar masses have cores that consist mainly of oxygen and neon. Theoretical models of stellar evolution predict which reactions happen next. Particularly important is a reaction sequence in which an atomic nucleus absorbs an electron, which combines with a proton to form a neutron. In that sequence, a high-energy (7 MeV) electron is absorbed by neon-20 to form fluorine-20, which promptly captures another electron to form oxygen-20. As a by-product of that reaction chain, gamma radiation is released and heats the stellar core enough to trigger the ignition of oxygen. Whether the energy liberated by oxygen ignition is enough to forestall collapse or trigger an explosion depends critically on the density at which the onset of electron capture on ^{20}Ne takes place.

A team led by Oliver Kirsebom (now at Dalhousie University in Nova Scotia, Canada) and Gabriel Martínez-Pinedo (GSI Helmholtz Center for Heavy Ion Research and Technische Universität Darmstadt in Germany) has recently found that the electron capture on ^{20}Ne occurs at lower densities and with a higher rate than previously expected. The researchers inferred experimentally the chain's first and rate-limiting step—the capture of electrons by ^{20}Ne—under conditions that prevail in a stellar interior. Stellar models based on the new rate suggest that thermonuclear explosion is the common end for many of our galaxy's stars.[1,2]

Forbidden transition

Atomic nuclei have different energy states. Which one a nucleus is most likely to inhabit depends on the temperature and density of the environment. At the temperatures in oxygen–neon stellar cores, most ^{20}Ne exists in its ground state. As the stellar core evolves, its density grows and the energy of the electrons, which comprise a degenerate gas in the core, increases. At some point, electrons will have enough energy, 7 MeV, to link in a decay chain the ground states of Ne and F.

The rate at which Ne captures electrons during the transition between the ground states of ^{20}Ne and ^{20}F nuclei can be directly related to the inverse process, the beta-decay in which radioactive ^{20}F emits an electron and produces ^{20}Ne. Under terrestrial conditions, ^{20}F decays to the first excited state of ^{20}Ne. However, that ground state transition has an extremely low likelihood and is considered forbidden. Forbidden means that the reaction links nuclear states with different spins, which results in a transition that is, in this case, supressed by six orders of magnitude compared to an allowed transition between same-spin states. As a result, quantifying the rate-limiting electron capture step is difficult.

To learn more about the neon–fluorine electron capture rate, Kirsebom and colleagues looked to an allowed version of the inverse beta-decay process. The decay that connects ^{20}F decays to the first excited state of ^{20}Ne can produce electrons that have from zero to 5.4 MeV of kinetic energy, whereas the decay connecting the ground states of ^{20}F and ^{20}Ne produces electrons up to a maximum kinetic energy of 7 MeV.[3] Electrons with energies up to 5.4 MeV mostly originate from the allowed decay to the excited state of ^{20}Ne; but any electrons with energies above 5.4 MeV must originate through the forbidden ground state decay. Kirsebom designed an experiment to measure how frequently ^{20}F emitted electrons with energies above 5.4 MeV, and thereby determine the strength of the forbidden transition.

Earthly measurements

Because ^{20}F decays extremely rapidly, with a half-life of 11 seconds, studying its behavior requires an advanced accelerator facility where the isotopes can be produced and quickly transported to a detection system. At the University of Jyväskylä accelerator laboratory in Finland the researchers bombarded carbon foil with a beam of ^{20}F nuclei. The laboratory is one of the few facilities worldwide that can produce a pure, intense, low-energy ^{20}F beam, free of contamination by other radioactive isotopes. On striking the carbon foil, the ^{20}F nuclei became embedded. Kirsebom and his colleagues, shown in figure 1, monitored the nuclei as they decayed and emitted energetic electrons. A specially designed scintillator detector with a magnetic transporter measured the electrons' energies.

The team paid particular attention to electrons that had kinetic energies 5 MeV and above. The resulting energy spectrum in figure 2 shows the count of electrons emitted at each energy during 105 hours of data collection. For energies below 5.4 MeV, the electron count exceeded by five orders of magnitude that emitted by background sources. The spectrum matched that obtained by simulations, which indicated frequent occurrence of the allowed decay of ^{20}F to excited ^{20}Ne. The background count rate was determined in separate measurements made with precisely the same setup but without the ^{20}F beam. Between 5.4 MeV and 7.0 MeV, the measured number of counts exceeded that expected from background sources. Electrons at those energies indicate occurrence of the forbidden decay of ^{20}F to ground state ^{20}Ne. For energies above 7 MeV, the entire electron count came from background cosmic rays. "Just looking at the large number of counts observed, one realizes that we are dealing with a rather strong forbidden transition," says Kirsebom.

The researchers concluded that 1 in 250 000 events produced ^{20}Ne in its ground state—a rate that should match that of the reverse process. Based on the measured transition probability, and

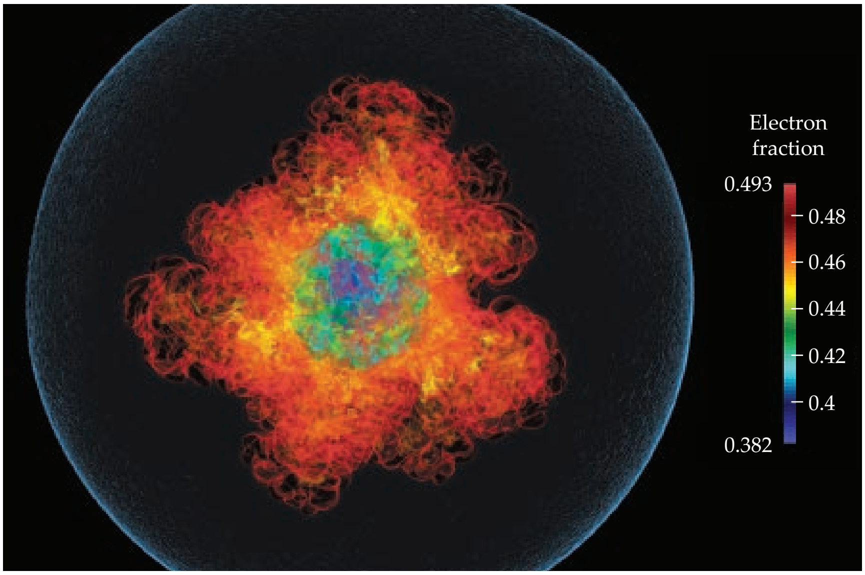

FIGURE 3. NUMERICAL SIMULATIONS SHOW THE SUPERNOVA that results from an oxygen–neon stellar core after the newly measured neon-20 electron capture triggers a thermonuclear explosion. The color key shows the explosion's electron fraction, which describes whether isotopes tend to be richer in protons or neutrons. For example, iron-56 has 26 protons and 30 neutrons, so its electron fraction is 26/56 or 0.464 and corresponds to the orange regions of the explosion. Iron-60 has an electron fraction of 26/60 or 0.433, corresponding to the turquoise region. The lowest electron fraction achieved in the simulation (blue) is below 0.40, which is 12% lower than regular supernovae. (Adapted from ref 5.)

considering stellar plasma densities of 10^9 g/cm^3, electron capture on ^{20}Ne was determined to occur eight orders of magnitude more often than assumed by previous calculations.

Stellar implications

Numerical simulations of stellar evolution that take into account the newly measured Ne–F transition rate suggest that the star's core begins to generate heat earlier than previous models predicted.[4] Once the core reaches 1.5×10^9 K, oxygen can fuse with itself; the earlier ignition happens, the higher the likelihood of a thermonuclear explosion.

The resulting supernova, like the one simulated in figure 3, differs from the type II supernova that ends the life of a star more massive than 11 solar masses. It also differs from the type Ia supernova in which a carbon–oxygen white dwarf fully explodes. It ejects more mass and it leaves behind an iron-rich white dwarf, as opposed to a neutron star or black hole.[5] The proportion of ejected elements also differs from both other supernova types; it is richer in calcium-48, titanium-50, chromium-54, and iron-60.

By itself, a high Ne–F transition rate isn't enough to preordain the explosion of a 7- to 11-solar-mass star. The energy released by electron capture on ^{20}Ne may trigger convection in the stellar core. Convection leads to mixing and could delay the onset of oxygen ignition, so that gravitational collapse would be the end of the star. Improved models of convection in the stellar core are needed.

The observation of iron-rich white dwarfs would clinch the case that the Ne–F transition drives a thermonuclear explosion. Several candidates have already been detected through observations of their atmospheres.[6] The associated explosions are expected to be characterized by specific spectral features that could, in principle, be observed.[5]

Rachel Berkowitz

References

1. O. S. Kirsebom et al., *Phys. Rev. Lett.* **123**, 262701 (2019).
2. O. S. Kirsebom et al., *Phys. Rev. C* **100**, 065805 (2019).
3. G. Martinez-Pinedo et al., *Phys. Rev. C* **89**, 045806 (2014).
4. J. Schwab, E. Quataert, L. Bildsten, *Mon. Not. R. Astron. Soc.* **453**, 1910 (2015).
5. S. Jones et al., *Astron. Astrophys.* **622**, A74 (2019).
6. R. Raddi et al., *Mon. Not. R. Astron. Soc.* **489**, 1489 (2019).

Doubt is cast on a mechanism of cancer nanomedicine

Leaky blood vessels seemed like the perfect conduit to deliver cancer-fighting drugs selectively to tumors. But the reality is starting to look more complicated.

Cancer is a disease of tissue growth gone wrong. Tumor cells proliferate uncontrollably and don't die as they should. When a solid tumor grows large enough to need to sprout its own blood vessels, those vessels, too, grow irregularly. The tumor vessel networks are tortuous and disorganized (see PHYSICS TODAY, February 2016, page 14), and the vessels' lining, or endothelium, is riddled with gaps hundreds of microns wide between cells.

The challenge of chemotherapy is to kill off the tumor cells without doing too much harm to healthy ones. The interendothelial gaps promised a way to do that. Nanoparticles up to 300 nm in diameter can fit through the gaps, and they can't permeate normal blood vessels the same way. So nanoparticles loaded with a drug should, it stands to reason, selectively enter and attack tumor tissue but leave healthy tissue alone. An inherently biomedical challenge was seemingly transformed into one of nanotechnology and fluid dynamics.

A quarter century of nanomedicine research has indeed yielded a few nanoparticle drug formulations that offer better performance or fewer side effects than their molecular counterparts. (See the article by Jennifer Grossman and Scott McNeil, PHYSICS TODAY, August 2012, page 38.) The mechanism of their action, however, has never been fully verified. No technique exists that can image nanoparticles *in vivo*, in real time, and with sufficient resolution to observe the particles slipping through the inter-

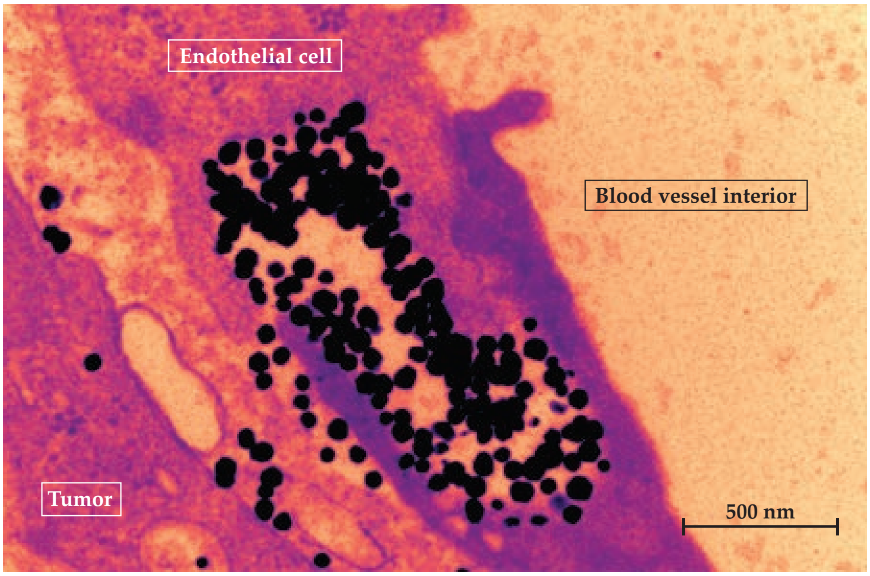

FIGURE 1. GOLD NANOPARTICLES (black) injected into the blood of a tumor-bearing mouse appear in the cytoplasm of the endothelial cells that line the tumor blood vessel; a few have been expelled into the tumor. Nanoparticles have been assumed to enter tumors through large gaps in the endothelium, but no such gap is visible in this transmission electron microscopy image. (Courtesy of Shrey Sindhwani.)

endothelial gaps in a tumor's blood vessels. The idea that they do has always been an assumption.

New research by Shrey Sindhwani, Abdullah Muhammad Syed (both with Warren Chan's laboratory at the University of Toronto), and their colleagues suggests that that assumption might not be correct. Most nanoparticles that end up in tumors, the researchers found, get there by passing through the endothelial cells, not between them.[1]

The underlying biological details are still murky. Several possible mechanisms fall under the umbrella of trans-endothelial pathways, and the researchers don't yet know which one predominates or why. For example, individual endothelial cells might engulf the nanoparticles and then expel them into the surrounding tumor, or the nanoparticles might pass through small intracellular pores that open up to exchange nutrients across the endothelium.

What the possible mechanisms have in common, however, is that they're all active cellular processes, so they're sensitive to nanoparticle surface chemistry and composition in ways that a passive physical mechanism isn't. The task of getting nanomedicines into tumors may therefore be a biological one rather than a physical one after all.

Mind the gaps

Chan and his colleagues have been testing the foundations of cancer nanomedicine for several years. In a controversial 2016 analysis of the literature, they found that among all published experiments in the field, a median of just 0.7% of the injected nanoparticles were delivered to the tumor.[2] Critics countered that some nanomaterials are delivered in quantities much greater than the median, that even 0.7% of the injected dose might be enough to treat a tumor, and that the amount of nanomaterial detectable in a tumor isn't necessarily the best measure of a drug's effectiveness.[3] But as Sindhwani explains, the Toronto researchers had their minds on a more fundamental question: "If there are all these gaps in the blood-vessel lining, why is the tumor accumulation so low? What are these gaps, and how many are there?"

Meanwhile, Sindhwani was also learning about Harold Dvorak's work on trans-endothelial mechanisms that can carry proteins as large as 5 nm into tumors. "That work is relatively unknown in the nano community," he says, "and nobody had looked at its relevance to nanoparticles."

It's relatively straightforward to show that trans-endothelial delivery of nanoparticles to tumors is possible. The researchers injected gold nanoparticles into a tumor-bearing mouse, allowed them to circulate, then extracted slices of the tumor and imaged them with transmission electron microscopy (TEM). Some of the images, including the one in figure 1, showed large caches of nanoparticles trapped in the endothelial cytoplasm, caught in the act of passing through an endothelial cell.

But which of the possible mechanisms predominates? That's a statistical question, and answering it required a lot of data—and a combination of methods. "It is really challenging to design experiments for looking at what nanoparticles are doing in the tumor," says Syed.

The first step was to determine how many inter-endothelial gaps there really were. The researchers took TEM images of hundreds of blood vessels from both mouse and human tumors, and they trained a team of nine colleagues to identify the inter-endothelial gaps. To reduce bias, they had each image independently evaluated by three randomly chosen team members who didn't talk to one another.

As it turned out, inter-endothelial gaps were surprisingly rare: Images of 313 blood vessels from mice showed just seven gaps in total, or about one per 20 000 square microns of endothelium. Human tumor vessels showed gaps in similarly small numbers. In a fluid-dynamical simulation of 50 nm nanoparticles, the observed density of gaps could account for just 1–2% of the already small number of nanoparticles known to reach the tumors.

Zombie mice

The researchers also wanted an experiment that could distinguish passive from active nanoparticle transport. For that, they developed a mouse model they called Zombie. Tumor-bearing Zombie mice, as the name suggests, are effectively animated corpses: dead, chemically treated to halt all cell activity, and hooked up to an external pump to keep their blood circulating. If nanoparticles enter tumors by passively flowing through inter-endothelial gaps, then just as many nanoparticles should reach the tumors in Zombie mice as in control, or live, tumor-bearing mice.

But that's not what happened. Fluorescence images in figure 2 show blood vessels in red and nanoparticles in green. Nanoparticles in the control mouse spread throughout the tumor, and some

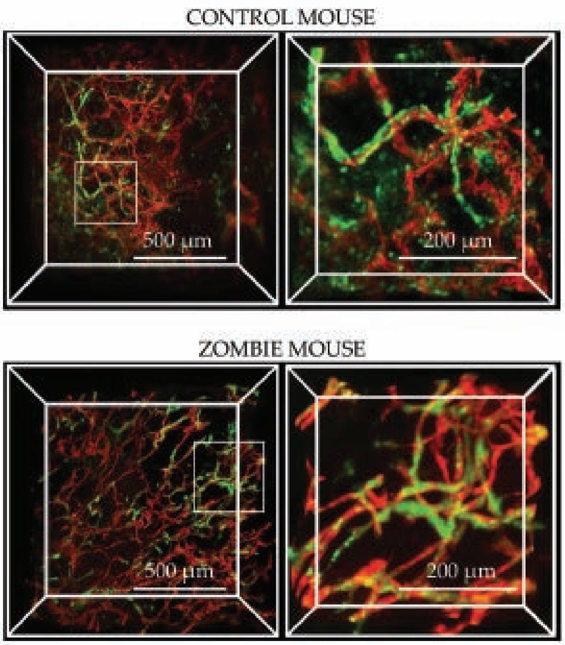

FIGURE 2. FLUORESCENCE IMAGES show the propagation of nanoparticles in the tumors of control tumor-bearing mice, which were alive, and Zombie mice, all of whose cells were dead. In the control mouse, nanoparticles (green) are able to escape the blood vessels (red), but in the Zombie mouse they can't. (Adapted from ref. 1.)

appear far from any blood vessels. But in the Zombie mouse, they remained confined to the tumor blood vessels. In other words, most nanoparticles escape the tumor blood vessels only when the cells in the vessel walls are alive.

Analysis of the Zombie experiment implied that for 50 nm gold nanoparticles, passive interendothelial transport accounts for just 3% of all nanoparticles entering the tumor. (Curiously, that fraction was greater—as high as 25%—for both larger and smaller nanoparticles, but it was always a minority.) The rough agreement between the experiment and simulation offers some confirmation of both methods. "That was a pleasant surprise," said Sindhwani, "and it gave us confidence."

All lines of the Toronto researchers' reasoning point to active trans-endothelial pathways as the primary means by which nanoparticles are delivered to tumors. But there's still work to be done. All their experiments so far used nanoparticles made of gold, which are easy to image but may not be representative of all nanomaterials. It's possible that passive transport doesn't work in exactly the same way in Zombie mice as in live ones. And the experiments don't reveal anything about what the predominant active molecular pathways are, what biomolecules are involved in regulating them, or—crucially for nanomedicine—how they compare to similar pathways at work in healthy tissue. "While we've made a first step," says Sindhwani, "we need a major collaborative undertaking to figure this out."

Johanna Miller

References

1. S. Sindhwani et al., *Nat. Mater.* (2020), doi:10.1038/s41563-019-0566-2.
2. S. Wilhelm et al., *Nat. Rev. Mater.* **1**, 16014 (2016).
3. S. E. McNeil, *Nat. Rev. Mater.* **1**, 16073 (2016); K. Bourzac, *Proc. Natl. Acad. Sci. USA* **113**, 12600 (2016).

PT


2020
IEEE NUCLEAR SCIENCE SYMPOSIUM
and MEDICAL IMAGING CONFERENCE
27th International Symposium on Room-Temperature Semiconductor Detectors, X-Ray and Gamma Detectors
BOSTON, MASSACHUSETTS
31 Oct – 7 Nov 2020 The Westin Boston Waterfront
ABSTRACT SUBMISSION DEADLINE – 7 MAY, 2020
IEEE NPSS
NUCLEAR & PLASMA SCIENCES SOCIETY
GENERAL CHAIR: Lorenzo Fabris
NSS CHAIR: Sara Pozzi
NSS DEPUTY CHAIR: Stefan Ritt
MIC CHAIR: Georges El Fakhri
MIC DEPUTY CHAIR: Ramsey Badawi
RTSD CO-CHAIRS: Ralph James and Michael Fiederle
nssmic2020@ieee.org
nssmic.ieee.org/2020

Brookhaven facility to be transformed into electron–ion collider

The Long Island lab prevailed over a rival proposal from the Thomas Jefferson National Accelerator Facility in Virginia.

The US Department of Energy has set in motion plans to build an electron–ion collider (EIC) at Brookhaven National Laboratory in New York. The 9 January announcement from DOE says the $1.6 billion–$2.6 billion EIC will "ensure U.S. leadership in nuclear physics" and that it will be "a game-changing resource for the international nuclear physics community."

The EIC is envisioned as an enhanced reprise of the Hadron–Electron Ring Accelerator (HERA) in Germany, which showed during its 1992–2007 run that gluons play an important role in determining a proton's properties. With the new facility, scientists will pursue ongoing questions of nuclear structure: How do protons get their mass and spin from their constituent quarks and gluons? How are quarks and gluons distributed inside atomic nuclei? How are protons and neutrons bound in nuclei? How closely can gluons be packed before they reach saturation? What are the properties of dense gluonic matter?

Talk about building a new electron–ion smasher began about 20 years ago. In 2015 the US nuclear physics community ranked it number one on its wish list for new facilities in a prioritization exercise by the Nuclear Science Advisory Committee (see PHYSICS TODAY, February 2015, page 20). In summer 2018, a review by the National Academies of Sciences, Engineering, and Medicine gave the proposed facility flying colors.

The detailed EIC design and cost estimate are in progress. DOE plans to begin operations around 2030.

Seeing the nucleus in a new way

Quantum chromodynamics (QCD), the theory of the strong force, describes the interactions between quarks and massless, force-carrying gluons in nuclei. The strong force increases as objects get farther apart, and it confines quarks in the nucleon; quarks and gluons are never found free outside a proton or neutron. "It's a beautiful theory. It explains nearly all visible matter," says Raju Venugopalan, a theorist at Brookhaven. "But there are many things we still do not understand in fundamental ways."

Collisions between electrons and protons or heavier ions produce fewer particles than hadron–hadron collisions such

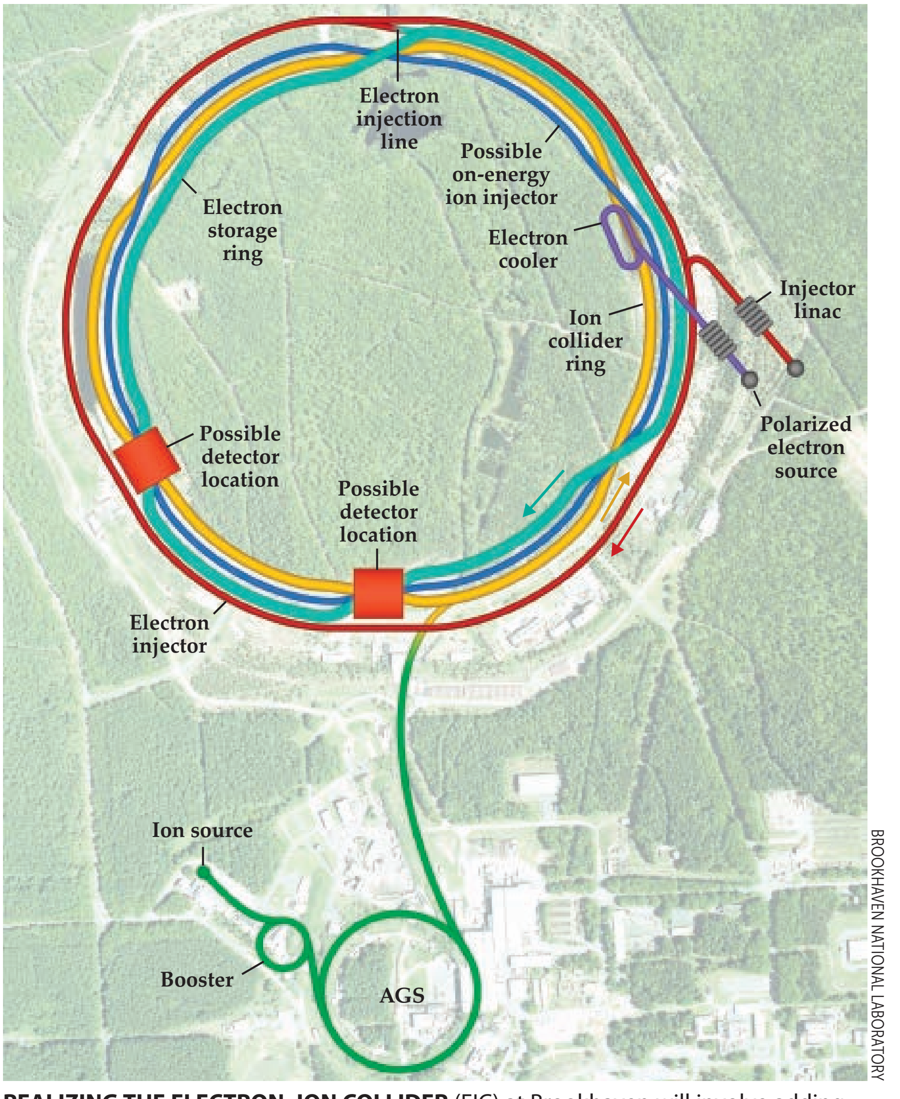

REALIZING THE ELECTRON–ION COLLIDER (EIC) at Brookhaven will involve adding an accelerator to produce a beam of polarized electrons and an electron storage ring (teal green) to the lab's existing Relativistic Heavy Ion Collider (RHIC). Electrons would collide at one or two sites (red blocks) with ions from the yellow ring. The Alternating Gradient Synchrotron (AGS; green ring at bottom) produces polarized ion beams and injects them into RHIC; it will do the same for the EIC.

as those at Brookhaven's current flagship Relativistic Heavy Ion Collider (RHIC), and they can therefore yield more precise information about the structure and dynamics inside nucleons. The EIC will smash electrons up to 18 GeV into protons up to 275 GeV. The collision center-of-mass energy will range from 20 GeV to 140 GeV; that's lower than HERA's 318 GeV, but the EIC will have the advantage of greater tunability for exploring interactions as a function of energy. Both beams at the EIC will be polarized, and the luminosity will be $10^{33–34}$ $cm^{-2}s^{-1}$, more than two orders of magnitude higher than at HERA. In addition to the wide energy range, polarized beams, and high luminosity, the EIC will be able to accelerate many different ion species. Those four characteristics combine to form "the ultimate QCD machine," says Venugopalan. "We will try to understand the strongest fields at the smallest distances possible."

An incident electron can scatter inelastically off individual quarks or gluons, or off clouds of gluons, or it can scatter elastically from the whole nucleus. The EIC will track and measure the electrons, photons, kaons, pions, protons, and other hadrons that emerge from collisions. It will identify and record particle mass, momentum, energy, and type.

The quark mass accounts for only 2% of the proton mass. And quarks account for only 30% of proton spin. One has to imagine a model in which the arrangement of quarks and gluons, their spins, and their orbital angular momenta contribute, says Carl Gagliardi of Texas A&M University. "Even antiquarks contribute to the spin of the proton. That means the ephemeral constituents play a real and visible role in the structures we are made of."

With the EIC, scientists will create three-dimensional spatial and momentum space images of quarks and gluons inside protons. Previous generations of experiments have looked mainly in the direction parallel to the beams, says Richard Milner of MIT, who is on the steering committee of the EIC users group. The EIC will implement new types of measurements, pioneered at the Thomas Jefferson National Accelerator Facility in Virginia, to look in the transverse direction, he says.

In addition to the three valence quarks that make up a proton, quark–antiquark pairs constantly appear and disappear in nuclei. Elke-Caroline Aschenauer, a Brookhaven nuclear physicist, asks where those fleeting particles reside. "Do they form a rim? Are they scattered throughout the nucleus?" By studying the spatial and momentum distributions inside protons, she says, "we may get a better understanding of what confines gluons and quarks to the nucleus."

If a quark is knocked out, the proton is destroyed and the quark binds with an antiquark or with other quarks to form a pion or other colorless hadron; jets of debris give clues to the quark distribution inside the original proton. Another possible outcome is deeply virtual Compton scattering, in which the energy is such that an electron–quark collision leaves the proton intact, and it, the scattered electron, and an ejected photon embody information about the quark's motion. Polarization results will be used to probe spin and, with high energies and heavy nuclei, gluon density.

The EIC could provide access to a new

state of gluonic matter. Theory predicts that gluons multiply, eventually reaching a maximum density, or saturated state, in the finite volume of a nucleus, says director of EIC science Abhay Deshpande. Gluonic matter has unique properties and should pervade all nuclei, he says. It would be observable at high energies, although it's not clear how high. The trick with the EIC, Deshpande says, is to enhance the nuclear gluon density by accelerating heavy ions, like lead or gold. That will allow "a more effective search for saturated gluonic matter" than was possible with HERA's higher-energy electron–proton collisions.

Understanding the structure of nuclei has broader implications too. Andrew Strominger of Harvard University is keen to compare EIC data with measurements at facilities such as LIGO, the Laser Interferometer Gravitational-Wave Observatory. The mathematics, he says, implies analogies between the "color memory" produced by the motion of quarks and antiquarks in dense color gluon shock waves and the "gravitational memory" produced by gravitational waves emitted in a black hole merger or other violent cosmological event. In both cases "memory" is information from the event that is retained in the system.

Jürgen Berges of the University of Heidelberg in Germany says theory describes "remarkable similarities" between gluons at saturation and cold atoms in a Bose condensate. By comparing data about the energy and momentum distributions of gluons and excitations in cold quantum gases, he says, links between the two different quantum systems may be found on vastly different energy scales. "The EIC is very interesting for studying this probable universality."

Site selection

Brookhaven's bid to host the EIC won out over a competing design by Jefferson Lab. DOE under secretary for science Paul Dabbar says the agency made the choice after the two proposals were reviewed by an international review panel, which considered six criteria: scientific merit, technical maturity, schedule, cost, project management, and the likely impact on other ongoing or planned DOE missions. "It was a standard DOE review process," he says.

Observers note that Jefferson Lab, which hosts an electron accelerator for fixed-target collisions, would have needed to add an ion accelerator, which would likely cost more than the electron accelerator and storage ring Brookhaven will have to install in its 4 km RHIC tunnel to realize an electron–ion collider. They also note that Brookhaven was more in need of a new raison d'être to maintain a vibrant nuclear physics program; Jefferson Lab's program extends further into the future than Brookhaven's would without the EIC.

Of course, scientists at Jefferson Lab are "quite disappointed," says Haiyan Gao, a Duke University physicist whose research is based at Jefferson Lab. But the lab is expected to be a major partner in the EIC and also has plans for new experiments, she says. "The bigger picture is that going ahead with the EIC is hugely positive news."

The technology for realizing the EIC's accelerators at Brookhaven already exists, says Robert Tribble, the lab's deputy director for science and technology. "We have the ion beams we need. The polarization exists at close to the levels we need."

BROOKHAVEN NATIONAL LABORATORY

BROOKHAVEN NATIONAL LABORATORY ENGINEER MATHEW PANICCIA next to accelerator beamlines in which low-energy electrons commingle with ions to extract heat and keep the ion bunches tightly packed. The approach may be applied in high-energy hadron cooling in the electron–ion collider.

BROOKHAVEN NATIONAL LABORATORY

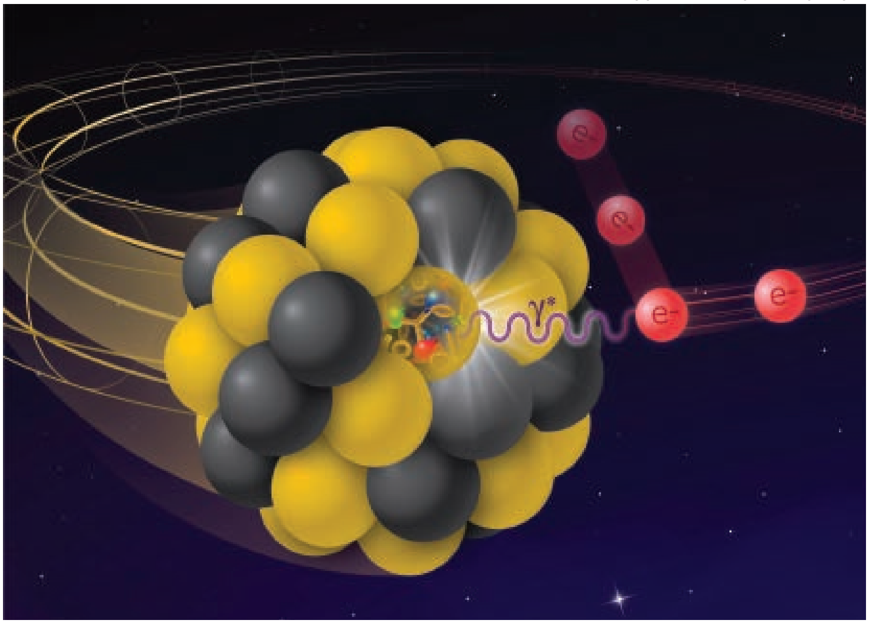

AN ELECTRON (RED) SCATTERS OFF A QUARK INSIDE A PROTON (yellow; neutrons are depicted in gray). The electron and the quark exchange a virtual photon and change direction in this deep inelastic collision. The schematic diagram illustrates one type of experiment with which the electron–ion collider to be built at Brookhaven National Laboratory will study nuclear structure and dynamics.

Minor modifications will be made to RHIC's existing configuration, he says. And a 150 MeV electron beam will propagate with the ions to cool them and thus maximize the collider luminosity.

The detectors, however, present many technical difficulties. They need to cover a wide range of angles, including small ones close to the beam pipes. Probably the most challenging technology is particle identification, says Brookhaven scientist Thomas Ullrich. Because the particles produced in the collisions come out with a broad range of energies, from 200 MeV up to 50 GeV, "the challenge cannot be met with a single technology." Overall, Cherenkov radiation detectors, gas and solid-state methods to detect and measure particle tracks and momentum, time-of-flight measurements, and calorimeters will be needed, he says.

So far, DOE has committed to just one detector site, although that could change. "We could cover both high energies and proton imaging at one [collision] site," says Tribble. "The community needs to decide if that's optimal." The majority of users prefer two detectors, says Silvia Dalla Torre, a nuclear physicist at INFN (Italy's National Institute for Nuclear Physics) in Trieste and spokeswoman for that country's participants in the EIC users group. "Each technology has advantages and disadvantages, and despite being clever when you make choices, nature always has surprises, so two complementary approaches would ensure better results." With two detectors, results could be confirmed, and each could be optimized for specific observations. That decision will be made in the coming months. It's not just a matter of money, according to Dabbar, who says the project can go ahead with US money alone. International partners are welcome, he adds.

In the world context, notes Dalla Torre, the EIC "is the only such project that is becoming concrete." Two other electron–ion colliders with different capabilities and scientific objectives are on the drawing boards: a higher-energy facility at CERN (see PHYSICS TODAY, May 2017, page 29) and a lower-energy one in China. The green light for the EIC is good news for the international science community, she says. More than 40% of the EIC users group's nearly 1000 members are based outside the US. "If a relevant nation like the US were to give up this kind of science, it would be noticed, and other countries might want to save money by cutting funding to this area. In going forward, the US sends a strong signal that this is strong science."

Toni Feder

What caused Australia's disastrous wildfires? It's complicated

The country's catastrophic bushfire season could either be a one-off or a new normal, experts say.

NASA

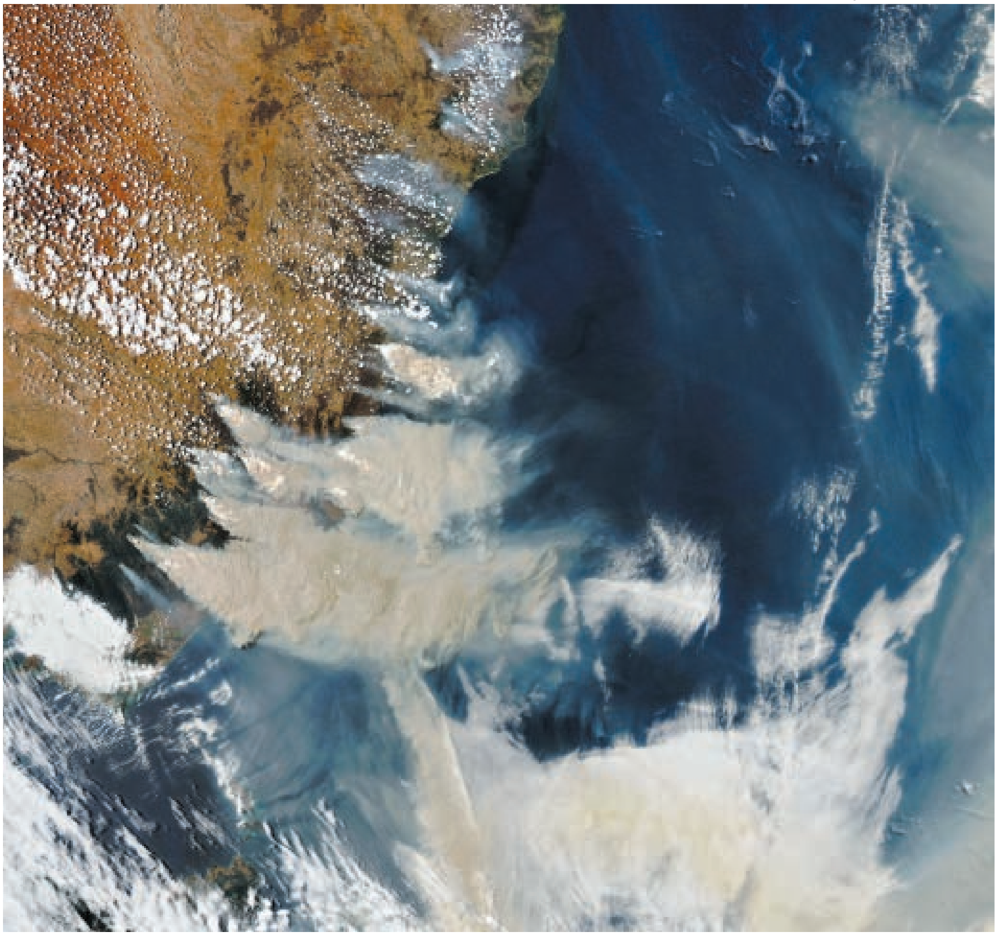

SMOKE FROM RAGING BUSHFIRES fills the skies in southeastern Australia and over the Tasman Sea in this natural-color image captured 4 January by the moderate-resolution imaging spectroradiometer aboard NASA's *Aqua* satellite. Smoke is tan; clouds are white. Some of the white patches above the smoke are likely pyrocumulonimbus clouds created by convection and heat rising from the fires.

As the world's attention was drawn to Australia's lethal bushfires, climate change was most invoked as the spark. But while global warming most certainly played some role in producing the worst fires in Australia's recent history, a number of perennial climate fluctuations also coalesced during the 2019–20 season, scientists say. It's likely those conditions will combine again, but probably not this year or even the one after that.

Bushfires are a regular feature of the Austral summer, but this season has been exceptional on several accounts. First, of course, is the extent of the burn—an estimated 11 million hectares as of 1 February. The surface area of the state of Virginia is about the same. The season began much earlier than is typical, as fires broke out during the first week of spring. And unlike most years, the fires have been concentrated near major population centers in southeastern Australia, filling the air in Sydney and other urban areas with unhealthy levels of smoke. According to the Global Fire Emissions Database, the number of active fires detected in New South Wales, Australia's most populous state, through early January was more than four times that in the previous record season of 2002–3.

The immediate cause for the extreme season was the parched lands that resulted from a drought that began three years ago. In a continent accustomed to periodic droughts, 2019 was the hottest and driest year ever recorded. The annual mean temperature was 1.5 °C above the 1961–90 average of 21.8°, surpassing the previous record of 1.33° set in 2013. (Coincidentally, 1.5° above preindustrial levels is the aspirational global ceiling set in the 2015 Paris climate agreement.) Australia had an all-time average high temperature of 40.3° on 17 December, but that was topped the next day with a reading of 40.7°. The nation's average rainfall totaled 277.6 mm last year, well below the previous record low of 314.5 mm established in 1902.

"It's not news to climate scientists that we've been experiencing an earlier extreme fire danger season and more intense bushfires," says David Karoly, leader of the Earth systems and climate change hub at the Commonwealth Scientific and Industrial Research Organisation (CSIRO), a government-funded agency. "There are numerous studies showing this in the observational data. Not every summer, but many summers are showing increases in the area burned and earlier occurrences of extreme fire. We don't like saying we told you so."

The highly flammable eucalyptus forests that predominate in Australia "virtually explode" and emit volatile organic compounds, says Karoly. "It is probably the worst tree in the world for wildfires."

Climate influences

A major global-scale cause of the extreme weather conditions in 2019 was the Indian Ocean Dipole (IOD), which last year moved into its strongest positive phase since 1997. The IOD is an oscillation that occurs in the sea-surface temperature between the western and eastern tropical Indian Ocean, analogous to the El Niño–Southern Oscillation in the Pacific Ocean. The relatively cool sea-surface temperatures near Australia during a positive IOD typically are linked to southeast

Australia's reduced spring rainfall. Last year's IOD persisted into the beginning of summer, before being dissipated by a delayed monsoon.

Most often, hot and dry conditions occur when a positive IOD coincides with an El Niño; this year's extremes occurred in the absence of one. "The fact we've had a really serious drought with only one of those factors is quite exceptional," says Mark Howden, director of the Climate Change Institute at the Australian National University (ANU).

Positive IODs don't occur that often. From 1960, when records began, there were 10 such events through 2016, according to Australia's Bureau of Meteorology. Scientists disagree on whether they will increase in number and strength as the climate continues to warm. "There are papers suggesting that the positive IOD will become stronger and more frequent, leading to drier conditions in winter and spring," says Julie Arblaster, an associate professor of Earth atmosphere and environment at Monash University. Some analyses indicate that a doubling of strongly positive IODs will occur with a global rise of 1.5°, says Howden.

But, according to Karoly, there's little evidence of an increase in climate models or in observations covering the period from the 1980s or 1990s to the present. He says that's mainly because the influence of increased greenhouse gases hasn't been strong enough yet.

A second global-scale influence on Australia is the Southern Annular Mode (SAM), the north–south movement of the westerly wind belt that circles around Antarctica. Historically, those westerlies and accompanying winter storms, known as the roaring 40s for their latitude, have brought rain to the south of Australia during the winter months, as the SAM shifts the westerlies to the north. Typically, the SAM moves poleward in summer and allows the subtropical ridge that sits over the continent to slide southward, which brings warm, dry weather. The high-pressure ridge itself has strengthened with climate change throughout the midlatitudes.

Human-induced climate change has caused the SAM to move more frequently into a positive phase during the winter, drawing the westerlies and the rains away from the southern coast, says Karoly. "I would argue the roaring 40s should be called the roaring 42s or 43s because they are shifted further south in winter," he says. Last year's dry winter set the stage for the disastrous fires. The same phenomenon led to a South African drought in which Cape Town nearly ran out of municipal water in 2018, he says. It has also helped to create the worst drought in Chile in 60 years.

AUSTRALIAN GOVERNMENT BUREAU OF METEOROLOGY

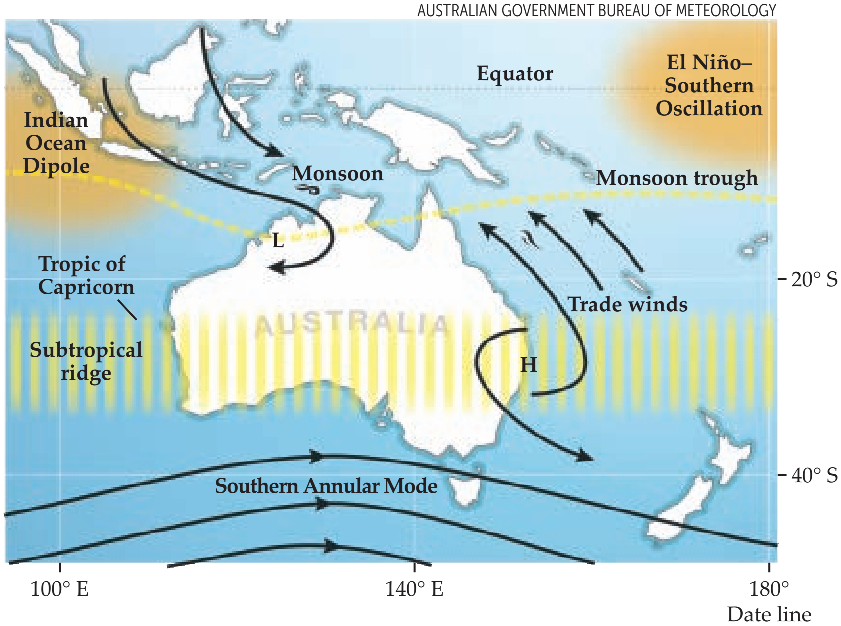

AUSTRALIA'S CLIMATE INFLUENCES acted in concert to produce record drought and heat during 2019. A southward shift of the Southern Annular Mode kept westerly winds south of the continent in winter. A strongly positive Indian Ocean Dipole (IOD) followed and maintained dry conditions throughout the spring and early summer. Absent last year was an El Niño, which typically works in tandem with the IOD to create droughts.

A rare event

One highly unusual occurrence, a breakdown of the Antarctic polar vortex due to sudden stratospheric warming, worsened fire conditions in Australia last year. Such events occur with some frequency in the Northern Hemisphere winter, but they are rare in the Antarctic. Prior to last year, the only other sudden warming was observed in 2002, though weakenings of the vortex have occurred more frequently. By coincidence, a paper Arblaster coauthored in the November 2019 issue of *Nature Geoscience* describing the effects of those weakenings on Australia's climate was in review when the actual event was in progress.

Like its counterpart in the Arctic, the southern polar vortex annually weakens in late spring as the atmosphere warms. But last August's sudden breakdown occurred months ahead of schedule. The effect was to increase the likelihood of spring hot and dry extremes across subtropical eastern Australia, as Arblaster and her colleagues described in their statistical analysis of observations over 40 years. Last year's collapse of the vortex caused the SAM and the surface westerlies to move northward and prevented the typical moisture-laden southeast trade winds from the Tasman Sea from reaching Australia's southeastern coast, says Karoly. It's far too early to draw a connection between climate change and the sudden warming, researchers agree.

Howden points to the extreme low humidity that accompanied the drought and heat waves as an apparent signal of climate change. The relative amount of moisture in the atmosphere has dropped across the midlatitudes that Australia occupies, compared with historical levels.

At the synoptic scale, the current fire season has featured a persistent high-pressure system, centered over the Tasman Sea, that circulated hot, dry air from Australia's interior desert to the southeastern part of the country, says Howden. When approaching cold fronts increased the pressure gradient in front of the high pressure, winds picked up and added fuel to the fires. Turbulent winds from multiple directions followed passage of the fronts and made the fires difficult to manage. According to Howden, some analyses have suggested that this pattern is likely to grow in frequency as the climate continues to transform.

Climate change

Australia is the most arid continent, and it features the greatest variability in rainfall from year to year—twice that of North America. Neville Nicholls, emeritus professor of Earth atmosphere and environment at Monash University, says that every influence on the nation's climate has been altered by climate change, even if the exact mechanism for how that is happening in each case isn't yet known. Australian daytime temperatures over land have increased by 1.25° in the past 25 years, or 5° per century. "That's a massive increase, and it overshadows the variations in temperature we get from year to year through what we used to call natural climate variations due to SAM or the IOD or El Niño," he says. "We can no longer say that anything is a purely natural phenomenon."

Among the developed nations, Australia is the most vulnerable to the impacts of climate change. *Climate Science for Australia's Future,* published in July 2019 by the National Climate Science Advisory Committee, says warming has caused increased intensity and frequency of extreme heat events and droughts, longer fire seasons, hotter and more acidic oceans, and rising sea levels that amplify the effects of high tides and storm surges on coastal communities and infrastructure. Australia's population is tightly concentrated in cities along its eastern coast.

Average April–October rainfall in southeast Australia has fallen 11% compared with the 1900–1998 period, according to the *State of the Climate 2018* report from Australia's Bureau of Meteorology and CSIRO. Nine of the country's top 10 hottest years have occurred since 2005.

"I've never been through a summer like this in my 70 years," says Nicholls. "In Melbourne, we have had massive hailstones, smoke from fires hundreds of kilometers away, and a massive dust storm in central Australia" that coated the city during rains. "The warming trend is so deep that definitely sometime in the next decade or so the record temperatures we set last year will be broken again," he says.

Howden points to a "mind-boggling storm" that on 20 January slammed the ANU Canberra campus and produced fist-sized hail that smashed car windows. Just 11 days later, a state of emergency was declared for the capital city as a bushfire approached from the south and the high reached 42°.

The impact of the bushfires on the ecosystem has been devastating, with some estimates putting the death toll of animals at a billion or more. For some species, fires destroyed most of their habitats. "The thing that really struck home to people was the pictures of the animals and the sheer number of wildlife that could have been affected," says Howden. "They've seen pictures of fires before and houses burnt down before, but pictures of koalas with singed feet and kangaroos barely escaping fire fronts really hit them hard."

Mitigation and adaptation

The increased duration of fire seasons across large parts of the continent since the 1950s has shrunk the available time in spring to conduct controlled burnings, which are of diminishing effectiveness during extreme fire conditions, researchers say. And because Australian bushfires are now overlapping with those in the US and Canada, the typical sharing of firefighting resources among the nations has become more difficult.

The so-called Black Saturday bushfires of 2009, which killed 173 in the state of Victoria, brought about policy changes. Officials now encourage Australians in the path of fires to leave their homes instead of trying to save them. New building codes require more fire-resistant structures. Near-real-time text and email warning systems also have been instituted. As a result, the death toll from this season's far more extensive fires, as of early February, remains relatively small at 33.

In a 10 January statement, Australian Academy of Science president John Shine said the response to bushfires must include more than rebuilding and recovery. "Everything, including urban planning; building standards; habitat restoration; biodiversity and species preservation; and land, water and wildlife management will need careful and measured consideration," he said. Improvements also are needed in threat forecasting, climate modeling, and the understanding of fire behavior.

With a population of roughly 25 million, Australia is the world's 16th largest emitter of greenhouse gases, producing 1.3% of the global total, according to the Global Carbon Project. Per capita emissions are among the highest of the developed countries, ahead of the US, Canada, the UK, and Russia. That's due in large part to the nation's high proportion of coal-generated electricity, much of which is fueled by lignite. Australia is the world's largest exporter of coal and liquefied natural gas.

In an open letter in the *Sydney Morning Herald* on 29 January, 81 Australian Research Council laureates warned, "If strong action is not taken, environmental degradation and social disruption will be much greater and in many cases adaptation will no longer be achievable. It would be naive to assume that such a world will still support human societies in their current form and maintain human wellbeing."

Nicholls says that "because we are at the frontline of being impacted by climate change of all the developed countries in the world, Australia has the most to lose from global warming. We've known that for 25 to 30 years." Accordingly, Australians should be pressuring the rest of the world to reduce greenhouse gas emissions. "It's in Australia's best interest to do that," he says, "not just out of the goodness of our hearts to save the rest of the world."

Howden agrees: "The really critical role Australia can play, together with the Scandinavian countries and New Zealand, is leadership. The pathway forward in terms of equitable solutions is being proactive in terms of responses and demonstrating how to do that in a way that's compatible with sustainable development."

Despite the bushfires, pockets of skepticism about human-caused climate change remain in Australian politics and media, says Nicholls. "You have to have your eyes completely shut to be a climate skeptic in Australia," he says. "You have to be ignoring the evidence in front of your eyes when you turn on the TV, when you talk to people who've been affected by the fires, when you talk to scientists who are monitoring the bleaching of the Great Barrier Reef."

David Kramer PT

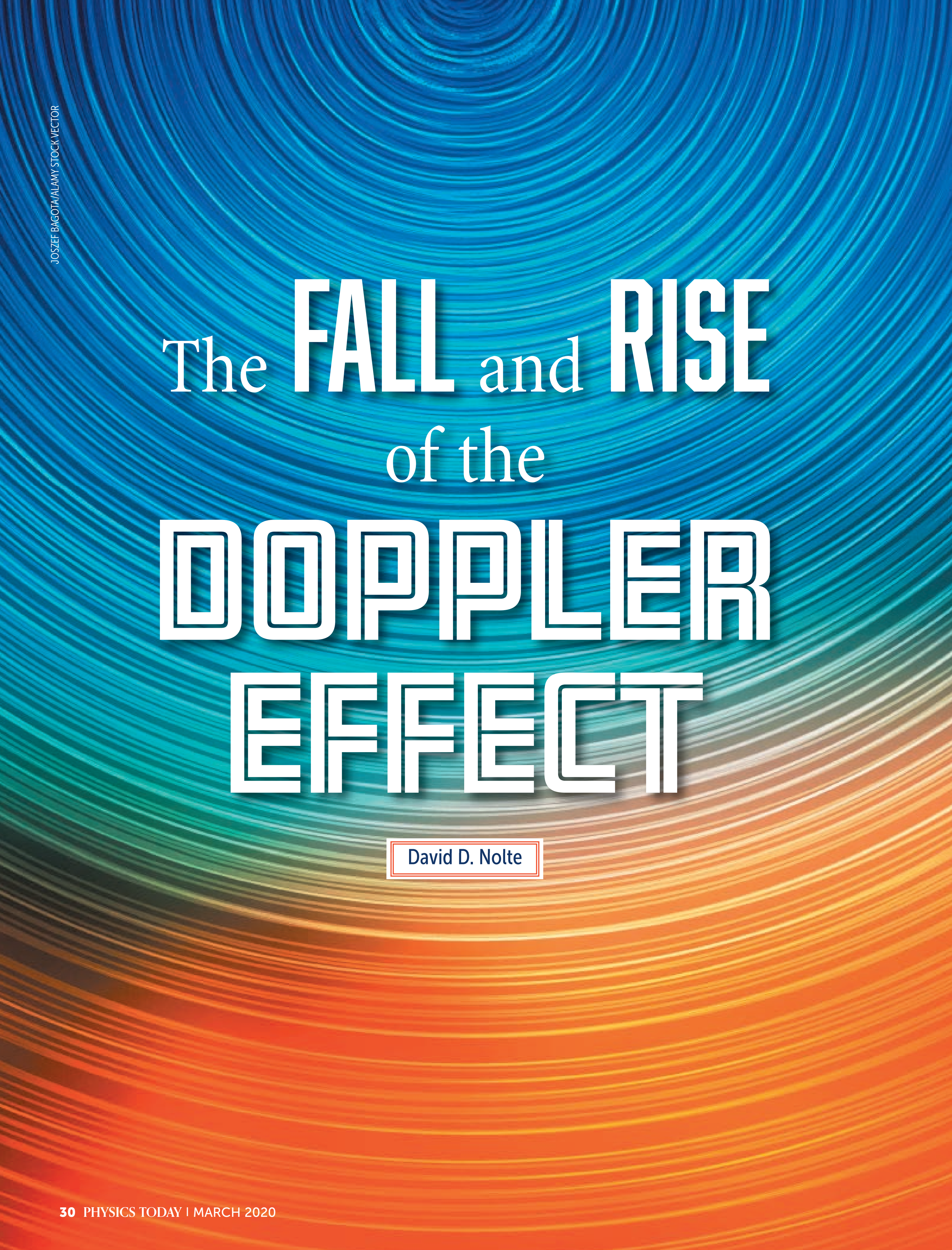

JOSZEF BAGOTA/ALAMY STOCK VECTOR

The FALL and RISE of the DOPPLER EFFECT

David D. Nolte

David Nolte is a distinguished professor of physics and astronomy at Purdue University in West Lafayette, Indiana, and is the author of *Galileo Unbound: A Path Across Life, the Universe and Everything* (2018) on the history of dynamics.

The phenomenon is so pervasive that we stake our lives on it, but Doppler's idea faced fierce criticism that took half a century to overcome.

Of all the eponymous discoveries that emerged from 19th-century physics—Young's fringes, the Biot–Savart law, the Fresnel lens, the Carnot cycle, the Faraday effect, Maxwell's equations, Michelson's interferometer, and many more—only one is heard daily on the evening news: the Doppler effect.[1] The effect, which describes the change in a wave's frequency heard by an observer moving relative to the wave source, is shown in figure 1. You experience the effect as you wait by the roadside for a train to pass by or a jet to fly overhead. Albert Einstein may have the most famous name in physics, but Christian Doppler's is probably the most commonly used. That's ironic because Doppler was hounded by a pompous nemesis, ridiculed for his effect, stripped of his university position, and forced to abandon Vienna in public disgrace and declining health. He finally retreated to Venice and died a few months later.

Despite Doppler's ignominious end, today his effect tells scientists of Earth's motion across the universe, allows physicists to cool atoms in laser traps to a fraction of a degree Kelvin, and is used to detect alien planets orbiting distant stars. With Doppler light scattering, scientists can see the flow of blood in arteries, and they are beginning to personalize chemotherapy by measuring tiny Doppler shifts from the motion of components inside living cells.[2] So why did his peers reject his idea, even years after his death, and how has it been rehabilitated so thoroughly that we now stake our lives on it? The answer begins with a troubled career that almost failed to launch.

Doppler's vision

Doppler was born in 1803 in Salzburg, Austria, to a long-standing family of stonemasons. By the age of 30, he was at the end of a temporary mathematics assistantship at the Imperial and Royal Polytechnic Institute (now TU Wien) in Vienna and could not find work except as a bookkeeper at a cotton factory. The Austrian empire in the early 19th century was a sprawling bureaucratic state with layers of regulations and armies of able applicants for any position. Doppler was lost in that environment despite his advanced education. His applications for permanent technical posts were denied, and he despaired of ever finding a suitable life, so he decided to emigrate to the US. He sold most of his possessions to pay for his journey and visited the US consulate in Munich to obtain the necessary paperwork. But on his return to Austria, on the eve of leaving Europe for an uncertain future, he received an offer for a teaching position in Prague, which he took in 1835.

He began to publish scholarly papers and in 1837 was appointed supplementary professor of higher mathematics and geometry at the Prague Polytechnical Institute (now Czech Technical University); in 1841 he was promoted to full professor of applied geometry. There he met Bernard Bolzano—a political agitator and a mathematician who developed rigorous concepts of mathematical limits. He is famous today for his part in the Bolzano–Weierstrass theorem in functional analysis. Bolzano presided as chairman over a meeting of the Royal Bohemian Society of Sciences on 25 May 1842, the day Doppler read a landmark paper on the color of stars to a meager assembly of only five regular members of the society.

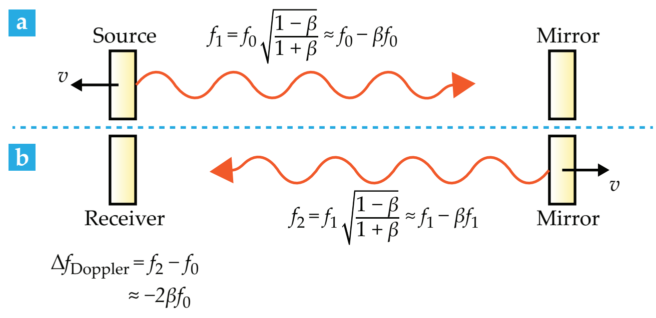

FIGURE 1. THE DOPPLER EFFECT in light backscattering is a relativistic effect that involves two different frames. The mirror in the first frame **(a)** sees a redshifted photon emitted from a receding source. The moving mirror in the second frame **(b)** re-emits the photon, which is redshifted again relative to the receiver, and produces twice the effect. The source frequency is f_0, the Doppler frequency shift on backscattering is $\Delta f_{\text{Doppler}}$, and the ratio of velocity v to the speed of light is β. (Image by David Nolte.)

Doppler had become fascinated by astronomy and by the phenomenon of stellar aberration. It was discovered by James Bradley in 1727 and could be explained by Earth's motion around the Sun combined with the finite speed of light, which causes the apparent position of a distant star to change slightly through a year. As Doppler studied Bradley's work, he wondered how Earth's relative motion would affect the color of the star. By making the simple analogy of a ship traveling with or against a series of ocean waves, he concluded that the frequency of the wave peaks hitting the ship's bow was no different from the peaks of light waves impinging on the eye. He concluded that the color of light would be shifted slightly to the blue if the eye was approaching towards, and to the red if it was receding from, the light source.

His interest in astronomy had made Doppler familiar with binary stars in which the relative motion of the light source might be large enough to cause color shifts. In fact, the star catalogs included examples of binaries that had complementary red and blue colors. Therefore, his paper, published in the *Proceedings of the Royal Bohemian Society of Sciences* a few months after he read it to the society, was titled "Über das farbige Licht der Doppelsterne und einiger anderer Gestirne des Himmels" ("On the colored light of the double stars and certain other stars of the heavens").[3] Although Doppler was mistaken in his assumption that stellar motion would cause a change in the broad-spectrum color of a star, his derivation of frequency shifts was correct. Figure 2 shows Doppler's own drawings of his effect at high speeds.

Many who heard of Doppler's theory did not believe it. Subsequently, on a cold February morning in 1845, Dutch scientist Christoph Buys Ballot, who had recently received his doctorate from the University of Utrecht, loaded an open train car with seasoned musicians and sent them blowing their horns down the railroad line between Utrecht and Maarssen. Buys Ballot did not think that stars would change color by moving, but having no means to test the effect on light, he decided to test it on sound. Unfortunately, the musicians were pelted with hail and snow, which prevented them from blowing their horns properly, so the experiment was reconvened in the milder month of June. That time, with Buys Ballot riding the footplate of the locomotive and the car of trumpeters holding a steady note, musicians standing beside the tracks could hear the approaching note a half-tone higher and the receding note a half-tone lower. The experiment validated Doppler's theory for sound.[1] Buys Ballot published a paper describing the experiment,[4] but he still refused to acknowledge that light could change color despite the close analogy between sound and light.

Petzval's attack

Doppler's prolific scientific output, combined with influential supporters who valued the importance of his work, brought him to the attention of the emperor of Austria, Franz Joseph, newly crowned after his uncle was forced to abdicate during the revolutions of 1848. Reforming education was a top priority for some of the emperor's advisers, and they persuaded him to found Austria's first institute of physics and to name Doppler as its first director. Excited by the prospects and full of ideas, Doppler threw himself into his new position. As a member of the Austrian Academy of Sciences, he proposed a prize for the development of photography to advance scientific inquiry. Unfortunately, photographic lenses were the specialty of another member, Joseph Petzval. His supporters in the academy quashed Doppler's prize proposal, possibly at Petzval's instigation.[1] More trouble from Petzval awaited Doppler and his effect.

At a meeting of the academy on 22 January 1852, Petzval read a paper criticizing Doppler's theory. At a later meeting on 21 May 1852, about 60 members and guests assembled to hear both sides of the argument. The large audience for the mock trial of the Doppler effect stands in ironic contrast to the mere five members of the Bohemian Society who first heard Doppler's ideas 10 years earlier. Petzval's speech, which was published later, attacked Doppler's theory for both sound and light. Petzval thought that no great science could come from a few simple lines of algebra: In his view, all natural phenomena were the manifestations of underlying differential equations. From that premise, he proposed a principle for the conservation of oscillation time in undulatory phenomena. Although he was a mathematician of some talent, he was adrift as a natural philosopher. Petzval conflated a source and receiver in relative motion with a stationary source and receiver embedded in a moving medium. He argued that the pure notes of a well-tuned orchestra would be just as harmonious to an audience on a blustery day as on a calm one; the notes would be unaffected

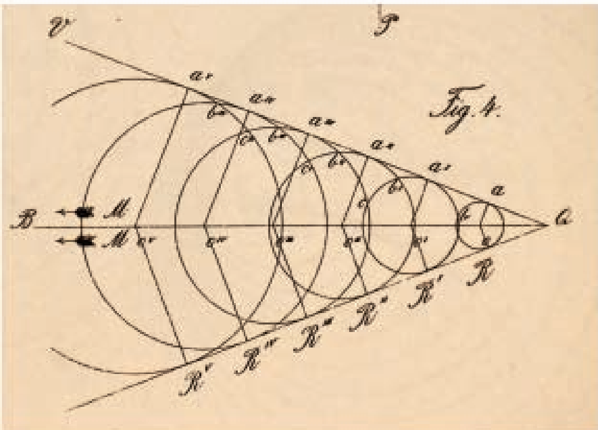

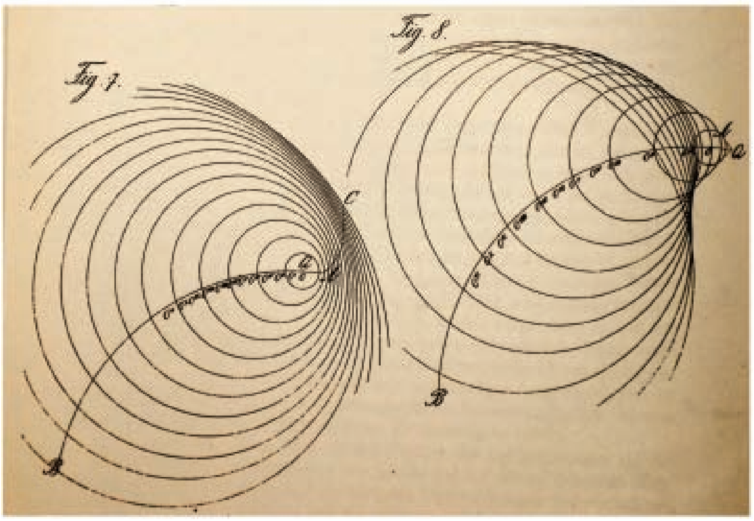

FIGURE 2. THESE DRAWINGS, from Doppler's 1847 paper,[17] illustrate his effect at high speeds and anticipate the Mach cone, which was predicted and photographed by Ernst Mach 40 years later. They also show shock-wave focusing for sources with angular velocity. (Harvard University Biodiversity Heritage Library, public domain.)

by the wind's motion. Ernst Mach later said that Doppler would agree but quipped that if the orchestra were falling from a great height, the audience would hear the piece in F major rather than E major.[5]

Doppler was nonplussed by Petzval's attack. His principle already had been verified for acoustic waves by Buys Ballot and by John Scott Russell, a UK railroad and naval engineer who later discovered solitons propagating in a canal. Furthermore, Hippolyte Fizeau in France had proposed the same theory for light in 1848. Unaware of Doppler's work, he had made the insightful prediction that the effect would be observable in shifts of narrow emission lines from stars in motion rather than from their overall change in color. Fizeau presented his results in a lecture to the Philomatic Society of Paris on 29 December 1848. Hence, the effect is sometimes called the Doppler–Fizeau effect.

Doppler defended himself against Petzval's onslaught simply by asking his opponent whether an observed phenomenon must be deemed nonexistent if it cannot be derived from differential equations. As reasonable as that argument is, a majority of the academy sided with Petzval, and only a few others, including Andreas von Ettingshausen, put up a defense for Doppler.

The academy's final decision was scheduled to take place during a meeting on 21 October 1852; once again Petzval was allowed to make his case. Doppler was unable to attend: The stress and disappointment of the Petzval affair had taken its toll on his health, which collapsed after years of battling tuberculosis. When academy members learned that he was making arrangements for a trip to Venice to improve his health, some mistakenly viewed it as a retreat from the fray and a concession of defeat. Members found in favor of Petzval and pronounced that Doppler's theory must be "abandoned, since it is false, as has been demonstrated."[1] Ten days later Doppler was officially stripped of his directorship of the Physics Institute of Vienna and replaced by Ettingshausen, but Doppler was already en route to Venice where he would die of his disease only four months later.

That might have been the end of the affair at the Physics Institute of Vienna, but Ettingshausen wasn't ready to abandon the Doppler effect just because a committee said it didn't exist. Several years later, he suggested to his student Ernst Mach that he construct a laboratory apparatus to directly demonstrate the acoustic Doppler effect. Mach built and tested a rotating-reed system with tubing that delivered air to the reed, causing it to vibrate at its natural frequency while directing its sound to a stationary observer. As the device spun, the reed approached and receded from the observer, who could hear the rapidly rising and falling tones.[6] Petzval continued denying the effect and accused Mach of youthful foolishness and of throwing away his chances at a career by pursuing an abandoned theory.[1] In response, Mach devised an even more ingenious apparatus, which allows one to listen in one direction to the rising and falling tones and in an orthogonal direction, in which the reed and observer are relatively stationary, to a constant pitch. That arrangement demonstrates even Petzval's preferred principle of frequency conservation. Despite such demonstrations, Petzval was never satisfied, and over the succeeding years Mach had to contend with persistent confusion and disbelief by many others until he finally refused to discuss the effect further.

Vogel's spectrum

Although experimental support for the acoustic Doppler effect accumulated steadily, corresponding demonstrations of the optical Doppler effect were slow to emerge. The breakthrough came in 1868 from William Huggins. He was an early pioneer in astronomical spectroscopy and was famous for discovering that some bright nebulae—planetary nebulae in our own galaxy—consist of atomic gases whereas others consist of unresolved emitting stars. Huggins corresponded with James Clerk Maxwell to confirm the soundness of Doppler's arguments, which Maxwell corroborated using his new electromagnetic theory. In May 1868 Huggins read a paper to the Royal Society of London reporting on observed shifts in the star's spectral lines.[7]

The importance of Huggins's report on the Doppler effect from Sirius was more psychologically important than scientifically accurate because it convinced the scientific community that the optical Doppler effect existed. Only one year later, Joseph Norman Lockyer, codiscoverer of helium, observed a

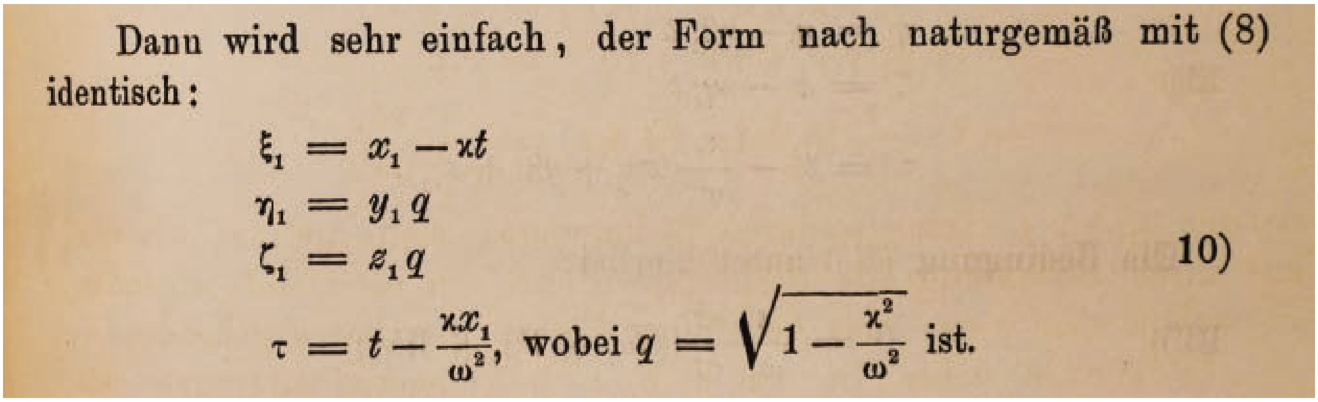

Dann wird sehr einfach, der Form nach naturgemäß mit (8) identisch:

$$\begin{aligned}\xi_1 &= x_1 - \varkappa t\\ \eta_1 &= y_1 q\\ \zeta_1 &= z_1 q\\ \tau &= t - \frac{\varkappa x_1}{\omega^2}, \text{ wobei } q = \sqrt{1 - \frac{\varkappa^2}{\omega^2}} \text{ ist.}\end{aligned} \qquad 10)$$

FIGURE 3. THE TRANSFORMATIONS that keep the wave equation for light invariant were stated in 1887 by Woldemar Voigt.[12] His factor q is the inverse of the Lorentz factor $\gamma = 1/q$. Voigt's equations are identical to the Lorentz transformation if each equation is divided by q. (Image from ref. 12.)

shift in the spectral lines of solar prominences—the high-speed motion of luminous gases ejected from the Sun.[8] Lockyer didn't mention the associated Doppler effect, and because there was no method to confirm the speed of the prominences, his observations were not a definitive demonstration of the optical Doppler effect.

A German astronomer, Hermann Vogel, began working with a new spectrograph that optically projected the spectrum from one side of the Sun next to a reversed spectrum from a point on the opposite side. That doubled the visible effect of the Doppler shift on sharp spectral lines, and Vogel was able to calculate an equatorial rotation speed of the Sun that closely matched the value obtained from the motion of sunspots. Vogel's results were published in 1872 as the first conclusive demonstration of the optical Doppler effect.[9]

Vogel was also working to improve the measurements of the radial velocity of stars—the speed along the line of sight—and was acutely aware that the many values quoted by Huggins and others for stellar velocities were nearly the same as the uncertainties in the measurement process. Using the human eye to observe the spectral lines was the chief problem. Astronomers had begun using photographic plates on telescopes, and Vogel adapted that new technology to the radial velocities problem. He installed photographic capabilities in the telescope and spectrograph at the Potsdam Observatory in 1887 and made observations of Doppler line shifts in stars through 1890. Vogel published an initial progress report in 1891, and his definitive paper in 1892 provided the first accurate stellar radial velocities.[10] Fifty years after Doppler read his paper to the Royal Bohemian Society of Sciences, the Doppler effect had become an established workhorse of quantitative astrophysics. Aristarkh Belopolsky, a Russian astronomer, finally achieved a laboratory demonstration of the phenomenon in 1901 by constructing a device with a narrow-linewidth light source and rapidly rotating mirrors.[11]

Voigt's transformation

At the January 1887 meeting of the Royal Society of Science in Göttingen, Germany, Woldemar Voigt delivered a paper in which he derived the longitudinal optical Doppler effect in an incompressible medium. He was responding to results published in 1886 by Albert Michelson and Edward Morley on their measurements of the Fresnel drag coefficient using an improved version of the 1851 Fizeau experiment that propagated light through moving water. Voigt pointed out that the wave equation for light is invariant under his transformations, shown in figure 3. From a modern vantage point, physicists immediately recognize, to within a scale factor, the Lorentz trans-

FIGURE 4. THE ORBITAL MOTION of the star 51 Pegasi was detected by the Doppler wobbles of the star and its Jupiter-mass planet relative to the system's center of mass (CM) **(a–c).** The velocity modulation is 60 m/s **(d).** (Panels a–c by David Nolte; panel d is adapted from ref. 14.)

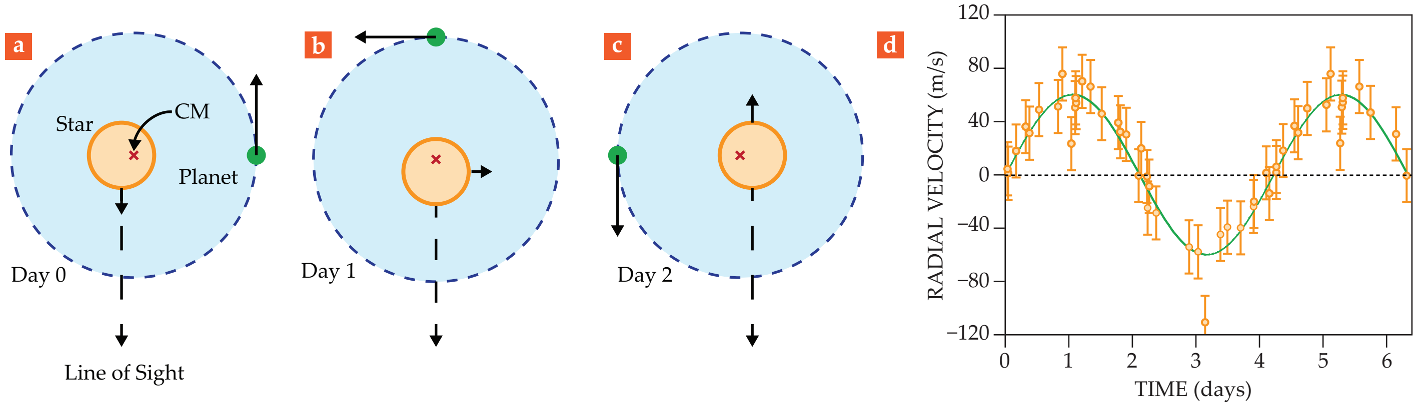

formation of relativity theory. Of particular note is the last equation,[12] which introduces a position-dependent time as an observer moves with speed κ relative to the speed of light ω. Therefore, Voigt derived the longitudinal Doppler effect by considering relativistic effects a few months prior to the epic Michelson and Morley experiment of 1887 on ether drift and two years before George Fitzgerald proposed length contraction.

Voigt's derivation takes a classic approach that is still used in today's textbooks to derive the Doppler effect. Twenty years later, Einstein completed the relativistic description of the Doppler effect by predicting the transverse Doppler effect for a source moving along a line perpendicular to an observer's line of sight.[13] That effect had not been predicted by either Doppler or Voigt.

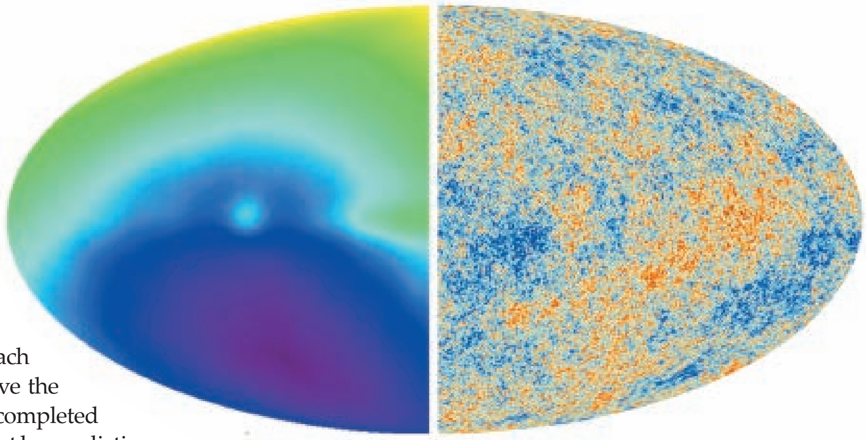

FIGURE 5. ANISOTROPY IN THE COSMIC MICROWAVE BACKGROUND. The Doppler dipole anisotropy (left) is caused by the motion of Earth. The small-angle anisotropy (right), after subtracting the dipole, is caused partly by Doppler scattering of photons in the early universe. (Images courtesy of NASA.)

Doppler spectroscopy

Almost two centuries have elapsed since Doppler published his simple idea using the analogy of a ship plowing through a series of ocean waves, and the idea now underlies our most sensitive forms of optical metrology of dynamical systems. Far beyond Doppler weather radar, the effect's applications extend from the ultrasmall, using Doppler cooling of atoms in the laboratory, to the ultralarge, using Doppler measurements of stellar wobble in the search for exoplanets. Until the launch of the *Kepler* satellite in 2008, most exoplanets had been discovered by detecting the Doppler shifts caused by small radial velocity variations as a star and an exoplanet orbit the system's center of mass. Using the Doppler wobble technique they reported in 1995, shown in figure 4, Michel Mayor and Didier Queloz discovered the first exoplanet, orbiting the star 51 Pegasi.[14] They received the 2019 Nobel Prize in Physics for their work (see PHYSICS TODAY, December 2019, page 17). Radial velocities as small as 3 m/s are resolved if measured over many years.

On a larger scale, the velocity curves of stars within galaxies, which provide some of the most compelling evidence for the existence of dark matter, are observed by Doppler spectroscopy. The relative velocities of the galaxies themselves, such as the streaming of the Virgo cluster of galaxies toward the Great Attractor, are also determined through the Doppler effect. At the largest scale, the Hubble effect is a cosmological redshift caused by the expansion of space rather than an actual Doppler effect. But the motion of Earth, 370 km/s relative to the local cosmic microwave background (CMB), is observed as the large-scale Doppler dipole anisotropy, as shown in figure 5. Doppler fluctuations caused by local motions in the early universe contributed to the small-scale CMB anisotropy that helps to determine the early uniformity of mass distributions and the fraction of dark matter in the universe.

In the life sciences, the acoustic Doppler effect is used in ultrasound imaging, first demonstrated in the 1960s for blood flow measurement,[15] and is now used routinely for Doppler imaging of internal motions, including the Doppler fetal monitor that detects a newborn's heartbeat in prenatal care. The optical Doppler effect is a major feature of dynamic light scattering to detect the directed motion of blood in optical tomography. The intracellular motions in living tissues produce Doppler signatures down to 10 mHz for speeds of several nanometers per second.[16] Subtle changes in intracellular speeds may eventually help doctors select the best treatments for cancer patients. Thus Doppler's eponymous effect has achieved a form of immortality he could never have imagined as he retreated from Vienna on his final journey to Italy, watching St. Stephen's steeple receding into the distance at a redshift of several MHz, though he could not perceive it.

I thank Olivier Darrigol for his helpful comments during the preparation of this article.

REFERENCES

1. A. Eden, *The Search for Christian Doppler*, Springer (1992); P. M. Schuster, *Moving the Stars: Christian Doppler, His Life, His Works and Principle, and the World After*, L. Wilmes, trans., Living Edition (2005); J. B. Hearnshaw, *The Analysis of Starlight: Two Centuries of Astronomical Spectroscopy*, Cambridge U. Press (2014).
2. H. Choi et al., *Biomed. Opt. Express* **9**, 2214 (2018).
3. C. Doppler, *Abh. Königl. Böhm. Ges. Wiss.* **2**, 465 (1842).
4. C. H. D. Buys Ballot, *Ann. Phys.* **142**, 321 (1845).
5. E. Mach, *Beiträge zur Doppler'schen Theorie der Ton-und Farbenänderung durch Bewegung (Contributions to Doppler's Theory of Tone and Color Change Through Movement)*, J. G. Calve'sche U. Buchhandlung (1873).
6. E. Mach, *Sitzungsber. K. Akad. Wiss. Wien* **77**, 299 (1878).
7. W. Huggins, *Philos. Trans. R. Soc. London* **158**, 529 (1868).
8. J. N. Lockyer, *Proc. R. Soc. London* **17**, 131 (1869).
9. H. Vogel, *Astron. Nachr.* **78**, 241 (1872).
10. H. C. Vogel, *Publ. Astrophys. Obs. Potsdam* **7**, 5 (1892).
11. A. Belopolsky, *Astrophys. J.* **13**, 15 (1901).
12. W. Voigt, *Nachr. Königl. Ges. Wiss. Univ. Göttingen* **2**, 41 (1887).
13. A. Einstein, *Ann. Phys.* **23**, 197 (1907).
14. M. Mayor, D. Queloz, *Nature* **378**, 355 (1995).
15. D. L. Franklin, W. Schlegel, R. F. Rushmer, *Science* **134**, 564 (1961).
16. Z. Li et al., *J. Opt. Soc. Am. A* **36**, 665 (2019).
17. C. Doppler, *Über den Einfluss der Bewegung des Fortpflanzungsmittels auf die Erscheinungen der Äther-, Luft- und Wasserwellen* (*Concerning the Influence of the Motion of the Transmitting Medium onto the Phenomena of the Waves of Ether, Air and Water*), Borrosch (1847).

PT

MULTISCALE MODELING BEYOND EQUILIBRIUM

Capturing the behavior of complex materials requires connecting dynamics on multiple scales.

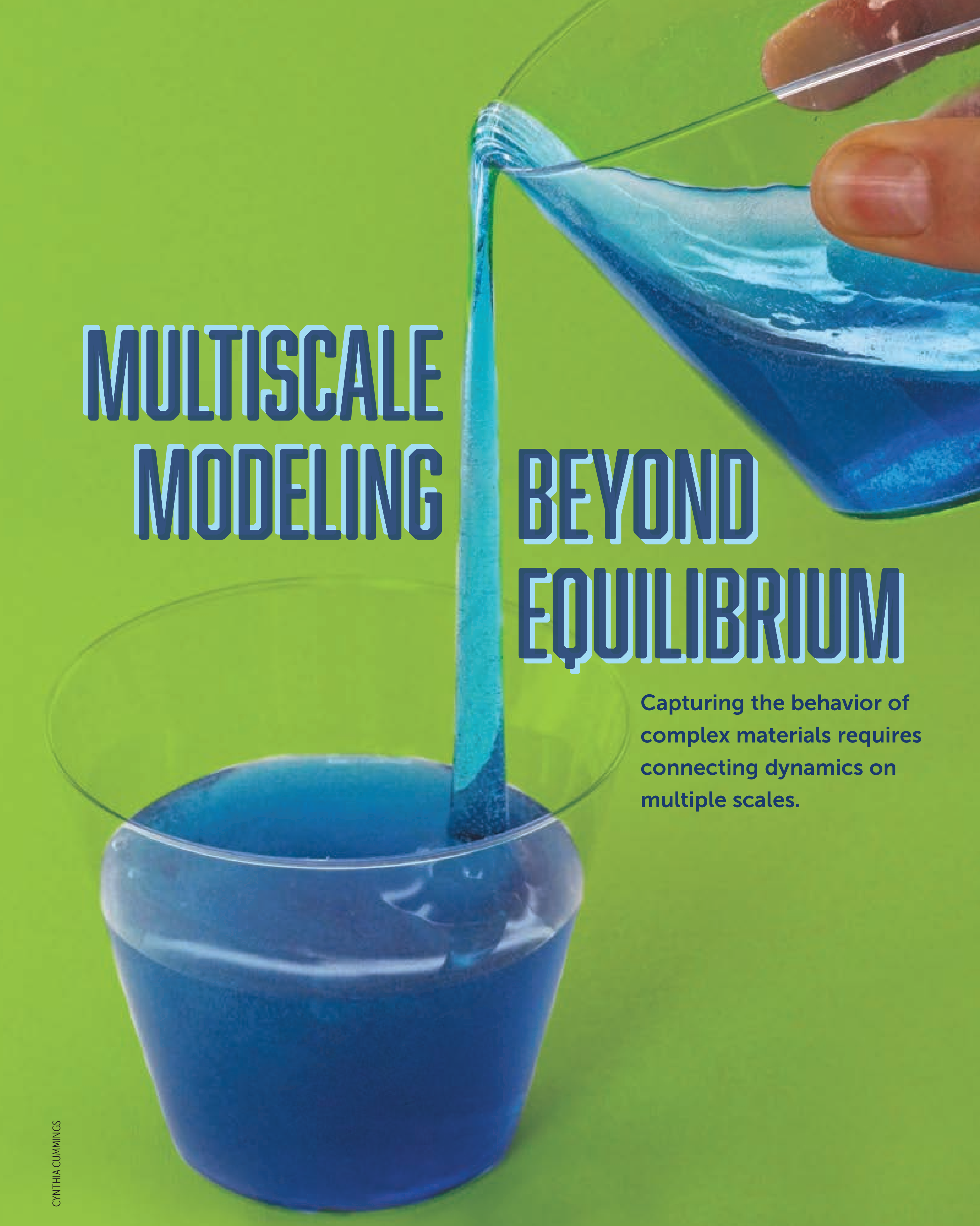

CYNTHIA CUMMINGS

Jay Schieber is a professor of physics, chemical engineering, and applied mathematics and the director of the Center for Molecular Study of Condensed Soft Matter at the Illinois Institute of Technology in Chicago. **Markus Hütter** is an associate professor of multiscale analysis of polymer systems in the polymer technology group of the mechanical engineering department at the Eindhoven University of Technology in the Netherlands.

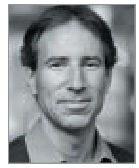

Jay D. Schieber and Markus Hütter

Engineered materials exhibit amazing and useful out-of-equilibrium properties. Some are soft but tough; others can harvest waste heat to produce electricity. Their properties often depend on how the materials are processed; during processing they can exhibit complex flow behavior unlike that of simple fluids. Classical descriptions like the Navier–Stokes equation or Hookean elasticity do not capture the mechanics of such materials. Instead, modeling emergent complex behavior requires simultaneous dynamical descriptions on both macroscopic and microscopic length scales (see the figure on page 38). Such multiscale modeling relies on physical insight; the examples discussed here, which use minimal mathematics, show that the growing field is ripe for contributions from physicists, mathematicians, materials scientists, and engineers.

Complex fluids can exhibit counterintuitive behavior. For example, inserting a rotating rod into a polymer solution or melt will cause the fluid to climb many centimeters up it. Known as the Weissenberg effect, the behavior is opposite that seen in fluids like water, whose flows are dominated by inertia. In simple fluids, a depression in the liquid's surface forms around the rod. Equally strange, if a bit of polymer liquid is pulled out of the top of a bucket, it can act as a kind of tubeless siphon and continue to flow over the edge on its own accord, as shown in the opening image. (For videos of the effects described here, see reference 1.)

Solid polymers display many equally interesting phenomena. Because their dynamics slow dramatically as they approach their glass transition temperature—the temperature below which a polymer behaves like a solid but remains noncrystalline—many polymers never reach equilibrium on cooling. In practice, polymers are not always uniform enough to fully crystallize. Solid, fully crystalline polymers are therefore scarce. If solidification occurs by rapid cooling either during or immediately after the material is deformed, the sample will stay deformed as long as it remains below the glass transition temperature, but it will go back to its original shape when heated. Applying a large plastic deformation to a solid polymer causes chain segments to become strongly oriented and can produce filaments with ultrahigh stiffness and strength. Those fibers are then used for many applications, such as cut-resistant gloves and strong, lightweight ropes for use at sea. For a more detailed description of semicrystalline polymers, see box 1.

Cross-linked networks of hydrophilic polymers in water form hydrogels that exhibit elastic behavior. Despite being mostly water, double-network hydrogels can sustain very high stresses—up to tens of megapascals—without breaking. Evidence suggests that the gel dissipates energy by irreversibly breaking the covalent bonds of one network while maintaining its strength through the second, unbroken network.

Simple beginnings for complex behavior

Continuum mechanics provides a well-established foundation for describing the macroscopic behaviors of both fluids and solids. Applying momentum conservation to a continuum generates the equation of motion known as the Cauchy momentum equation:[2]

$$\rho \frac{\mathrm{D}}{\mathrm{D}t}\mathbf{v} = -\nabla \cdot \boldsymbol{\Pi} + \rho \mathbf{g}\,.$$

The left side contains the mass density ρ, the macroscopic fluid velocity $\mathbf{v}$, and the material time derivative. The right side captures the forces on a point in the continuum through the total pressure tensor $\boldsymbol{\Pi}$ and body-force vector $\mathbf{g}$. Simply put, the equation is force equals mass times acceleration.

Adding a restrictive assumption—that the pressure tensor has the usual isotropic thermodynamic pressure plus a contribution that is linearly proportional to the instantaneous velocity gradient—yields the famous Navier–Stokes equation. The assumption implies that deformations on molecular length scales relax so quickly that the microscopic components of the material always behave as if they are locally at equilibrium.[3] It also guarantees nonnegative entropy production. The idea is intuitively appealing, and for fluids like water, whose small molecules relax rapidly compared with macroscopic strain rates, the Navier–Stokes equation indeed appears to be exact.

However, for polymers, proteins, colloids, liquid crystals, emulsions, and other materials with larger constituent parts, microscopic relaxation rates can become comparable to macroscopic strain rates, which causes the local equilibrium assumption to fail. (See the article by Byron Bird and Charles Curtiss, PHYSICS TODAY, January 1984, page 36.) Researchers recognized the shortcomings of the Navier–Stokes equation for such materials early on; they then began searching for a fix, and the field of rheology was born. Although Cauchy's equation was safe, it contained that unknown pressure tensor term $\boldsymbol{\Pi}$, which could no longer simply be replaced by a pressure term plus a term proportional to the velocity gradient. The modeling of complex fluids still starts with the velocity field, but adjustments are needed to account for noninstantaneous microscopic relaxation by bringing elastic effects into the otherwise purely viscous description.

FIGURE. POLYMERIC MATERIALS exhibit different structures on a wide range of length scales. If a material is deformed, the structures relax on disparate characteristic time scales, from tens of picoseconds for monomers to hours or even years for bulk materials. Models of multiscale materials aim to describe bulk properties by capturing structural dynamics across length and time scales. (Adapted from Y. Li et al., *Polymers* **5**, 751, 2013.)

Like fluid mechanics, solid mechanics also begins with the conservation of linear momentum. However, the resulting equation is usually recast in terms of the Lagrangian deformation field χ, which for elastic solids is more natural than a velocity field. The simplifying assumption for describing solid-like behavior is that the pressure tensor is linearly proportional to instantaneous strain, a component that is closely related to the spatial derivative of χ. Not surprisingly, the assumption introduces several limitations that make it inappropriate for complex materials. Even with moderate deformations, stresses can depend nonlinearly on strains. And as anyone who has tried to repair a bent wire coat hanger knows, solid deformations can be irreversible. Linear elasticity, on the other hand, has no entropy generation, so it should always be reversible. Therefore, an accurate description of complex solids needs to be extended to account for relaxation effects.

The simplified fluid description has dissipation with no elasticity; the simplified solid has elasticity but no dissipation. The former implies an infinitely fast relaxation of the material's microscopic components, whereas the latter implies no relax-

BOX 1. SEMICRYSTALLINE POLYMERS

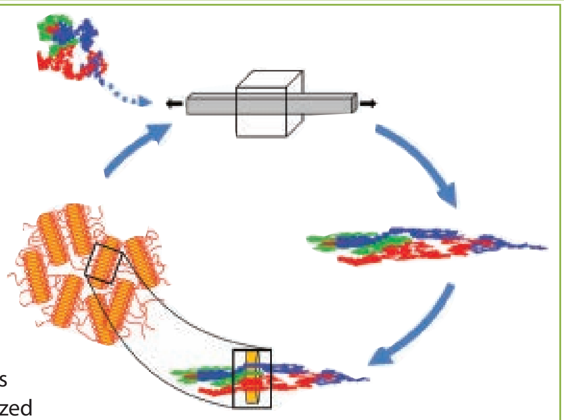

Cooling a polymer below its crystallization temperature typically does not result in a fully crystalline material. Instead, crystallization is arrested by topological constraints and a dramatic slowing as the system approaches its glass transition temperature.[12,13] Processing conditions, such as how the polymer is cooled and deformed, have a strong effect on the resulting microstructure and determine properties like the volume fraction of crystals, the thickness of lamellae, and the structure's overall anisotropy.

The diagram outlines how flow-induced crystallization in a polymer can control the material's mechanical properties. When isotropic polymers (top) undergo a macroscopic deformation, they can become oriented and stretched (right). At sufficiently low temperatures, that stretching enhances their crystallization (bottom). Chain segments locally pack into small organized structures, such as lamellae or shish kebabs, that can assemble into superstructures.

The semicrystalline morphology of those superstructures (left) can affect the macroscopic behavior of the crystallizing material, including its effective linear elastic properties, yield stress, birefringence, and conductivity. When producing ultrahigh-strength polymer fibers, crystallinity is relevant only during the intermediate processing steps. Achieving the desired mechanical properties requires finding the right density of chain entanglements. A lower entanglement density, which can be achieved by dilution, not only helps to produce thin fibers but also increases the fiber's drawability, which gives the filament its ultrahigh strength. (Image courtesy of Markus Hütter.)

BOX 2. CRYSTALLINE METALS

Solid metals are typically imperfect crystals. When they experience sufficiently high stress, new dislocations—line defects in the crystal structure—are created in large numbers. The dislocations cause irreversible plastic deformation by moving through the crystal lattice,[14,15] a feature that is absent in the solid mechanics of elasticity. Interactions between dislocations increase the stress required for yielding and result in work hardening. Dislocations can be described in various levels of detail: parametrization of each dislocation, a statistical description of the orientation of dislocation segments, or simply a density of dislocation segments.

The diagram shows different microstructural levels of description for a crystalline metal. A full-detail atomistic lattice with line defects is shown in the lower left. In the lower right is a phase-field description of dislocations that does not explicitly account for the lattice. The upper right shows a large number of dislocations, each of which is represented by a discrete line.

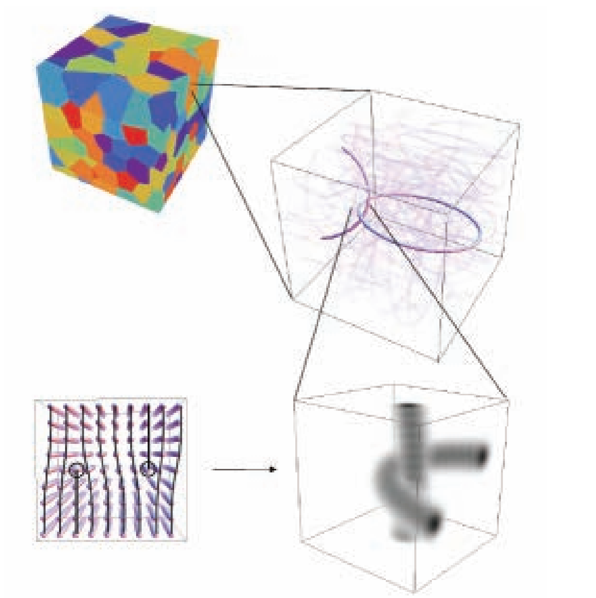

Macroscopic samples are typically not single crystalline. Rather, they are polycrystalline and contain grains—smaller single-crystalline volumes that make up the larger structure seen in the upper left. The presence of grain boundaries hinders the stress-activated motion of dislocations, so the grain size has a strong effect on the plastic deformation behavior of metals; smaller grains make the metal stronger.

Quantifying the rich microstructure and capturing the interplay between the microstructure and the macroscopic behavior depend on exactly which phenomena one wants to study. Macroscopic stress leads to the creation and motion of dislocations, which also couple back to the macroscopic scale. The characteristics of the dislocations, such as their Burgers vectors, density, and velocities, inform the so-called plastic strain-rate tensor on the macroscopic level, which is the key ingredient for enriching elasticity theory with plasticity. (Image courtesy of Markus Hütter.)

ation at all. Irrespective of whether one takes a fluid or a solid as the starting point, extension, or rather enrichment, is clearly required to account for the finite-time relaxation found in real materials.

Microstructure

To describe complex solids and liquids, researchers first had to develop the idea of microstructure, which is captured by variables on an intermediate length scale that relax slowly and have a clear connection to a system's dynamics on the atomistic scale. The number of such variables should be many orders of magnitude smaller than the number of atoms in the system but still capture the physical phenomena of interest. Any discarded degrees of freedom are typically assumed to be near equilibrium and provide a sort of thermal bath for the more slowly relaxing degrees of freedom.

Physical insight from experiments or atomistic simulations can guide the development of evolution equations for microstructural variables. That process, known as coarse graining,[4] raises three questions:

- What are useful microstructural variables?
- What equations describe their evolution?
- How are macroscopic quantities, such as stress, related to the microstructural variables?

Answering each question requires insight, intuition, and innovation. Systematic ways of finding the right microstructural variables rarely exist. But whether the starting point is a fluid or a solid, the goal of incorporating microstructural variables is to bring finite-time relaxation processes into the overall description. Boxes 1, 2, and 3 give examples of continuum approaches that have been enriched by including microstructure.

A concrete set of variables that accurately describes the microstructure in a complex material is paramount. The variables must include sufficient detail about the microstructure, and simplifications must discard only unnecessary information. The model is then more likely to retain the necessary physics to capture many phenomena. For example, a set of microstructural variables might simultaneously describe mechanical and dielectric phenomena, birefringence, and direct structural information obtained by scattering experiments. However, the variables should only retain the necessary physics for the problem of interest. An overly detailed model can become cumbersome and have too many adjustable parameters.

If a wide separation exists between the macroscopic and microstructural length scales, it should be reflected in the variable choice. Typically, a separation of time scales accompanies the separation of length scales, which makes possible the use of fluctuation–dissipation theorems.[5]

Without a more prescriptive set of instructions, choosing the variables for each physical system falls largely to physical insight. But that is not a shortcoming. It is an essential step toward physics-based, rather than algorithm-based, coarse graining.

Introducing microstructural variables into a dynamic model should decrease, not increase, the model's complexity. It should allow observed phenomena to be expressed in physically intuitive terms and relate seemingly distinct aspects,

BOX 3. MORE POLYMER MODELS

Polymers come in multiple shapes and sizes, and different models are needed to describe their dynamics. One example is a simple model for an idealized branched, entangled chain architecture called the pom-pom.[16] Each chain has a linear backbone with q branches of identical molecular weight on each end. The microstructure is characterized by two parameters: a conformation tensor $\mathbf{c}$ that describes the average orientation of the backbone and a stretch ratio Λ that characterizes the average stretch of the backbone relative to the average equilibrium length that results from flow. The arms slow down the backbone's relaxation, but otherwise, their direct contributions to observables are neglected.

The pom-pom model complies with thermodynamics, and researchers have identified an expression for its free energy that captures both the driving force of the dynamics and the dependence of the pressure tensor on microstructural conformations. The appropriate orientational relaxation is determined by

$$\frac{\partial \mathbf{c}}{\partial t} + \mathbf{v}\cdot\nabla\mathbf{c} = (\nabla\mathbf{v})^{\dagger}\cdot\mathbf{c} + \mathbf{c}\cdot(\nabla\mathbf{v}) - \frac{1}{\tau_b}\left(\mathbf{c} - \frac{1}{3}\boldsymbol{\delta}\right),$$

where τ_b is a frictional relaxation time constant for the backbone. The stretch dynamics are coupled with the conformation tensor and the velocity gradient, which stretches the backbone according to

Atomistic simulations of entangled polymer chains

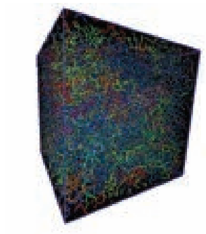

Primitive path analysis to find model parameters

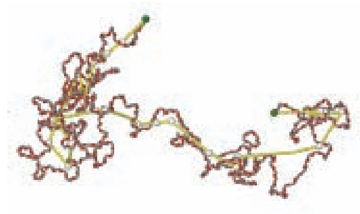

$$\frac{\partial \Lambda}{\partial t} + \mathbf{v}\cdot\nabla\Lambda = \Lambda\mathbf{c} : (\nabla\mathbf{v}) - \frac{\Lambda}{\tau_s f(\Lambda)}\left[min(\Lambda, q) - \frac{1}{\Lambda}\right],$$

where τ_s is a stretch relaxation time and is assumed to be much smaller than τ_b. The function f equals $1 + \Lambda$ if $\Lambda \le q$, or $\Lambda - 1/q$ otherwise. That jump captures a sudden relaxation in the polymer's dynamics, which is attributed to its branches withdrawing into the tube already occupied by its backbone when doing so becomes entropically favorable.

Solving the pom-pom model requires calculating the velocity field $\mathbf{v}$ and the two microstructural variables, $\mathbf{c}$ and Λ, simultaneously at every point in the flow domain. All three parameters are coupled. The continuum level feeds the velocity gradient to the microstructure, which relays the pressure tensor to the continuum. The model can describe qualitative differences such as how the concept of entangled polymer chains helps elucidate the counterintuitive Weissenberg and tubeless-siphon effects.

Thermodynamics, but with friction

Modeling the nonequilibrium thermodynamics of dynamic, multiscale systems relies on thermodynamic potentials, such as the Helmholtz free energy. The potentials for such systems, which can be derived from statistical mechanics, do not just determine static properties, but also provide the driving forces for the fluxes and relaxation processes of the microstructural variables. Statistical mechanics can also be applied outside equilibrium, not just to macroscopic variables like volume but also to microstructural variables. That strategy was first used by Werner Kuhn in 1934 to describe polymers.[6] However, because the microscopic and macroscopic descriptions have different amounts of entropy, it is important that the free energies on both levels be compatible: Performing two successive coarse-graining steps, from atomistic to mesoscopic and then to macroscopic, must yield the same free energy as that obtained in a single step from atomistic to macroscopic.

Thermodynamic potentials also help to determine with minimal phenomenology the elusive pressure tensor $\mathbf{\Pi}$. Although they may seem like restrictions, thermodynamic constraints are actually quite liberating. As long as new models and microscopic variables conform to those constraints, they will avoid the risk of creating energy *ex nihilo*, destroying entropy in the universe, or masking other forbidden features.[4]

Once the microstructural variables are chosen, they need associated evolution equations, which must conform to fundamental physical constraints like the first and second laws of thermodynamics and the fluctuation–dissipation theorem. Parameter values for those equations, such as friction coefficients, may have to be obtained from molecular dynamics simulations or another highly detailed description. In practice, that might mean that the system's dynamics are described on three levels: atomistic, microstructural, and continuum. However, once the necessary parameter values are found, the atomistic simulations can be discarded, and the model is left with only two remaining variable sets: microscopic—or more accurately, mesoscopic—and macroscopic. In simulations, the two sets must communicate with one another at all times.

No monologues, but a dialogue

Multiscale modeling links the dynamics of the structure on the mesoscopic level with a macroscopic dynamic formulation. The time evolution of macroscopic variables like those typically used in fluid and solid mechanics is refined by time-dependent information from the microstructure. The coupling should be bidirectional: A macroscopic deformation distorts the microstructure, and, in turn, the forces of the deformed microstructure give rise to out-of-equilibrium stresses on the macroscale. The pressure tensor is thus not expressed directly in terms of a macroscopic velocity or displacement gradient; rather, it depends on the mesoscale's structural state. Such a scenario is typical, and nonequilibrium thermodynamics is often

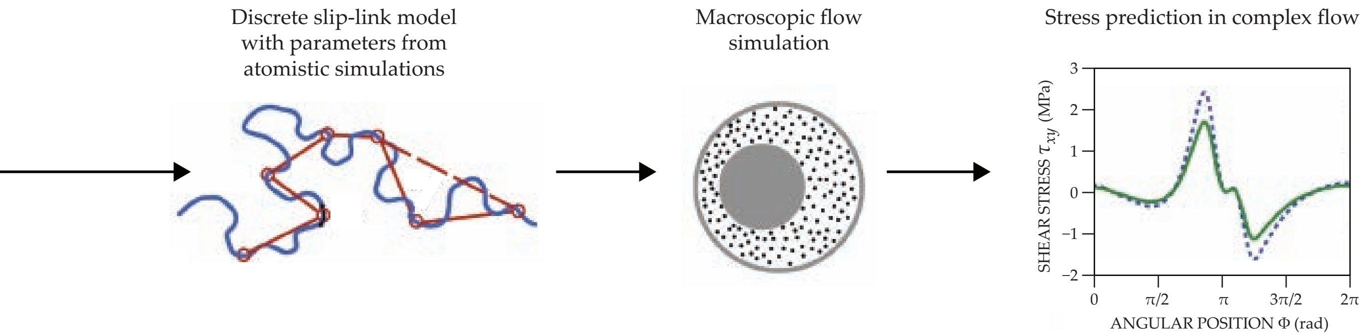

that have been observed in shear and elongation experiments for branched-chain-polymer architectures but not observed in linear chains. There also exist several modifications to the model that were suggested either by thermodynamic considerations or by improved agreement with experiment.

Similarly, the microscopic dynamics of an ensemble of independent stochastic trajectories can be solved numerically, akin to using Brownian dynamics simulations to extract information from Fokker–Planck equations. A method called smoothed particle hydrodynamics can be used for the macroscopic-level calculations. Embedded in each particle is an ensemble of several thousand coarse-grained polymer chains. The chains are stochastically independent, but all feel the same local velocity gradient. Taking the proper average over the ensemble of chains yields the local polymeric contribution to stress and the self-consistent motion of the particles.

The slip-link model, illustrated here in tandem with smoothed particle hydrodynamics, is used to describe linear entangled chains. It has fewer adjustable parameters and greater fidelity with experiments than the pom-pom model. On the left, an atomistic simulation shows dense polymer chains at equilibrium. Topological analysis can uncover entanglements in each chain, as shown in the next image. Entanglement parameters are found by matching the statistics from all the chains with the coarse-grained slip-link model (center). An ensemble of chains is placed in each particle of the smoothed particle hydrodynamics simulation, shown in the next image, to find the macroscopic flow. Those simulations can then predict the stresses or other macroscopic properties anywhere inside the flow (right). (Image adapted from *Mol. Syst. Des. Eng.* **1**, 6, 2016.)

employed to achieve bidirectional coupling in a way that is compatible with fundamental principles of thermodynamics.[4]

Although derivatives of thermodynamic potentials act as driving forces for dynamics, frictional transport coefficients are also needed to describe relaxation phenomena. Like entropy, friction increases when moving to coarser levels of description. The most famous assertion of that fact is the fluctuation–dissipation theorem, which relates the magnitude of certain fluctuations on one level of description, like forces or velocities, to friction on a coarser level. Originally, the theorem was derived from purely deterministic dynamics without any friction to put restrictions on coarse-grained dynamics.

Models are more useful when they are well-defined mathematical objects and not just computer algorithms. A mathematical object can be tested rigorously for adherence to the principles of thermodynamics. And when an asymptotic solution to a model exists, it can also be used to test the convergence of algorithms. In our own work, we used the mathematical formulation of the slip-link model to derive an algorithm for graphical processors. It exploits the parallel computing power of inexpensive video cards to perform simulations that are two orders of magnitude faster than those on central processing units but that yield identical results. The speedup could not have been achieved without a well-defined mathematical object.

Using a nonequilibrium thermodynamics route for the model formulation guarantees that the first and second laws, among other restrictions, are respected. The numerical algorithm must therefore converge to a thermodynamically acceptable solution. Moreover, forcing the discretized dynamics of the algorithm to obey thermodynamics can improve the numerical stability of the simulations.[7]

Everything flows, including microstructure

The quintessential system for applying multiscale modeling is polymers. The simplest microstructural variable for a polymeric liquid, and one that is slowest to relax, is the conformation tensor $\mathbf{c} \equiv \langle \mathbf{R}_{ee}\mathbf{R}_{ee} \rangle$, where $\mathbf{R}_{ee}$ is the end-to-end vector of one polymer chain and $\langle \ldots \rangle$ is an ensemble average. If the chains become stretched out by a flow field, their entropy decreases, but their energetics are not changed significantly, which produces a strong thermodynamic drive for the polymers to return to their shorter, isotropic conformations. That retraction naturally gives rise to shear and normal stresses, which easily occur in polymers. In fact, the Weissenberg effect, in which polymeric fluid climbs up a rotating rod, is due to the presence of anisotropic normal stresses, which provide tension along curved streamlines in the flow. So-called hoop stresses form, squeeze the fluid, and cause it to move up the rod.

Observations of atomistic simulations or the scattering properties of real systems can be incorporated into a conformation tensor. Hence that microstructural variable easily connects simple molecular descriptions to macroscopic phenomena.

But things aren't always that straightforward: Chain uncrossability in concentrated polymers leads to entanglements.[8] The spacing between entanglements is a length scale that is independent of molecular weight and is intermediate to the polymer's persistence length and the overall size of the polymer coil. In several articles in the 1970s Masao Doi and Sam Edwards proposed describing the microstructure of a polymer in terms of the probability density for the orientation of a tube segment that surrounds a particular length of polymer. With that level of description and a simple proposal for anisotropic dynamics, their tube model accurately described the stress relaxation in nonlinear step-strain experiments. (For more on polymer entanglement, see the article by Tom McLeish, PHYSICS TODAY, August 2008, page 40.)

The single-segment theory of Doi and Edwards is not sufficient to make quantitative predictions or describe more detailed phenomena. That shortcoming led to the development of more detailed models, such as the so-called slip-link models,[9] which have successfully described entangled polymer melts. Their microstructural variables include fluctuations in entanglement number, entanglement spacing, and monomer density between entanglements. The entanglement parameters characterizing the relevant statistics can all be found with atomistic simulations. Because of their finer level of description, the slip-link models discussed in box 3 capture the broad spectrum of phenomena displayed by polymer melts.

No time to relax yet

Plenty of opportunities exist to build new multiscale models. For example, the dynamics that underlie dislocation-based plasticity may not exhibit a clear separation of time scales,[10] which implies that the fluctuation–dissipation theorem might not hold. Systems without time-scale separation clearly warrant further investigation.

Brittle fracture is also governed by communication between large and small length scales, which makes it a good candidate for multiscale modeling. However, unlike the examples above, in which the microstructure exists throughout the continuum and its effects can be averaged, fracture contains an isolated crack tip in an otherwise elastic continuum. The stress field around the crack tip is long ranged and drives the fracture, but the crack tip itself exists on a small scale. Continuum mechanics are therefore typically applied far away from the crack tip, but atomistic and even quantum mechanical descriptions are used nearby. Intricate coupling is needed to connect the two regions. Because it incorporates the effects of disparities in both length and time scales, multiscale modeling offers opportunities for advancing models of brittle fracture.

Although this article focuses on the responses of materials to deformation, similar issues arise when materials are exposed to other stimuli, such as temperature gradients and electromagnetic fields. In those cases, the details of a dynamic multiscale model—the particular choice of variables and the model's formulation—depend on which stimuli and phenomena are being studied. But the general philosophy of multiscale modeling presented here can still be applied. Multicomponent materials and the coarse graining of active matter, such as molecular motors in a gel or swarms of swimming Janus particles, also present unique challenges that might benefit from multiscale modeling.

Researchers should not think of microstructural variables only as necessary mathematical simplifications. When coarse graining is successful, it yields deep insights into the physics that underlies interesting phenomena and helps scientists develop intuition for molecular engineering. Atomistic simulations are most useful when they are accompanied by a guiding coarse-grained level of description that can facilitate the extraction of useful information. Even when coarse graining fails, it uncovers information about the assumptions that went into it. A coarse-grained model that eliminates some essential physics will fail to agree with experiment, and that in itself is useful to know. So instead of making apologies for coarse graining, we say that one has no excuse for not doing it.[11]

Many open questions, both fundamental and practical, remain, and each new problem requires deep physical insight and creative intuition to find the appropriate level of description. Despite their impressive accomplishments, machine-learning algorithms are not likely to uncover the proper way to model entanglements. Physicists have a lot to contribute in the field.

Great progress has been made in developing robust numerical algorithms for multiscale modeling, but it seems that every new model presents unforeseen numerical challenges. Both fundamental and applied mathematicians can make important contributions on that front, and the tools they develop for modeling multiscale systems are not only intriguing from a fundamental perspective. They have tremendous potential for applications in engineering and may eventually lead to the designing of molecules that exhibit desired nonequilibrium properties.

Markus Hütter would like to acknowledge stimulating discussions with Marc Geers, Varvara Kouznetsova, and Theo Tervoort. Jay Schieber would like to thank David Venerus for useful feedback on the manuscript.

REFERENCES

1. See, for example, the Weissenberg effect, www.youtube.com/watch?v=0-WmJy9edlA; the tubeless siphon, www.youtube.com/watch?v=g4od-h7VoRk; and recovery on reheating, www.youtube.com/watch?v=3wKNAPJ-0ug.
2. R. B. Bird, W. E. Stewart, E. N. Lightfoot, *Transport Phenomena*, 2nd ed., Wiley (2002).
3. S. R. de Groot, P. Mazur, *Non-equilibrium Thermodynamics*, Dover (1984).
4. H. C. Öttinger, *Beyond Equilibrium Thermodynamics*, Wiley-Interscience (2005).
5. R. Kubo, M. Toda, N. Hashitsume, *Statistical Physics II: Nonequilibrium Statistical Mechanics*, Springer (1985).
6. W. Kuhn, *Kolloid-Z.* **68**, 2 (1934).
7. C. P. Zinner, H. C. Öttinger, *J. Non-equilib. Thermodyn.* **44**, 43 (2019).
8. S. F. Edwards, *Proc. Phys. Soc.* **92**, 9 (1967).
9. H. Feng et al., *Mol. Syst. Des. Eng.* **1**, 99 (2016); J. D. Schieber, M. Andreev, *Annu. Rev. Chem. Biomol. Eng.* **5**, 367 (2014).
10. M. Kooiman, M. Hütter, M. G. D. Geers, *J. Mech. Phys. Solids* **90**, 77 (2016).
11. H. C. Öttinger, *J. Rheol.* **53**, 1285 (2009).
12. H. E. H. Meijer, ed., *Processing of Polymers*, Wiley (1997).
13. G. Reiter, G. R. Strobl, eds., *Progress in Understanding of Polymer Crystallization*, Springer (2007).
14. J. P. Hirth, J. Lothe, *Theory of Dislocations*, 2nd ed., Wiley (1982).
15. D. Raabe, *Computational Materials Science: The Simulation of Materials, Microstructures and Properties*, Wiley (1998).
16. H. C. Öttinger, *Rheol. Acta* **40**, 317 (2001); T. C. B. McLeish, R. G. Larson, *J. Rheol.* **42**, 81 (1998); W. M. H. Verbeeten, G. W. M. Peters, F. P. T. Baaijens, *J. Non-Newtonian Fluid Mech.* **108**, 301 (2002).

PT

The emergence of MAGNETIC SKYRMIONS

Alexei N. Bogdanov and Christos Panagopoulos

The nanometer-scale localized objects share a nonlinear mathematical framework with systems from water waves to elementary particles.

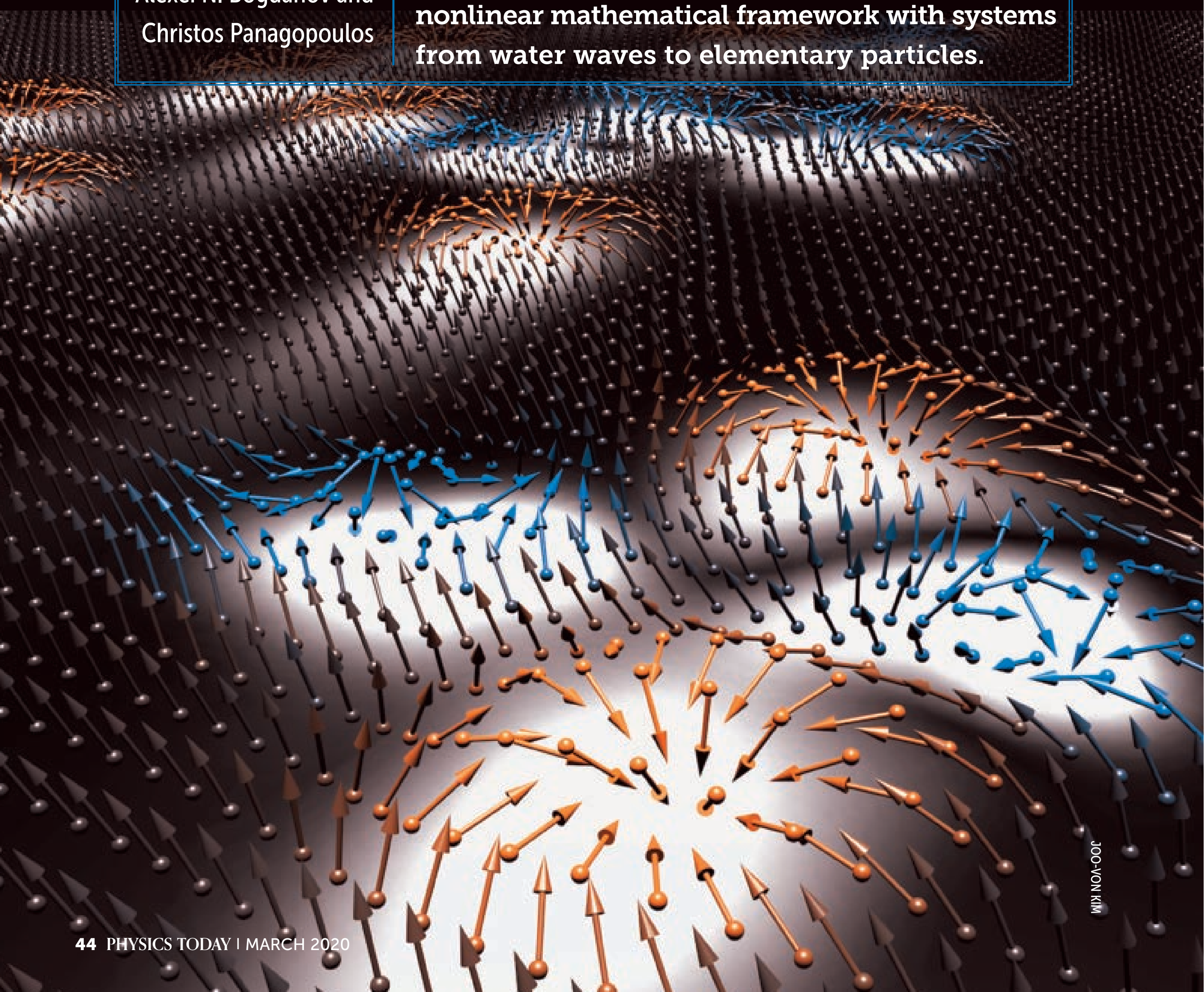

JOO-VON KIM


Alexei Bogdanov is a senior researcher at the Leibniz Institute for Solid State and Materials Research Dresden in Germany and a project professor in the Chirality Research Center at Hiroshima University in Japan. **Christos Panagopoulos** is a professor of physics at Nanyang Technological University and an investigator at the National Research Foundation, both in Singapore.

Magnetic skyrmions, sometimes teasingly called magic knots or mysterious particles, are nanometer-scale whirling cylinders of magnetization (see figure 1). The spatially localized objects are highly mobile and the smallest possible magnetic configurations in nature. They are thus promising for applications in the emerging field of spintronics, which uses the electron spin as an information carrier in addition to or instead of the electron charge. To explore the unconventional and potentially useful features of skyrmions, research to date has focused on novel classes of bulk and recently synthesized nanolayers and multilayers of magnetic metals.[1,2]

For many years the primary question surrounding skyrmions was whether they even exist. Mathematically, in the majority of physical systems, localized structures similar to skyrmions are unstable and collapse spontaneously into linear singularities. But three decades ago, a surprising mathematical development identified a group of low-symmetry magnetic materials that defy the general rule of instability.[3]

In asymmetric compounds, specific magnetic interactions counteract the collapse and stabilize finite-sized structures, or spin textures, such as magnetic skyrmions.[3,4] Skyrmions are one example of a self-supporting particle-like object known as a soliton. The physics that governs solitons began with a remarkable observation made almost two centuries ago.

The birth of solitons

In August 1834 engineer John Scott Russell noticed that when a boat suddenly stopped in a narrow water canal, a resulting localized wave flowed virtually unchanged for many miles. He noted that "the mass of water in the channel which [the boat] had put in motion … rolled forward with great velocity, assuming the form of a large solitary elevation, a rounded, smooth and well-defined heap of water, which continued its course along the channel apparently without change of form or diminution of speed" (reference 5, page 3).

Inspired by the observation, Russell built pools at his house and experimented with such so-called solitary waves. He was convinced of their fundamental importance. But his work was viewed with skepticism, primarily because his findings and conclusions didn't agree with the properties of water in the prevailing theory at the time.

Russell's solitary wave is described by a superposition of harmonic waves. The phase speeds of harmonic waves depend on their wavelengths—a phenomenon known as the dispersion effect. Once formed, the waves gradually spread and decay. But solitary waves show an enigmatic stability. In 1871 physicist Joseph Boussinesq figured out that the seabed stabilizes solitary waves but only in shallow waters. Six years later he introduced an equation to describe the phenomenon:[3]

$$\underbrace{\frac{1}{v_0}\frac{\mathrm{d}\eta}{\mathrm{d}t}+\frac{\mathrm{d}\eta}{\mathrm{d}x}}_{\text{Transport}}+\underbrace{\frac{h^2}{6}\frac{\mathrm{d}^3\mathrm{d}\eta}{\mathrm{d}x^3}}_{\text{Dispersion}}+\underbrace{\frac{3}{2h}\eta\frac{\mathrm{d}\eta}{\mathrm{d}x}}_{\text{Interaction with seabed}}=0.$$

In which $v_0 = \sqrt{gh}$. The function η depends on the distance x and time t, and the equation changes with the depth of the water h and gravitation acceleration g. It became known as the Korteweg–de Vries (KdV) equation in honor of the physicists who in 1895 published detailed studies of the localized and periodic solutions. The KdV equation's first two terms, which are labeled as transport, yield solutions for nondispersive waves traveling at speed v_0. The next term describes the wave's dispersion, and the last term accounts for its interaction with the seabed.

When h is a factor of 20 or more smaller than the wavelength L, the equation yields localized solutions with bell-shaped profiles[5] $\eta_s(x, t)$, shown in figure 2a, that describe solitary waves.[6] Contrary to deep-water waves, the balance of dispersion and the interaction with the seabed keeps shallow solitary waves stable and preserves their bell-shaped profile.

Despite that mathematical description, researchers ignored solitary waves for decades. But in the 1960s, scientists discovered localized states in various physical systems. Since then researchers have used modern mathematical methods and numerical simulations to study solitary waves and other self-supporting localized states, which are referred to as solitons, a term coined by Martin Kruskal of Princeton University and Norman Zabusky, who worked at Bell Labs in New Jersey at the time.[7]

Physics beyond the linear world

In the KdV equation, solitary waves are stabilized because of the quadratic term in the function η; the other terms are linear and do not support the formation of localized states. Nonlinearity is the characteristic feature of soliton mathematics, but most physical systems have linear models from Maxwell's equations to the Schrödinger equation. In a linear model, the net response from two or more stimuli is the sum of the isolated responses. But sufficiently strong distortions make a system become nonlinear—that is, the net response is not the sum of its parts. (For more on localized states in nonlinear systems, see the article by David Campbell, Sergej Flach, and Yuri Kivshar, PHYSICS TODAY, January 2004, page 43.)

The transformation from linear to nonlinear is clear in the simplified model of waves shown in figure 2b. In deep water, although waves propagate, particles below the surface orbit in circles. The orbits' diameters decrease with increasing distance from the surface and become zero at a distance $L/2$ below the surface. In shallow water with h less than $L/2$, the orbits are increasingly elliptical with distance from the surface and become horizontal oscillations at the seabed. The distortion of the particle orbits increases with decreasing total depth of the water. In extremely shallow water with h less than $L/20$, the distortions are strong enough to suppress dispersion and stabilize solitary waves.

As a local energy minimum of the system, solitary waves are extremely stable. They preserve their shape not only while in motion but during interactions with other solitary waves; in other words, they behave similarly to solid particles. The shallow-water mathematical model represents the extended class of self-supported and particle-like solitons that emerge in nonlinear physical systems—for example, magnetic skyrmions.

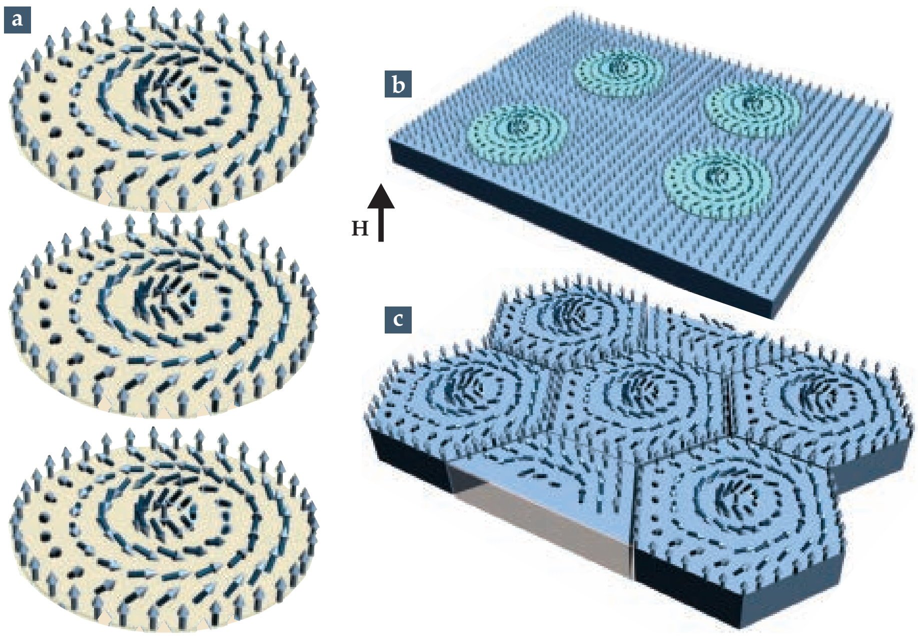

FIGURE 1. MAGNETIC SKYRMIONS are nanoscale cylinders of spinning magnetization **(a)** embedded in a ferromagnet **(b)** under an applied magnetic field **H**. The skyrmions' magnetization is antiparallel to **H** at their centers, is parallel to **H** at distances far from the centers, and rotates radially with a fixed chirality for distances between. They're known as Bloch-type skyrmions, one of the five possible configurations in uniaxial ferromagnets. For small values of **H**, isolated skyrmions condense into a hexagonal lattice **(c)**. (Courtesy of A. N. Bogdanov and C. Panagopoulos.)

Stability of magnetic skyrmions

Unlike the one-dimensional solitons described by the KdV equation, magnetic skyrmions are two-dimensional axisymmetric configurations of the magnetization (see arrows in figure 1). Solutions for 1D solitons can be derived from established mathematical methods for many nonlinear equations.[5] But theorists have proven that 2D and 3D solitons are unstable in most models. The Derrick–Hobart theorem, for example, states that skyrmions in ferromagnets should shrink and collapse to a linear singularity.

The Derrick–Hobart theorem is generally true, but it doesn't apply to models in which instabilities are eliminated by terms with higher-order spatial derivatives. In 1961 mathematical physicist Tony Skyrme, for whom skyrmions are named, introduced solutions for one case of 3D solitons—the subatomic particles called mesons and baryons.[8] Whether those multidimensional solutions described any real physical phenomena wasn't yet clear. In condensed-matter physics, for example, no obvious physical interactions are described by higher-order degrees of spatial derivatives.

Theorists later established that magnetic skyrmions emerge in magnetic compounds without inversion symmetry—that is, noncentrosymmetric crystals.[3] Chiral magnetic materials, or those with broken mirror symmetry, are a common and well-investigated group of noncentrosymmetric ferromagnets that host magnetic skyrmions. A chiral object and its mirror image have two distinguishable forms of the crystal: left- and right-handed enantiomers. The enantiomeric pair of cubic iron monogermanide, FeGe, is shown in figure 3.

In chiral ferromagnets, the underlying structure induces magnetic Dzyaloshinskii–Moriya interactions,[4] and those forces give rise to helical spatial modulations of the magnetization perpendicular to the direction of propagation **p**. Such helical strings are known as Bloch-type magnetic skymions, as shown in figure 1. In polar noncentrosymmetric ferromagnets, Dzyaloshinskii–Moriya interactions stabilize strings with magnetization rotation along the propagation direction. Those so-called Neel-type skyrmions, shown in figure 4a, are one of the five possible configurations.[3]

Dzyaloshinskii–Moriya interactions result in energy contributions composed of Lifshitz invariant functionals $L^{(k)}_{ij} = M_i(\partial M_j/\partial x_k) - M_j(\partial M_i/\partial x_k)$. Those invariants[4] are linear in the first spatial derivatives of the magnetization **M**, which produce rotating magnetization in the ij-plane and propagation along the k-axis. The $L^{(z)}_{xy}$ invariant, for example, stabilizes helices propagating along the z-axis with magnetization rotating in the xy-plane. In a cubic chiral ferromagnet, the Dzyaloshinskii–Moriya energy is

$$w_D(\mathbf{M}) = D(\mathcal{L}^{(z)}_{yx} + \mathcal{L}^{(y)}_{xz} + \mathcal{L}^{(x)}_{zy}) = D(\mathbf{M}\cdot\nabla\times\mathbf{M}).$$

The equation favors helices propagating along three spatial axes with the rotational direction determined by the sign of a constant D, which depends on the symmetry of the material. Mathematically, Lifshitz invariants violate the Derrick–Hobart theorem and stabilize 2D and 3D localized skyrmions.[3,9]

Although the term skyrmion was introduced in nuclear physics, the term has spread, and now it describes various physical phenomena in condensed matter, string theory, and particle and nuclear physics.[10] The term's wide use creates issues similar to that explained by Umberto Eco in the postscript of his novel *The Name of the Rose*: "because the rose is a symbolic figure so rich in meanings that by now it hardly has any meaning left." For skyrmions, such a wealth of meanings sometimes leads to the misunderstanding that they are a fundamental entity, similar to electrons or quarks, with shared common physical properties.

In condensed matter, skyrmions are specifically nonsingular, localized, and topologically stable configurations and distinct from singular localized states, such as disclinations in liquid crystals. Their nontrivial topology protects them from unwinding into homogeneous states, but they can collapse. The nature of magnetic skyrmions is best understood by picturing them as particle-like objects—that is, as solitons.

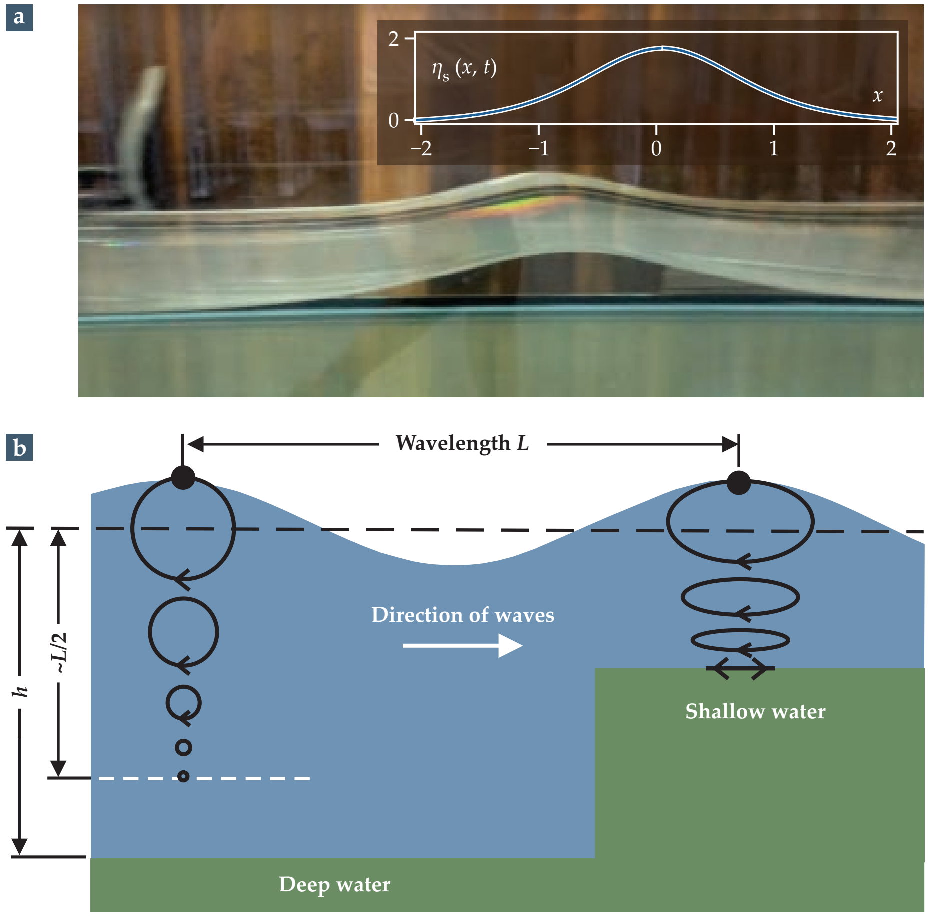

FIGURE 2. JOHN SCOTT RUSSELL'S SOLITARY-WAVE SOLITONS occur in shallow water channels, as shown in a laboratory reconstruction **(a)** of his original observation. (Adapted from ref. 6.) The inset is a typical localized solution of the Korteweg–de Vries equation for extremely shallow water. (Adapted from ref. 5.) **(b)** In deep water, waves propagate from left to right, whereas water particles orbit in circles around their average position. The diameters of the circular orbits shrink gradually with increasing distance from the surface down to half the wavelength L. In shallow waters with depth h less than $L/2$, the orbits become elliptical and essentially flat at the bottom of the tank or seabed. (Image by A. N. Bogdanov and C. Panagopoulos, adapted by Donna Padian.)

Isolated skyrmions and lattices

Experimentalists have discovered Bloch-type skyrmions in many chiral cubic helimagnets, including FeGe, manganese silicide, and copper selenium oxide.[1,2,11] Neel-type skyrmions have appeared in polar noncentrosymmetric ferromagnet gallium vanadium sulphide and in nanolayers with engineered Dzyaloshinskii–Moriya interactions.[1,11–13]

A simplified model for the energy w_0 of a chiral cubic ferromagnet in an applied magnetic field $\mathbf{H}$ is

$$w_0(\mathbf{M}) = \underbrace{A(\nabla \cdot \mathbf{M})^2}_{\text{Exchange}} - \mathbf{M} \cdot \mathbf{H} - \underbrace{D(\mathbf{M} \cdot \nabla \times \mathbf{M})}_{\text{Dzyaloshinskii–Moriya interaction}}.$$

The equation has three energy components, which contribute to the formation of magnetic skyrmions. The first ferromagnetic exchange energy term, with constant A, imposes parallel ordering of the magnetic moments. The second term, which is the interaction with the applied magnetic field, favors magnetization oriented along $\mathbf{H}$. The final Dzyaloshinskii–Moriya term induces helical modulations. The model introduces two fundamental parameters: the helix period $L_D = 4\pi A/|D|$ and the saturation field $H_D = D^2M/(2A)$ that suppresses chiral modulations.[1,9] For the two most studied cubic helimagnets, MnSi and FeGe, $L_D = 18$ nm and 70 nm and $\mu_0 H_D = 620$ mT and 359 mT, respectively, in terms of the vacuum permeability μ_0.

At high magnetic fields, minimizing the energy functional $w(\mathbf{M})$ yields isolated skyrmions in the form of weakly repulsive localized states in an otherwise uniformly magnetized state, as seen in figure 1b. They arise from a subtle balance of the competing magnetic forces. Similar to solitary waves and other solitons, isolated magnetic skyrmions manifest as internally stable, particle-like objects in a continuous medium: Numerical simulations demonstrate colliding and scattering magnetic skyrmions in narrow channels.[14]

Figure 4b plots the evolution of the skyrmion core diameter L_S as a function of an applied magnetic field. The antiparallel magnetization at the skyrmion center is energetically unfavorable in the presence of an applied magnetic field, so the

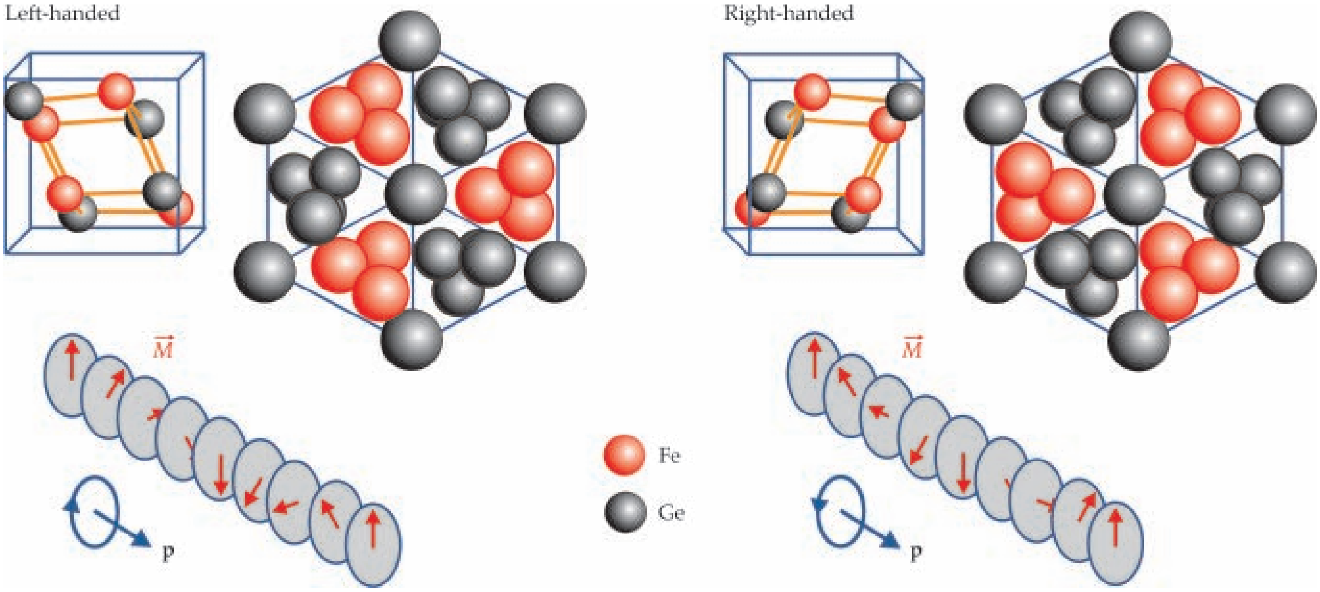

FIGURE 3. LEFT- AND RIGHT-HANDED ENANTIOMERS of chiral cubic crystal iron monogermanide do not have mirror symmetry. Magnetic interactions in FeGe stabilize Bloch-like strings of magnetization **M** with a fixed helicity relative to the direction of propagation **p**. (Courtesy of A. N. Bogdanov and C. Panagopoulos.)

skyrmion core gradually shrinks with increasing magnetic field. Below a transition field $H_S = 0.801\ H_D$, isolated skyrmions condense into a lattice, although the scenario is realized only if they nucleate. Otherwise, isolated skyrmions persist below H_S, elongate, and expand into a 1D band below an external magnetic field $H_{el} = 0.534\ H_D$, known as the elliptic instability field. Experimentally, skyrmions gradually elongate from circular to elliptic to 1D modulations in iron-palladium-iridium nanolayers in a decreasing magnetic field,[11,12] as shown in the spin-polarized scanning tunneling microscopy images in figures 4c–4g.

In model w_0, isolated skyrmions exist only in applied magnetic fields larger than the elliptic instability field. But in some highly anisotropic ferromagnetic bulk crystals and artificially synthesized magnetic nanolayers and multilayers, internal magnetic interactions can stabilize skyrmions even in the absence of an applied magnetic field,[3,11] as has been observed in FePd/Ir nanolayers.[13]

With decreasing magnetic field, isolated skyrmions (indicated by the right white square in figure 5) often transform into a lattice, usually with hexagonal symmetry. A demonstration on FeGe nanolayers, as shown in figure 5, reveals transitions between a skyrmion lattice and competing 1D phases.[9,12,15]

The flexibility to tune spin textures has led to intensive experimental and theoretical investigations in noncentrosymmetric ferromagnets and magnetic nanolayers and multilayers. A broad spectrum of unique capabilities of magnetic skyrmions has already emerged—for example, their creation, deletion, and motion using a magnetic tip.[12]

Perspective and potential technology

Magnetic skyrmions constitute a promising new direction for data storage and spintronics. They are countable objects that can be created and manipulated in, for example, layers of magnetically soft materials to develop versatile nanoscale magnetic patterns.[2,16] Skyrmions thus offer a route to localized magnetic inhomogeneities in low-coercivity materials, which are not viable for traditional magnetic recording.

Interactions similar to Dzyaloshinskii–Moriya arise in a wide range of condensed-matter systems with broken inversion symmetry. The introduction of chiral interactions in those systems provides the stabilization mechanism for solitonic states analogous to magnetic skyrmions. For example, axisymmetric solitons appear in chiral liquid crystals,[17] a state of matter thermodynamically located between an isotropic liquid and a 3D ordered solid. In ferroelectrics, which display spontaneous electric polarization, layered oxide architectures host emerging magnetic solitons.[18] Noncentrosymmetric condensed-matter systems broadly form a class of materials with multidimensional solitonic states.[9]

For condensed-matter physicists, the Dzyaloshinskii–Moriya interaction in particular offers a playground for investigations that only require a lack of inversion symmetry. In addition to naturally occurring systems, such as chiral cubic helimagnets, researchers can engineer a structure that cannot be inverted—for example, the interface between two materials. The interface between a ferromagnet and a strong spin-orbit metal gives rise to tunable-strength Dzyaloshinskii–Moriya interactions, which vary with the material selection.[1,2,16] The interfacial effects can even dominate if the ferromagnet is sufficiently thin.

The flexibility to design the host and tune the skyrmion properties offers versatility for technological applications. Skyrmion-based devices have the potential to store and process information in unprecedentedly small spaces.[1,2,14,16] The presence or absence of a skyrmion could serve as a 1 or 0 in a data bit for racetrack memory, and multiple skyrmions could aggregate to form storage devices. The states of such devices could be modulated by an electric current that drives skyrmions in and out of the devices, analogous to biological synapses. The

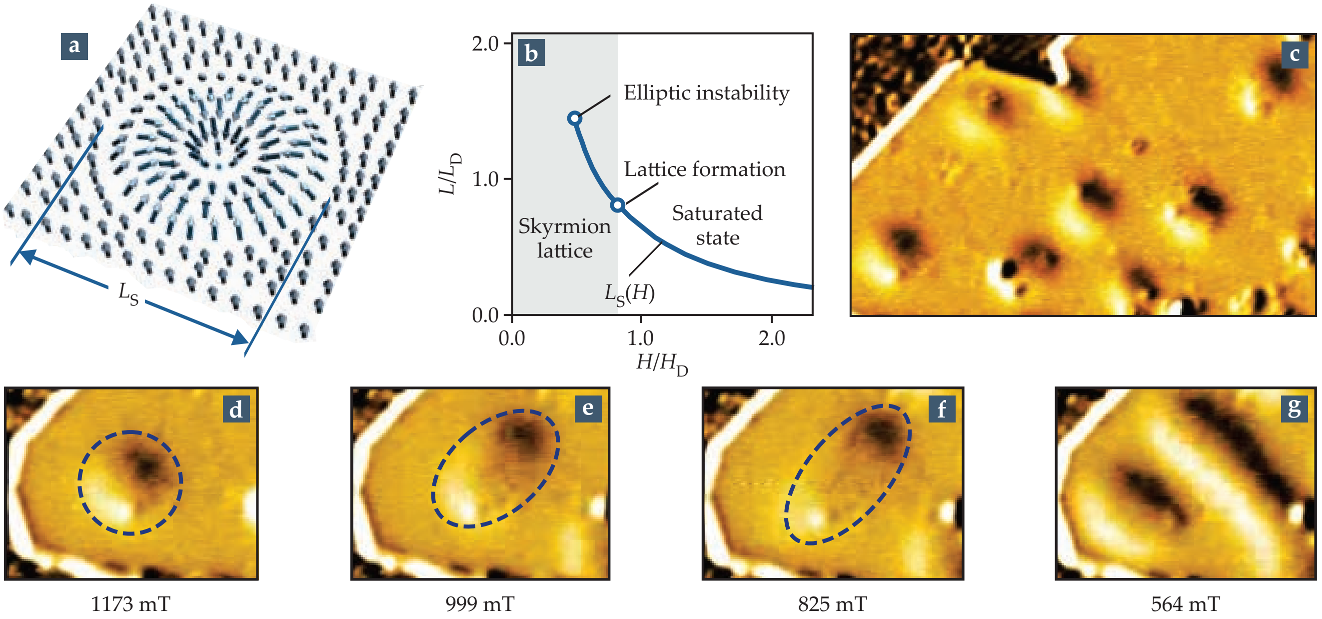

FIGURE 4. ISOLATED NEEL-TYPE SKYRMIONS (a) have magnetization rotating along the direction of propagation. **(b)** The calculated skyrmion diameter L_S shrinks as the applied magnetic field increases. The characteristic parameters L_D and H_D are the helix period and saturation field, respectively. **(c)** Skyrmions in an iron-palladium-iridium nanolayer are isolated at an applied magnetic field $\mu_0 H = 1280$ mT. With decreasing magnetic field, a skyrmion (circled) deforms into an ellipse and terminates as a one-dimensional modulation **(d–g)**. (Adapted from ref. 11.)

devices could thus potentially perform neuromorphic pattern-recognition computing.

Researchers have already engineered interfacial skyrmions in magnetic multilayers at up to room temperature.[16] Those skyrmions offer an opportunity to bring topology into consumer-friendly nanoscale electronics. In the magnetic multilayers, exotic skyrmion configurations also form under the combined influence of chiral interactions and magnetodipolar effects. Such skyrmion hybrids present a novel class of localized states that have yet to be explored in depth.

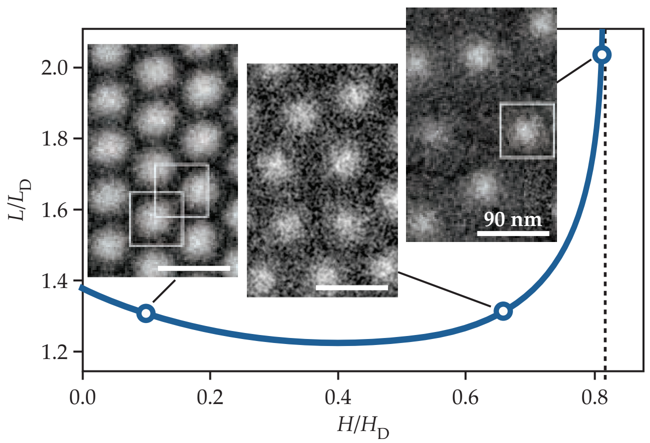

FIGURE 5. A HEXAGONAL SKYRMION LATTICE evolves in the presence of weaker applied magnetic fields in materials that allow nucleation. The calculated size L of the skyrmion cell varies with the reduced applied magnetic field, H/H_D. The characteristic parameters L_D and H_D are the helix period and saturation field, respectively. The insets are three electron holography images of skyrmion lattices in a thin layer of iron monogermanide for different applied magnetic fields—from left to right, 100 mT, 350 mT, and 400 mT. The white squares indicate individual skyrmions. (Adapted from ref. 15.)

But there are still fundamental properties to investigate, such as the wave–particle duality of skyrmions, their interaction with other magnetic textures, and skyrmion lattices as magnonic crystals. The interaction between magnetic skyrmions and light or other topological excitations—for example, superconducting vortices—could also lead to new exotic states of matter. Investigating those topics will require new material architectures and advancements in characterization techniques.

REFERENCES

1. R. Wiesendanger, *Nat. Rev. Mater.* **1**, 16044 (2016).
2. A. Fert, N. Reyren, V. Cros, *Nat. Rev. Mater.* **2**, 17031 (2017).
3. A. N. Bogdanov, D. A. Yablonskii, *J. Exp. Theor. Phys.* **68**, 101 (1989).
4. I. E. Dzyaloshinskii, *J. Exp. Theor. Phys.* **19**, 960 (1964).
5. M. Remoissenet, *Waves Called Solitons: Concepts and Experiments*, 3rd ed., Springer (1999).
6. N. Pizzo, "Shallow water wave generation," www.youtube.com/watch?v=w-oDnvbV8mY.
7. N. J. Zabusky, M. D. Kruskal, *Phys. Rev. Lett.* **15**, 240 (1965).
8. T. H. R. Skyrme, *Proc. R. Soc. A* **260**, 127 (1961).
9. U. K. Rößler, A. N. Bogdanov, C. Pfleiderer, *Nature* **442**, 797 (2006).
10. G. E. Brown, M. Rho, eds., *The Multifaceted Skyrmion*, World Scientific (2010).
11. A. O. Leonov et al., *New J. Phys.* **18**, 065003 (2016).
12. N. Romming et al., *Science* **341**, 636 (2013).
13. S. Meyer et al., *Nat. Commun.* **10**, 3823 (2019).
14. A. Fert, V. Cros, J. Sampaio, *Nat. Nanotechnol.* **8**, 152 (2013).
15. A. Kovács et al., *Appl. Phys. Lett.* **111**, 192410 (2017).
16. A. Soumyanarayanan et al., *Nature* **539**, 509 (2016).
17. P. J. Ackerman et al., *Phys. Rev. E* **90**, 012505 (2014).
18. S. Das et al., *Nature* **568**, 368 (2019). PT

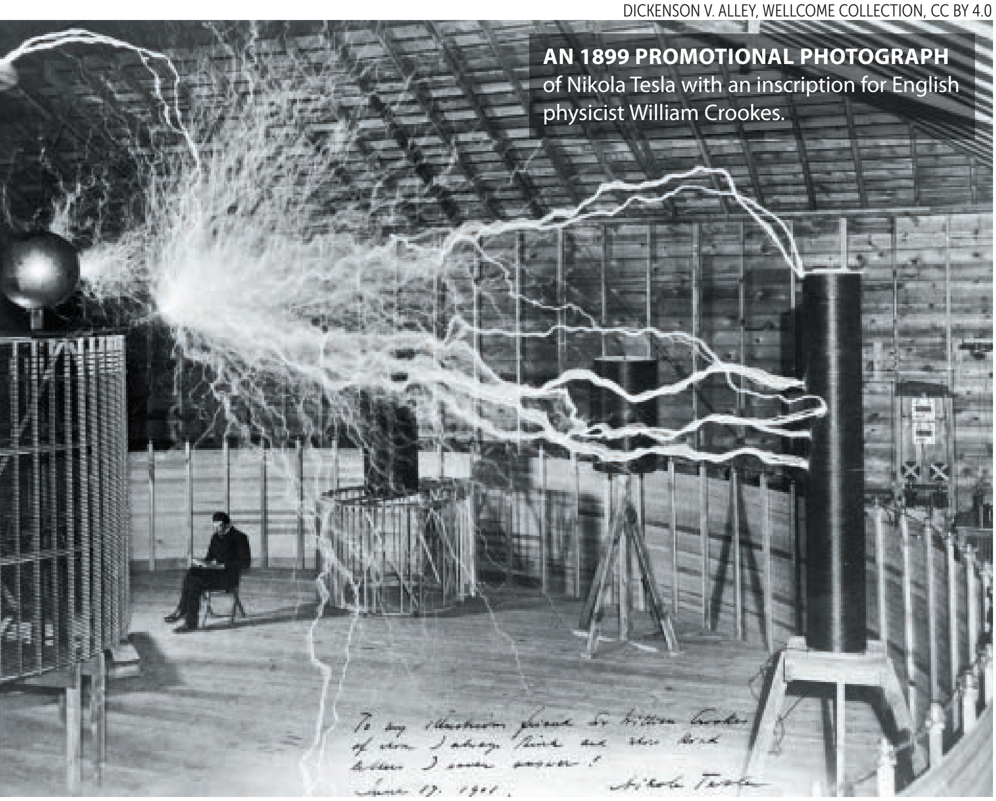

AN 1899 PROMOTIONAL PHOTOGRAPH of Nikola Tesla with an inscription for English physicist William Crookes.

Nikola Tesla, a man of his time

Today, a futuristic electric car carries the name Tesla in honor of a man who, more than a century ago, imagined transforming the world. Nikola Tesla was an electrical engineer notable for his innovative work on alternating current (AC) power distribution systems, polyphase motors, and induction coils. Many biographies of Tesla written after his death in 1943, such as Margaret Cheney's *Tesla: Man Out of Time* (1981), paint him as an esoteric genius and a neglected underdog out of step with the cutthroat entrepreneurial culture of the Victorian era. Is this a true portrait of the man or a caricature?

In *Nikola Tesla and the Electrical Future*, historian of science Iwan Rhys Morus examines this "man of apparent contradictions" in the context of the cultural and technological revolutions of the late 19th century. The book includes an extensive bibliography and endnotes; the author clearly is an authority on the history of electrical technology. Morus convincingly dispels the image of Tesla as a man out of time and replaces it with a more realistic view of a brilliant inventor who was nevertheless the product of his era, his interests and activities shaped by the world in which he lived.

Nikola Tesla and the Electrical Future

Iwan Rhys Morus
Icon Books, 2019. $22.95

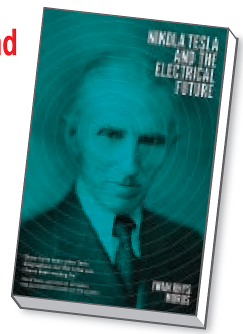

Morus's journey into the world of Nikola Tesla has five parts. The first, "The Electrical Century," describes how the Industrial Revolution influenced Tesla from his early childhood in Croatia through his college years and up to his first job at Thomas Edison's incandescent bulb factory in Paris. Part 2, "Battle of the Systems," recounts Tesla's decision to come to the US to work in Edison's laboratory. Tesla had viewed Edison as a hero, but that hero worship quickly soured and was replaced by a new conviction that he alone was responsible for his destiny as an inventor.

Morus delves into the famous AC/DC controversy, which pitted Edison's preferred direct current (DC) distribution against Tesla's more stable AC system, and explains the roles that both Tesla and businessman George Westinghouse played in the conflict with Edison. Although Edison initially gained ground by instilling unwarranted fear in the public's eye about the dangers of AC, its technological superiority, lower cost, and more manageable safety risks would eventually enable AC systems to flourish.

In part 3, "Scientific Showman," Morus examines Tesla's epiphany that being an inventor required business savvy and self-promotional efforts in addition to new ideas. The author describes Tesla's involvement with a successful hydroelectric power plant at Niagara Falls in New York and his public lectures at international exhibitions where he became known as a master showman, able to exploit the power of spectacle to promote his ideas. However, Tesla's dream of limitless power distribution and worldwide communications via Earth's crust, as Morus shows in part 4, "Selling the Future," ended in dismal failure when his massive communications tower, the Wardenclyffe, failed to produce the breakthroughs for which he had hoped. The book concludes with an examination of Tesla's life, his prognostications, and his posthumous image in the final part, "Visions of Tomorrow."

Morus's argument that Tesla was a product of his time is carefully developed and supported with clear and convincing evidence. Tesla lived in a world where the wonders of electricity appeared boundless. The grand exhibitions of the day provided a glimpse into the future for everyone to see, and larger-than-life personalities like Edison were the iconic figures whom many, including Tesla, sought to emulate. But Tesla quickly discovered that he wasn't the type of person who collaborated well with others—he wanted to control the outcome of his visions. Succeeding as an inventor, however, required him not just to make new things, but to sell a vision of the future to those who had the money to back him. Morus shows the reader how Tesla learned from his experiences and crafted an image as an iconic, eccentric inventor through his showmanship and connections with the media.

Morus emphasizes that Tesla was a great inventor with a gift for visualizing new apparatuses and accurately imagining how a new instrument would work in response to various stimuli. But *Nikola Tesla and the Electrical Future* also shows that the man was not a traditional scientist or engineer. He appreciated only his version of the future and downplayed major breakthroughs by others; for instance, he dismissed the "illusion of Hertzian waves" and declared that "there is no such element as Radium." Furthermore, although Tesla's visions always held great promise for the future of society, they often lacked the details necessary to make his imagined future a reality.

Nikola Tesla and the Electrical Future is not simply another biography of Tesla, but rather, a scholarly study of him in the context of his place and time. In a seamless and comprehensive narrative, Morus successfully weaves together Tesla's personal life with the cultural influences that shaped it and illuminates a very complex person. The clear and engaging writing is a pleasure to read. Although the book was written for a general audience, it would also serve nicely as supplemental reading in a course on the history of technology.

Morus concludes the book by examining how our ideas about the art of invention have and have not changed since Tesla's day. The melding of invention with business has strengthened over the years, while the role of individualism has waned. Nonetheless, inventiveness—the cornerstone of Tesla's life and afterlife—can have far-reaching and perhaps unintended consequences. There is an important lesson here for all of us.

Richard Bradley
National Radio Astronomy Observatory
Charlottesville, Virginia

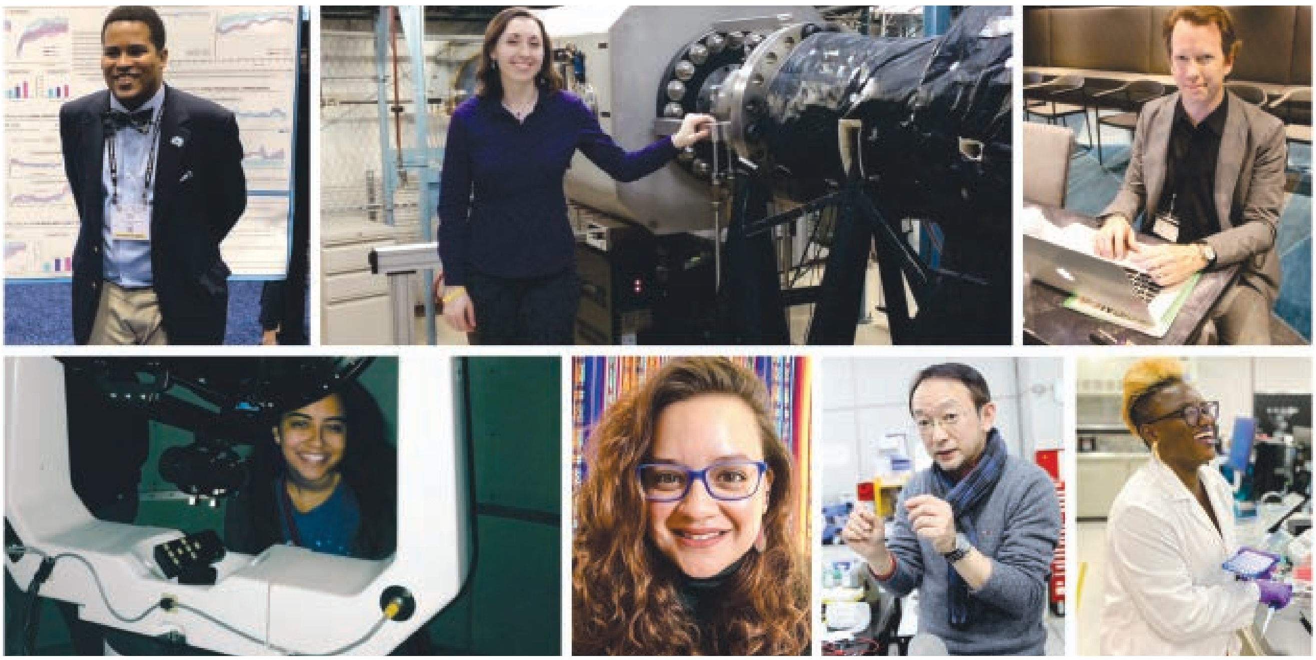

A COLLAGE OF REAL SCIENTISTS—and just one tie. Clockwise from top left: Jared Boyce, Nicole Sharp, Sean Carroll, Danielle Twum, Yeom Han-Woong, Ximena Cid, and Suchi Narayanan. (Photo of Nicole Sharp by Kelley Sharp; Sean Carroll by Sgerbic, CC BY-SA 4.0; Danielle Twum by Susana Jett; Yeom Han-Woong by Rickinasia, CC BY-SA 4.0; and Suchi Narayanan by Orion Lyau. All others provided by their subjects.)

Essays from a career in science writing

Real Scientists Don't Wear Ties
When Science Meets Culture
Sidney Perkowitz
Jenny Stanford Publishing, 2019. $29.95

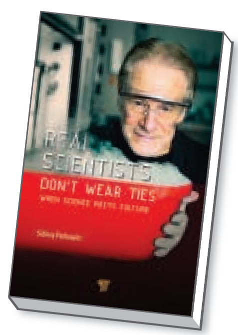

How can scientists share their insights with laypeople in a way that encourages audience members to reframe their perspective? Sidney Perkowitz, a popular science writer and professor of solid-state physics, has been attacking that question from all angles since his retirement from academia in 1990. His new book *Real Scientists Don't Wear Ties: When Science Meets Culture* is an anthology of 50 essays he wrote between 1989 and 2018. The pieces are diverse in form and subject; articles explaining research concepts and technological innovations sit beside musings on science's relationship with art and society. Over the course of the collection, Perkowitz triumphs, entertains, and stumbles, illustrating the full breadth of his career writing for the public.

Real Scientists Don't Wear Ties has

three sections—Science, Technology, and Culture—which could be read independently but also flow well if read continuously. In the first, Perkowitz breaks down scientific ideas from quantum entanglement to the meaning of the fundamental constants. Each article stands alone, but all describe complicated ideas for an audience of nonscientists. The book ends up repeating explanations of major concepts such as quantum principles, particle physics, and gravitation, although Perkowitz's prose contains enough vivid metaphors to keep the reading enjoyable. For instance, one stellar essay draws parallels between the ancient four elements—earth, air, water, and fire—and the modern understanding of materials science; it shows how Greek and Enlightenment philosophers were right and wrong about our universe. Here and elsewhere, Perkowitz balances gradual pacing for learners with getting to the point for more knowledgeable readers.

The middle section, Technology, transitions from raw science to real-world application and touches on topics from space travel to artificial intelligence to genetic engineering. Standout essays include an ambitiously concise cultural history of lasers and a personal tale of cataract surgery—a story linked to the lives of artists like Monet, who could paint into old age because of advancing medical technology. In his musings, Perkowitz doesn't shy away from politically thorny topics. One piece tracks eugenics from Nazis to the sci-fi film *Gattaca*; another one, discussing predictive policing by computer algorithms, includes interviews with police officers, software developers, and civil rights activists. Even on controversial topics, Perkowitz delivers valuable and nonpartisan information. He shows how new technology can change society and why we all ought to be aware of applications on the horizon.

Perkowitz is at his loftiest in the last section, Culture, which covers wide ground from humor to fine art to popular media. These final essays draw freewheeling parallels between scientific and artistic perspectives, analyze scientific realism in movies, and discuss the development of genres like science fiction. No matter your feelings about how science is portrayed in pop culture, there's no question that the average person hears more about science through media channels than from scientists themselves. Perkowitz lays out how society (mis)understands research and researchers, which helps us in the physics community relate to our audience and address possible misconceptions immediately.

Given the chronological span of this anthology, it's no surprise some essays have aged poorly. The title essay, "Real Scientists Don't Wear Ties" (1991), on how scientists "reveal themselves by their dress," is the oddest in that regard. I can swallow—wincingly—the title, an out-of-context quote from a woman describing a physics conference crowd. What reads more crudely, after a long exposition about beards and pocket protectors, is a gendered reference to female physicists' clothing. Perkowitz writes that though women "suffer in their choices for insignia of rank," they often communicate "nuances of position and success to other women" through jewelry. Nearly three decades later, physics is marginally more gender balanced, and happily we are also more receptive to a wider range of gender expressions. Female, non-binary, and male physicists are now more welcome to be "real scientists" in whichever choices of dress they prefer.

Such dips are contextualized by glimmers of self-importance, such as the author's self-portrait cover and the almost boastful material in the foreword. Furthermore, although the content of *Real Scientists Don't Wear Ties* is diverse, the collection can feel repetitive. Most of the essays have a structure derived from the recipe Perkowitz outlines in the introduction: They start with an anecdote, move to "a look at the history of the subject," and include "plentiful application of metaphor." Still, for scientists trying their own hand at public communication, Perkowitz's style is a good one to study.

The book's grandiose yet comprehensive overviews of science topics bring to mind another recent book, *Liquid Rules: The Delightful and Dangerous Substances That Flow Through Our Lives* (2019) by materials scientist Mark Miodownik (see the review by Michelle Driscoll, PHYSICS TODAY, August 2019, page 54). That book also explains a wealth of scientific concepts, but uses the theme of examining liquids on an airplane to make the topics cohere into a single narrative. In comparison, *Real Scientists Don't Wear Ties* feels scattered at times. However, readers of all backgrounds will still benefit from the engaging prose in Perkowitz's diverse collection. Let us hope that if more physicists read this book, more of us will be convinced to distill our own research and ideas into writing for public consumption.

Brian Kraus
Princeton University
Princeton, New Jersey

NASA/JPL/ASU

A descriptive overview of astronomy

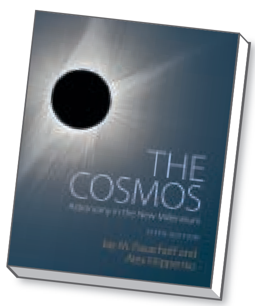

The Cosmos
Astronomy in the New Millennium
Jay Pasachoff and Alex Filippenko
Cambridge U. Press, 2019 (5th ed.). $79.99 (paper)

Introductory astronomy is one of the most popular general education STEM (science, technology, engineering, and mathematics) classes at colleges and universities. Most students who enroll in it are nonscience majors, and astronomy is the last, or perhaps only, college-level science course they will ever take. *The Cosmos: Astronomy in the New Millennium*, now in its fifth edition, offers a descriptive presentation of astronomy with that audience in mind. Authors Jay Pasachoff and Alex Filippenko are accomplished astronomers, celebrated educators, and champions of science popularization. Their experience communicating science to nonprofessionals is evident in the updated edition of *The Cosmos*, a comprehensive, easy-to-read survey of astronomy appropriate for use in a general-education science course.

The diverse array of topics presented in *The Cosmos* allows professors great flexibility when using the book in their courses. The text could be assigned for either a one-semester survey course emphasizing selected topics or a two-semester introductory sequence using the entire book. The first few chapters cover general ideas about the nature of astronomy, light, telescopes, celestial motions, and gravity. The book moves on to a grand tour of the universe, beginning with Earth and moving outward through space and introducing readers to topics such as stars, stellar evolution, black holes, galaxies, and cosmology. The newest edition includes recent developments such as the results of the New Horizons mission to Pluto and Ultima Thule, the 2017 total solar eclipse, gravitational wave detections, and the Kepler and TESS missions—additions I appreciate.

To help students engage with the material, the authors have included several interesting pedagogical features, such as the "Star Parties" and "Lives in Science" boxes interspersed throughout the text. "Star Parties" boxes contain observational exercises related to the material. For example, students are instructed on how they could re-create Galileo's observations with a small telescope or track the motion of Jupiter and Saturn through the sky over the course of several days. Those features encourage students to connect to the material outside the classroom.

As the name suggests, "Lives in Science" boxes provide short biographies about notable scientists. I think they have the potential to foster an inclusive classroom atmosphere by portraying scientists as real people; biographical stories help students feel that they, too, can make meaningful contributions to science. I was therefore surprised to find that only six individuals were featured: Nicolaus Copernicus, Tycho Brahe, Johannes Kepler, Galileo Galilei, Isaac Newton, and Albert Einstein. I am disappointed that the book did not include stories of more recent and diverse scientists.

Furthermore, although the authors successfully provide a descriptive presentation of astronomy, I have concerns about some gaps and omissions in the text. *The Cosmos* occasionally lacks depth, and the choices of key terms are not always carefully thought through. For example, the concepts of continuous spectra and absorption lines are well developed, and both terms appear in boldface for easy identification. However, the authors do not provide the same level of description for the equally important emission lines; the text mentions them only briefly and does not put the term in bold. Similarly, the beginning of the section describing the appearance of the Moon reads, "Even binoculars reveal that the Moon's surface is pockmarked with craters. Other areas, called maria […], are relatively smooth and dark." That description makes no mention of the lunar highlands, a major feature of the Moon's appearance. Such inconsistencies and omissions in the coverage of important terms are troubling.

The authors do an excellent job of using figures and photographs to aid in the explanation of concepts and hold students' interest. However, not all of the images are well presented or pedagogically useful. Several pictures are grouped into multipart figures with one overwhelmingly long caption describing the set. In many instances, the captions contain more information about the concept than the text itself. Although I appreciate the number of images, I wish some of them were better incorporated into the text.

Astronomy educators often debate the appropriate amount of quantitative material for an introductory astronomy course. Pasachoff and Filippenko acknowledge that many instructors will prefer a more mathematical description of the universe's physical processes than the one provided in their book. I view astronomy as a quantitative science, and *The Cosmos* includes too little math for my taste. If you are looking for an introductory astronomy textbook that includes a significant quantitative component, then this is not the book for you.

Overall, *The Cosmos* provides an excellent tour of the universe for those interested in a qualitative description of a broad array of topics in astronomy. Several features will encourage student engagement and allow instructors in diverse astronomy classes to customize their use of the text. However, the textbook occasionally lacks sufficient depth. I would suggest that instructors looking for more than a basic overview consider supplementing *The Cosmos* with deeper discussions of physical phenomena and quantitative ideas.

Kristen Thompson
Davidson College
Davidson, North Carolina

NEW BOOKS & MEDIA

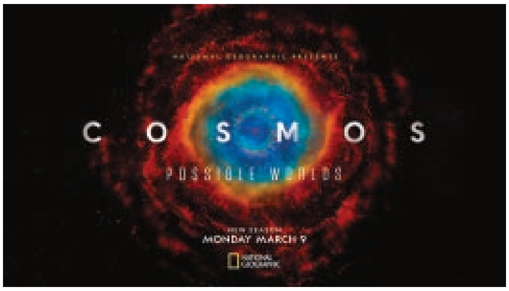

Cosmos
Possible Worlds

Neil deGrasse Tyson (host) and Ann Druyan (executive producer)
Cosmos Studios, 2020 (3rd season)

In its third season, the successor to Carl Sagan's celebrated 1980s *Cosmos* series tackles nothing less than humanity's future, discussing themes and concepts related to space exploration, human evolution, and climate change. As in previous seasons, the show's visual style blends colorful animations, live-action reenactments, beautiful nature cinematography, and 3D renderings of spaceships and cities in imagined futures. Some episodes have a sci-fi feeling to them as they paint hopeful pictures of humans in space. Others, such as a spotlight on persecuted geneticist Nikolai Vavilov, focus more on science's past. Host Neil deGrasse Tyson narrates. The first episode of the new season will air Wednesday, 9 March, on the National Geographic Channel; episodes will also air on the FOX network later this year. —MB

Marie Curie and Radioactivity

Jordi Bayarri
Graphic Universe/Lerner Publishing, 2020. $8.99 (ebook)

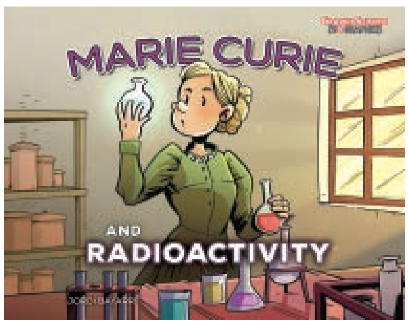

One of a series of graphic science biographies offered by children's book publisher Lerner, *Marie Curie and Radioactivity* is a 30-page visual narrative relating the life of the celebrated physicist, chemist, and multiple Nobel laureate. Written and illustrated by cartoonist Jordi Bayarri, the book includes a timeline, glossary, list of resources, and index. The image-heavy format, which is aimed at readers ages 10–14, is intended to be both entertaining and educational. To ensure historical and scientific accuracy, Bayarri consulted science historian Tayra Lanuza. Other physicists covered in the series include Albert Einstein and Isaac Newton. —CC

The Expanse

Amazon Prime Video
Alcon Entertainment/Sean Daniel Company, 2019 (4th season)

This sci-fi television series based on James S. A. Corey's popular novels imagines a future in which humans live not only on Earth, but in domes on Mars and on space stations in the Kuiper Belt. Those in the Belt have adapted to low gravity but still face limited air and water, communication lags, and the menace of a mysterious life form known as the protomolecule. As season 4 opens, an extraordinary new discovery has enabled humans to travel to potentially habitable exoplanets, but tensions between Earthers, Martians, and Belters are still running high as factions compete for land and resources on a newly discovered world. *The Expanse* offers a grittier and more grounded vision of humans in space than utopian takes like *Star Trek*, and the show's writers make smart use of planetary science to build their stories. *Torchwood* alum Burn Gorman joins the cast as ruthless security officer Adolphus Murtry. —MB

The Joy of x

Steven Strogatz, host
Quanta Magazine, 2020

In this informative podcast from *Quanta* magazine, applied mathematician Steven Strogatz interviews scientists about their work. Each episode is a freewheeling, hour-long conversation about career path, current projects, and interests outside science. Strogatz's enthusiasm and curiosity make him an ideal host; he will frequently ask a guest to explain an interesting turn of phrase or to dig deeper into an intriguing concept. Early episodes feature cosmologists Priya Natarajan and Brian Keating, neurobiologist Cori Bargmann, and psychologist Brian Nosek. New installments are released weekly on Wednesdays. —MB

How Cosmologists Explain the Universe to Friends and Family

Karim A. Malik and David R. Matravers
Springer, 2019. $29.99 (paper)

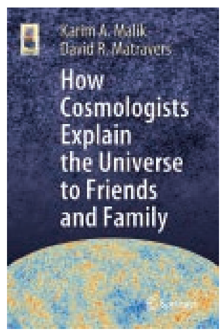

How did the universe begin, and how did it evolve to look as it does today? Those are just some of the questions addressed by theoretical cosmologists Karim Malik and David Matravers in this overview of modern cosmology. Their aim, they say, is to explain their highly complex area of research as thoroughly as possible to readers who may not have a math or physics background. They begin with a discussion of the scientific method before moving on to recent observations, the astronomical tools used to make them, what constitutes normal and exotic matter, and the forces that shape the universe. Then they take the reader on a journey back in time to the very beginning. Images, drawings, tables, and diagrams supplement the text. —CC PT

AMERICAN PHYSICAL SOCIETY SEEKS NEW CEO

The American Physical Society (APS) seeks a compelling leader with top-level management experience as its next CEO to create a high-performance culture that inspires members, staff, and the broader physical sciences community.

The APS is a strong and successful 501(c)(3) nonprofit membership corporation, headquartered in College Park, Maryland with offices in Ridge, New York and in Washington, DC. The new CEO will advance the mission of the world's leading physics professional society with a budget of $68 million, leading and managing more than 55,000 members and 250 staff.

The ideal candidate is excited by the evolution of scientific discovery and research dissemination, the changing scientific publishing landscape, and opportunities to ensure long-term sustainability of the Society. They will address membership growth and retention, effective meeting strategies, and will further strengthen APS through collaboration with scientists and staff at all levels of the profession. The successful CEO will:

- Possess excellent management, strategic, communication, and diplomacy skills
- Advance and diffuse the knowledge of physics
- Engage, support, and further energize an active, multidisciplinary, and diverse membership
- Advance scientific discovery and research dissemination through world class journals and meetings
- Advocate for physics and physicists, amplifying the voice for science
- Promote effective physics education at all levels
- Promote opportunities for underrepresented groups, valuing diversity, inclusion, and equity
- Bring their own vision and values to a highly functioning strategic framework, implementing initiatives through clear business processes, goals, and resource allocation

The top candidate will be a qualified scientific leader with knowledge of the U.S. legislative process, science policy, and global scientific collaboration. They will have experience with the needs of diverse, multidisciplinary audiences and appreciate the intricacies of working with member-elected governing bodies. They will manage, lead, and inspire staff and members to accelerate organizational change and resilience.

Jackie Eder-Van Hook, PhD, President, Transition Management Consulting, Inc. is conducting this search for APS. Interested candidates should read the Organizational and Candidate Profile at www.TransitionCEO.com/careers and submit their cover letter, resume, and salary expectations as soon as possible, but not later than **Thursday, April 30, 2020**. Questions should be mailed to **APS2020_Search@TransitionCEO.com**.

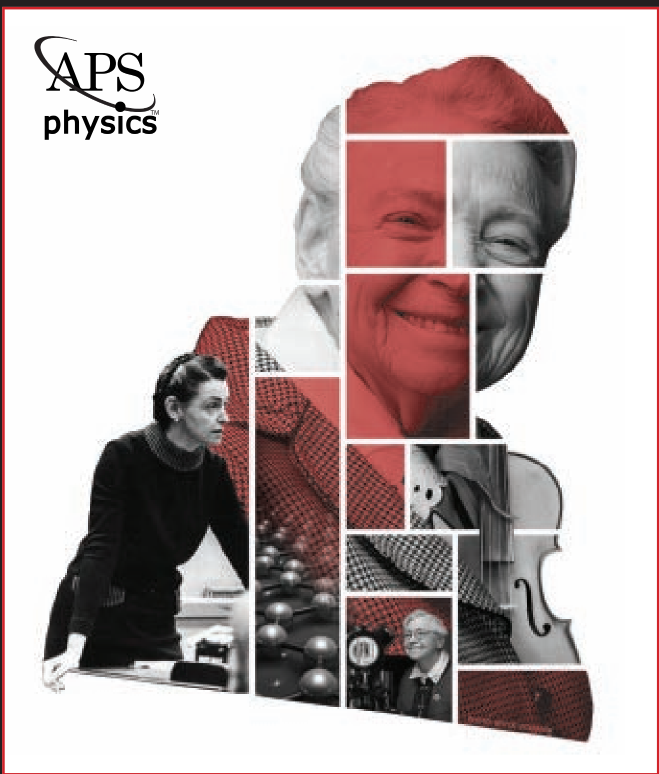

MILLIE DRESSELHAUS

Fund for Science and Society

Created by the American Physical Society to honor the remarkable scientific career and community legacy of the late Millie Dresselhaus.

To learn more, please visit go.aps.org/dresselhaus

or contact Mariam Y. Mehter, APS Campaign and Donor Relations Manager at (301) 209-3639 or mehter@aps.org.

NEW PRODUCTS

Focus on test, measurement, and data acquisition

The descriptions of the new products listed in this section are based on information supplied to us by the manufacturers. PHYSICS TODAY can assume no responsibility for their accuracy. For more information about a particular product, visit the website at the end of its description. Please send all new products submissions to ptpub@aip.org.

Andreas Mandelis

PCB efficiency testing device

Keysight designed its i3070 Series 6 in-circuit test (ICT) suite to improve the throughput and operational efficiency of printed circuit board assembly (PCBA) manufacturing. The i3070 Series 6 ICT supports a wide range of PCBA sizes for applications that include the internet of things, 5G wireless technology, and the energy industry. According to the company, the i3070 features the shortest signal path between measurement circuitry and devices under test. That minimizes parasitic capacitance, cross-talk interference, and stray signal coupling and thereby facilitates delivery of consistent, repeatable measurements. Up to 4× faster boundary scan, silicon nails, and dynamic flash programming optimize test efficiency and throughput. Certified machine-to-machine capabilities reduce response times and operating expenses and improve test-data insights. ***Keysight Technologies***, *1400 Fountaingrove Pkwy, Santa Rosa, CA 95403-1738, www.keysight.com*

High-amplitude signal generators

Spectrum Instrumentation has added six arbitrary waveform generators (AWGs) to its M2p.65xx series of PCIe cards. The new AWGs extend the product family's capabilities by boosting the available output range, so that waveforms can be generated with amplitude swings of up to ±12 V into 1 MΩ or ±6 V into 50 Ω. To achieve the higher output voltage ranges, the cards have been fitted with additional amplification and larger cooling plates. The slightly wider cards occupy two PCIe slots, but they are just 168 mm long and can fit into almost any PC. The M2p.65xx series AWGs use the latest 16-bit digital-to-analog converters and feature a fast PCIe ×4 interface with up to 700 MB/s streaming speed. Users can select output speed rates of either 40 MS/s (M2p.654x series) or 125 MS/s (M2p.657x series) and models with one, two, or four channels per card. ***Spectrum Instrumentation Corp***, *401 Hackensack Ave, 4th Fl, Hackensack, NJ 07601, https://spectrum-instrumentation.com*

Fourier-transform IR imaging microscope

Bruker's Lumos II Fourier-transform IR imaging microscope provides ultrafast data acquisition in mapping and focal-plane array imaging modes. The Lumos II can identify particles, determine coatings and contaminations, and reveal polymeric compositions. According to the company, it delivers excellent results in transmission and reflection and attenuated total reflection measurements. The fully automated, software-controlled microscope features an easily accessible sample stage. The retractable crystal is controlled by high-precision piezoelectrical motors and integrated into the lens to give a clear view of the sample. The Lumos II offers a very large field of view and spatial resolution of 0.6 μm/pixel. It is suitable for use in quality control and failure analysis in many fields, including polymers, electronics, and pharmaceuticals, and for life sciences and forensics applications. ***Bruker Optics Inc***, *40 Manning Rd, Billerica, MA 01821, www.bruker.com*

Photoelastic modulator controller

Hinds Instruments has introduced the PEM-200 all-in-one controller for its photoelastic modulators. The device's primary function is to control the peak retardation of the photoelastic modulator optical head. In the past, that was an analog circuit with an electronic head. The new digital PEM-200 sets the transducer vibration amplitude and thus the strain amplitude in the optical element. It improves over its predecessor by providing a 50/50 duty cycle, a simplified connection (dual SMA cables from optical head to controller), USB 2.0 communication, and a low 1.7 W power requirement. The new controller has the same polarization purity, stability, and sensitivity as the previous model, and old PEM optical heads can be used with it. ***Hinds Instruments Inc****, 7245 NE Evergreen Pkwy, Hillsboro, OR 97124, www.hindsinstruments.com*

Large-aperture pulsed-laser-energy sensor

MKS Instruments, which includes Ophir-Spiricon, has announced the Ophir L2000W-PF-120 water-cooled laser power and energy sensor for measuring large pulsed lasers. The thermal sensor measures powers of 1–2000 W and energies of 6–6000 J over the spectral range of 0.3–2.2 μm. It features a large 120 mm aperture to accommodate high energy densities and short pulses. A fast 7 s response time allows the device both to measure fast drifts and instabilities and to handle high energy levels. The L2000W-PF-120 laser sensor is designed for use with large-diameter pulsed nanosecond or picosecond lasers. To address the optical damage that such short pulses can induce, the sensor features Ophir's PF-type volume absorber, which can withstand higher average energies and energy densities of up to 3 J/cm^2. ***Ophir-Spiricon LLC****, 3050 N 300 W, North Logan, UT 84341, www.ophiropt.com*

Inductive plasma-spectrometry system

Agilent has announced new inductively coupled plasma–optical emission spectrometry (ICP-OES) systems with patent-pending free-form optics. According to the company, the 5800 and 5900 models are the smallest and fastest ICP-OES systems available. They incorporate novel instrument intelligence that can deliver insight into samples, processes, and operational status. Sensors linked to software tools guide laboratory users through analyses, help them avoid unplanned downtime, and reduce their need to remeasure samples. The ICP-OES systems are suitable for users at all expertise levels in laboratories serving the environmental, food, energy, chemical, and materials fields. ***Agilent Technologies Inc****, 5301 Stevens Creek Blvd, Santa Clara, CA 95051, www.agilent.com*

Compact quadrupole analyzer

Hiden's pQA portable gas analyzer is a versatile mass spectrometer with interchangeable sampling inlets. It can be used in a broad range of applications, including gas analyses in which sample volume is small and environmental analyses that require detection of low concentration levels. The lightweight pQA system allows high-sensitivity, high-dynamic-range multigas analysis by mass spectrometry (MS) to be performed in the field, on riverbanks, at sea, and in the laboratory. Membrane-introduction MS inlets enable analysis of dissolved species in groundwater, fermentation cultures, soil samples, and other applications that require dissolved species in liquid samples. The pQA system has a mass range of 200 amu and sub-ppb detection levels. An extended mass range to 300 amu is optional. ***Hiden Analytical Inc****, 37699 Schoolcraft Rd, Livonia, MI 48150, www.hidenanalytical.com*

High-speed IR detection module

Boston Electronics, through its partner Vigo System SA, now offers the UHS-M high-performance, high-bandwidth IR detector and preamplifier module. The UHS-M features a minimum 1 GHz bandwidth, detector sensitivity of 3–11+ μm, and a high signal-to-noise ratio. According to the company, it is easy to use. Applications include fast pulsed-laser measurements, dual-comb spectroscopy, heterodyne detection, and free-space optical communication. The UHS-M module is contained in one compact package with the IR detector, preamplifier, thermoelectric cooler controller, and power supply. It is equipped with two analog signal outputs: AC–main broadband and DC–DC. ***Boston Electronics Corporation****, 91 Boylston St, Brookline, MA 02445, www.boselec.com*

Radiometric power and energy measurement

Gamma Scientific has released its UDT series of enhanced radiometric sensors. According to the company, the sensors deliver highly accurate results, including femtoamp-level sensitivity for ultralow-light measurement. Configuration options include miniature, low-profile, blue- and UV-optimized, indium gallium arsenide, and cooled sensors for a wide variety of applications ranging from 190 nm to 1750 nm. With rise times to 1 μsec, pulsed-energy measurements are also possible. Most configurations can easily be combined with the Gamma Scientific range of integrating spheres and other full test solutions for laboratories, production-line testing, and OEM use. All products feature NIST-traceable calibration. ***Gamma Scientific****, 9925 Carroll Canyon Rd, San Diego, CA 92131, www.gamma-sci.com*

Wideband digitizer for RF applications

The ADQ7WB wideband digitizer from Teledyne SP Devices is available in PCI Express and PXI Express form factors and features 12-bit resolution. Its high analog input bandwidth of 6.5 GHz combined with a sampling rate of 5 gigasamples/s/channel allows for wideband capture of intermediate-frequency, quadrature, and RF signals. The AC-coupled analog front end is optimized for high linearity. Proprietary ADX digital performance enhancement technology helps the ADQ7WB achieve high spurious-free dynamic range. The optional FW4DDC firmware package adds real-time radio digital-signal-processing functions that can help reduce data rates to a manageable level. In addition to the onboard real-time processing, the ADQ7WB supports data streaming at high rates. Applications include RF monitoring, recording, and production testing; low-level RF; radar; satellite monitoring; and signals intelligence. ***Teledyne SP Devices***, *700 Chestnut Ridge Rd, Chestnut Ridge, NY 10977, https://spdevices.com*

Materials fatigue testing

Waters Corp has brought to market the MSF16 multispecimen fatigue instrument from its subsidiary TA Instruments. The MSF16 delivers insights into the failure limits of materials, components, and products that experience repetitive forces (stresses and strains), such as those in the aircraft, automobile, and medical devices industries. Failure quantification requires 10–100 specimens be tested for millions, even hundreds of millions, of cycles. Equipped with TA's patented, frictionless ElectroForce motor, the MSF16 offers 3000 N force capacity and high accelerations. According to the company, the instrument enables faster test frequencies and thereby reduces testing time. It features 16-sample simultaneous loading, precision specimen-to-specimen adjustments, and convenient features such as an auto-fill bath. ***TA Instruments***, *159 Lukens Dr, New Castle, DE 19720, www.tainstruments.com*

Lens centering system

Trioptics OptiCentric products are used for optical centration testing and manual and automated cementing and bonding of lenses and lens assemblies. According to the company, its OptiCentric 3D 101 with new optimized software is the only system available that allows the combined measurement of lens centering, air gap, and center thickness. Instead of using nominal values for the multilens calculation of internal centering errors, the OptiCentric 3D 101, with a patented procedure, uses the real distances for center thickness and air gaps. The company claims the method improves the accuracy of multilens measurements and the alignment of achromatic lenses. The system also offers increased accuracy for multivalve measurements. An ultrastable, vibration-free design enables high measurement speed and improved alignment processes. ***Trioptics USA****, 9087 Arrow Rte, Unit 180, Rancho Cucamonga, CA 91730, https://trioptics.com*

Image- and surface-analysis software

Digital Surf has released its Mountains 8 software platform for surface metrology and image analysis. Mountains 8, which builds on the previous Mountains 7 platform, combines Mountains' profilometer and scanning electron microscope data analysis with SPIP (scanning probe image processor) software from Image Metrology. Mountains 8 provides faster calculation speeds, new types of surface data, greater interactivity, and more than a hundred new features. Three families of instrument-specific products are offered: MountainsMap for profilometers, including 2D and 3D contact and noncontact profilers; MountainsSEM for scanning electron microscopes; and MountainsSPIP for scanning probe microscopes, such as atomic force and scanning tunneling microscopes. Research laboratories using multiple types of instruments can benefit from new MountainsLab software, a superset product designed to ensure multiple-source data confluence. ***Digital Surf****, 16 rue Lavoisier, 25000 Besançon, France, www.digitalsurf.com* PT

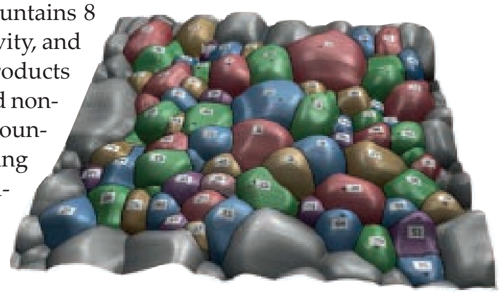

Lower jitter, more channels, faster edges

DG645 Delay Generator ... only from SRS

- Up to 8 output channels
- Delay & pulse-width control
- <25 ps jitter
- 1 ns rise/fall time
- Trigger rates to 10 MHz
- Precision rate generator
- Externally triggered burst mode
- GPIB, RS-232 & Ethernet interfaces

The DG645 generates four independent pulsed outputs — each with its own delay, pulse width, amplitude, and BNC output channel. There is less than 25 ps of jitter between a trigger any of the outputs, and less than 15 ps of channel-to-channel jitter. A built-in trigger rate generator is provided with less than100 ps of clock jitter.

A 10 MHz reference input/output lets you synchronize with mode locked lasers and other sources, and an optional rubidium clock or crystal timebase offers improved accuracy and jitter.

The DG645 can also be ordered with eight output channels in several optional configurations.

DG645 ... $4495 (U.S. list)

SRS Stanford Research Systems

www.thinksrs.com/products/dg645.html
Tel: (408)744-9040

John Warren Wilkins

John Warren Wilkins, Ohio Eminent Scholar and professor of physics emeritus at the Ohio State University (OSU), died on 6 December 2019 in Columbus, Ohio.

Born on 11 March 1936 in Des Moines, Iowa, John obtained a BS in engineering at Northwestern University in 1959. Four years later, under J. Robert Schrieffer, he earned his PhD in physics from the University of Illinois at Urbana-Champaign.

After an NSF postdoc at Cambridge University, John was appointed as an assistant professor of physics at Cornell University in 1964. He left as a full professor in 1988 to join OSU as an Ohio Eminent Scholar and a physics professor. Over his 53-year career in many areas of condensed-matter theory and interdisciplinary research, John mentored 45 PhD students and 59 postdocs, hosted 12 faculty visitors, and published hundreds of papers.

The three of us met John and each other 50 years ago, when John was a young faculty member at Cornell and we were students in theory and experiment. John's excitement about physics was contagious. His interests and expertise spanned both the theoretical and experimental frontiers. His infectious laugh, insatiable scientific curiosity, and willingness to provide advice and guidance to everyone who sought him out had an enormous, positive, lifelong influence on us—scientifically, professionally, and personally.

When recently asked what his most significant accomplishment in physics was, John responded, "My students and postdocs"—men and women of many backgrounds and ethnicities.

John's broad range of research included electron–electron interactions in metals and quantum dots, hybrid density functional theory for III–V semiconductor alloys, magnetic and electronic properties of rare earths, dilute magnetic alloys, x-ray absorption, and heavy-fermion materials.

At Cornell, soon after Kenneth Wilson developed his theory of the renormalization group for critical phenomena, John, Wilson, and their graduate student H. R. Krishnamurthy applied it to solve the Anderson impurity problem. Bubbling with ideas and questions, John was an inspiring presence to students and postdocs in his frequent visits to the low-temperature experimental labs of David Lee, John Reppy, and Robert Richardson. He facilitated exchange visits with European low-temperature physicists that resulted in collaborations and lasting relationships. His behind-the-scenes efforts led directly to the foundation of CHESS, the Cornell High Energy Synchrotron Source. John was the strong link that brought together many theorists and experimentalists at Cornell.

As an Ohio Eminent Scholar, John worked with OSU leadership to enhance investment in research and spur the growth of the Ohio Supercomputer Center and the OSU library. He paved the way for the NSF-supported Center for Emergent Materials. John was instrumental in the expansion of the physics department and in hiring efforts that included attracting Wilson to OSU.

John chaired the American Physical Society's division of condensed-matter physics and received a lifetime award as an APS Outstanding Referee. He served as an editor on several journals. He was an adviser to the US Department of Energy, national and company laboratories, and US and European universities. John's broad and deep knowledge, tireless service, discerning eye, unabashedly forthright questions, and thoughtful constructive criticism made him an indispensable member of numerous national and international advisory and review committees.

John had a lasting effect on condensed-matter physics in the Nordic countries, starting in 1968 when Stig Lundqvist at Chalmers University of Technology invited him to visit Gothenburg, Sweden. Subsequently, John made a long-term commitment to the Nordic Institute for Theoretical Physics to help establish a solid-state program. He made many extended visits to Chalmers and to the Niels Bohr and Hans Christian Oersted Institutes in Copenhagen, and he helped arrange numerous exchanges for professors, postdocs, and students from Denmark, Sweden, and Finland. His direct and hands-on approach to theoretical physics, his boundless energy, his sense of humor, and his willingness to enter into any argument were sources of constant inspiration.

BENGT LUNDQVIST/CHALMERS UNIVERSITY

John Warren Wilkins

John often took students on his sabbaticals to Denmark and Sweden and to the Kavli Institute for Theoretical Physics at the University of California, Santa Barbara. On a sabbatical to Denmark and Sweden in 1972–73, John helped organize Nobel Symposium 24, which was attended by nine previous and future Nobel Prize recipients. After serving as drivers and slide projectionists, we students got to hear the talks and go to the banquet. It was a unique and unforgettable experience.

John left substantial bequests to enhance physics in the future. Cornell will have two endowed John W. Wilkins postdoctoral fellowships in condensed-matter physics—one theoretical and one experimental. OSU will have an endowed professorship.

Our remarks represent the sentiments of hundreds of students, colleagues, and friends, and we thank Jan Herbst, Henrik Smith, Jeevak Parpia, Bengt Lundqvist, Avik Ghosh, Bill Halperin, and Terry Miller for their contributions.

Carl Kukkonen
VIASPACE
Santa Cruz, California
Caltech/NASA Jet Propulsion Laboratory
Pasadena, California
Robert Buhrman
Cornell University
Ithaca, New York
Tin-Lun (Jason) Ho
Ohio State University
Columbus PT

INDEX TO ADVERTISERS

ADVERTISING SALES MANAGEMENT

American Institute of Physics
One Physics Ellipse
College Park, MD 20740
+1 301.209.3393
www.physicstoday.org/advertising

Sales and Marketing Manager
Christina Unger Ramos • cunger@aip.org

Recruitment Advertising
ptjobs@aip.org

Ad Traffic Coordinator
Unique Carter • ucarter@aip.org

ADVERTISING SALES CONSULTANTS

USA and CANADA

AL, AK, AZ, AR, CO, HI, ID, IL, IN, IA, KS, KY, LA, MI, MN, MS, MO, MT, NE, NV, NM, ND, OH, OK, SD, TN, UT, WV, WI, WY
CEL Associates II
Merrie Lynch
+1 617.594.4943
merrie.lynch@celassociates2.com

CA, CT, DE, FL, GA, ME, MD, MA, NH, NJ, NY, NC, OR, PA, RI, SC, VT, VA, WA, and Canada
CEL Associates II
Jody Estabrook
p: +1 774.283.4528
m: +1 978.835.2013
jodyestabrook@comcast.net

INTERNATIONAL

Northern and Western Europe
John Gold
+44 208.641.7717
johnfgold@gmail.com

Central and Eastern Europe
Leo Ploner
+49 172.8231.062
leo@ploner.de

Asia/Pacific
Jake Wilson
+61(0)413 949 644
jwilson@imraust.com.au

PHYSICS TODAY

www.physicstoday.org/advertising

QUICK STUDY

Larry Townsend is the Chancellor's Professor Emeritus at the University of Tennessee, in Knoxville.

Space weather on the Moon

Lawrence W. Townsend

Apollo missions placed astronauts outside Earth's protective magnetosphere for days at a time. Future missions risk exposing them to solar and cosmic radiation for months.

No one has been to the Moon since 1972. Nearly half a century later, NASA is planning a return visit—the Artemis mission (see PHYSICS TODAY, July 2019, page 8)—to establish sustainable exploration. The effort would be a radical departure from our previous experience. During nine earlier missions, only six of them landing on the lunar surface, Apollo astronauts spent a cumulative time of less than three months in space over a four-year period. Altogether, the astronauts spent just 80 hours outside the lunar module.

Radiation dosimeters measured the crews' total skin exposure on those six missions to be between 160 and 1400 mGy, below levels that would trigger health concerns. Currently established skin-absorbed dose limits are 1500 mGy within a 30-day period. During future missions, astronauts are likely to spend far more time outside. (One gray, the energy absorbed from ionizing radiation per unit mass, is defined as 1 J/kg.)

An unfiltered sky

The surface of the Moon is itself a dangerous environment. Aside from its lack of a large magnetic field to deflect charged particles, the airless surface is covered with a finely granulated layer of dust, made up mainly of silicon dioxide crystals. The crystals, which have the consistency of flour, are abrasive, easily disturbed, and hazardous to both humans and equipment. In the weak gravitational field, kicked or otherwise disturbed dust particles are lofted above the surface for longer times than on Earth, and their angular surfaces adhere to lunar rovers, habitats, and space suits. Although the toxicity of lunar dust is unclear, Apollo astronauts commonly complained about eye, nose, and lung irritation.

Crews on the Moon also need protection from its extreme variations in temperature; a lunar day reaches as high as 127 °C (260 °F), and a lunar night dips as low as −173 °C (−280 °F). Space suits can insulate against those temperature swings. Astronauts and electronics are far more likely to be affected by exposure to space weather—the natural radiation environment in deep space.

Space weather includes the solar wind, solar flares, coronal mass ejections (CMEs)—the release of billions of tons of plasma from the Sun's corona, as figure 1 illustrates—galactic cosmic rays (GCRs), and micrometeoroid bombardments. Solar flares and the shock waves from CMEs can yield protons, electrons, and energetic ions—collectively known as solar energetic particles (SEPs). Earth's magnetic field and atmosphere shield us on the ground from most of that radiation, and our exposure—a combination of dose rate and duration—mainly comes from small particle fluxes of muons and neutrons. Above the atmosphere, charged particles can leak through Earth's magnetic field and damage the control systems and solar cells of satellites traversing the planet's van Allen belts (see the article by Daniel Baker and Mikhail Panasyuk, PHYSICS TODAY, December 2017, page 46).

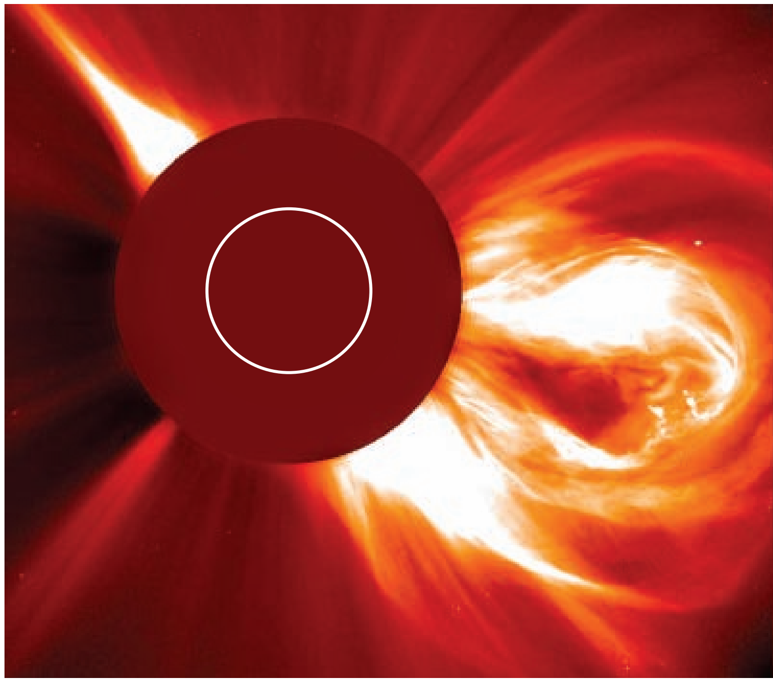

FIGURE 1. THIS IMAGE OF A CORONAL MASS EJECTION and solar flare was taken on 2 December 2003 by the *Solar and Heliospheric Observatory* (*SOHO*).The occulting disk blocks the brightness of the Sun (outlined in white) and its corona. (Courtesy of *SOHO*.)

The bursts of electromagnetic energy emitted in solar flares pose virtually no hazard to crews of missions beyond Earth; x rays are blocked by space suits and the intensities of gammas are too low to worry anyone. But SEPs are a different story. Protons, which make up about 95% of the SEP spectrum, are of most concern because they are charged and can ionize cellular components, damage DNA strands, and at high exposure levels kill cells and cause irreparable organ damage.

Solar-particle releases are random events, and the longer the time spent outside Earth's magnetosphere, the higher the exposure risk. Most SEP events pose little threat because their proton spectra have low fluence levels (flux integrated over time) and are mainly composed of low-kinetic-energy protons. Even thin spacecraft structures or modest surface habitats—including such natural enclosures as caves and underground lava tubes—can shield against them.

But a single 11-year solar cycle may see several SEP events large enough to threaten crews on the lunar surface. One such event, whose energy spectrum is shown in figure 2, occurred in August 1972 between the flights of *Apollo 16* and *Apollo 17*. It would have exposed a crew on the lunar surface to far higher radiation levels than are allowable. Astronauts protected only by a space suit would have received more than 10 Gy to the skin and 2 Gy to the bone marrow, resulting in severe skin blistering, ulceration, and tissue necrosis, often accompanied by nausea, vomiting, and diarrhea. Doses to the spleen and other blood-forming organs would likely also have damaged bone marrow and begun destroying stem cells.

Even a 2-cm-thick skin of aluminum on a spacecraft would have significantly reduced the organ doses, though not below an astronaut's allowable limit. (NASA's effective dose limit is not a fixed number; rather, it's based on a mission-specific 3% risk of exposure-induced death.) A protective storm shelter with a thickness of about 7.4 cm of Al would provide adequate protection for almost all SEP events. However, recent studies found historical evidence of an SEP event in AD 775 whose proton fluence was far larger than any event from the current era of space travel.

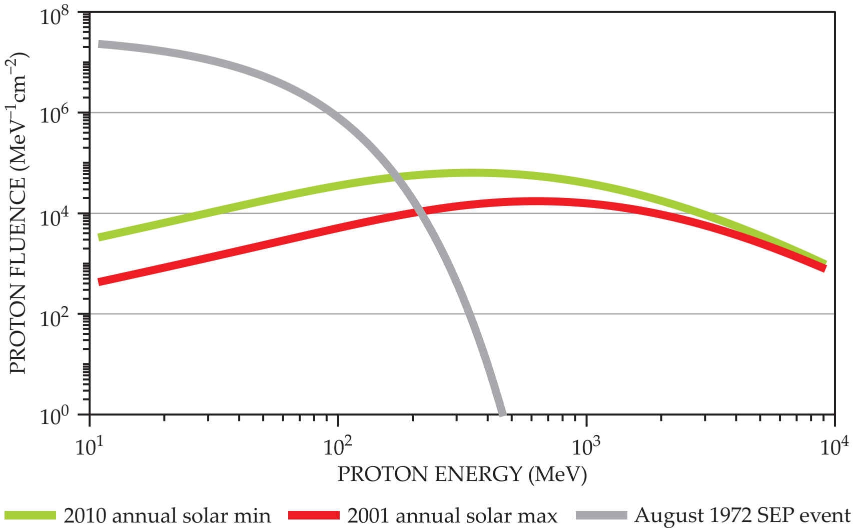

FIGURE 2. ANNUAL PROTON FLUENCES measured during the 2001 solar maximum (red) and the 2010 solar minimum (green) as a function of energy. Also displayed is the three-day proton fluence (gray) of a 1972 solar energetic particle event. The SEP event is four orders of magnitude higher in proton fluence at lower energies than galactic cosmic-ray protons, and the dose it delivered would have far exceeded NASA's allowable limit. At higher energies the GCR spectra clearly dominate. (Image by Lawrence Townsend.)

Galactic cosmic rays

The most dangerous radiation environment is the GCR background, composed of all naturally occurring elements and arising from supernovae explosions. Only elemental nickel and lighter species are abundant enough to deliver worryingly high exposures, but they are unavoidable. The GCR particles have kinetic energies up to tens of GeV/nucleon and beyond—they are much more energetic than typical SEP protons.

Galactic cosmic-ray particle fluxes are anticorrelated with solar activity. During times of high solar activity, the high magnetic fields associated with CMEs deflect the lower-energy GCR particles from the inner solar system, and fewer reach the Moon. The deflection reduces the GCR fluxes at kinetic energies below about 2 GeV/nucleon. Conversely, during solar minimum periods, the solar wind is less disturbed, which allows more lower-energy GCR particles to flood the inner solar system.

Because of their relatively low fluxes, GCR particles pose little risk of acute radiation sickness for crews on the lunar surface. In 2009 NASA's *Lunar Reconnaissance Orbiter* spacecraft was launched into lunar orbit carrying the Cosmic Ray Telescope for the Effects of Radiation (CRaTER) instrument. Shielded by less than 2 cm of aluminum, the dosimeter inside CRaTER indicated that the doses are about 130 mGy per year—almost entirely due to GCR ion exposures. That level is well below the blood-forming-organ limit of 250 mGy within 30 days.

However, GCRs do pose an increased risk of longer-term effects, including cancer mortality and cell damage to the heart, brain, and lenses of the eyes. GCR ions travel at close to the speed of light. Because they are charged, they release copious numbers of electrons and densely ionized tracks as the ions penetrate deep into human tissue. The ions frequently collide with spacecraft and the lunar surface, which generate many secondary ions and neutrons that penetrate further still.

Single ions can kill or damage multiple cells. In 2009 estimates of the effective dose measured by the Mars Science Lab on the *Curiosity* rover during its deep-space trip to Mars averaged about 0.66 Sv over the instrument's one-year travel time. (A measure of equivalent dose, one sievert equals 1 Gy multiplied by a biological factor that accounts for an organ or body part's radiation sensitivity.) Halving that estimate to account for shielding by the Moon's bulk suggests an annual effective dose of GCRs on the lunar surface of 330 mSv. That's about 140 times the average annual exposure on Earth.

Additional resources

▶ J. Guo et al., "MSL–RAD radiation environment measurements," *Radiat. Prot. Dosim.* **166**, 290 (2015).

▶ J. E. Mazur et al., "Update on radiation dose from galactic and solar protons at the Moon using the LRO/CRaTER microdosimeter," *Space Weather* **13**, 363 (2015).

▶ D. V. Reames, *Solar Energetic Particles: A Modern Primer on Understanding Sources, Acceleration and Propagation*, Springer (2017).

▶ I. G. Usoskin et al., "The AD775 cosmic event revisited: The Sun is to blame," *Astron. Astrophys.* **552**, L3 (2013). PT

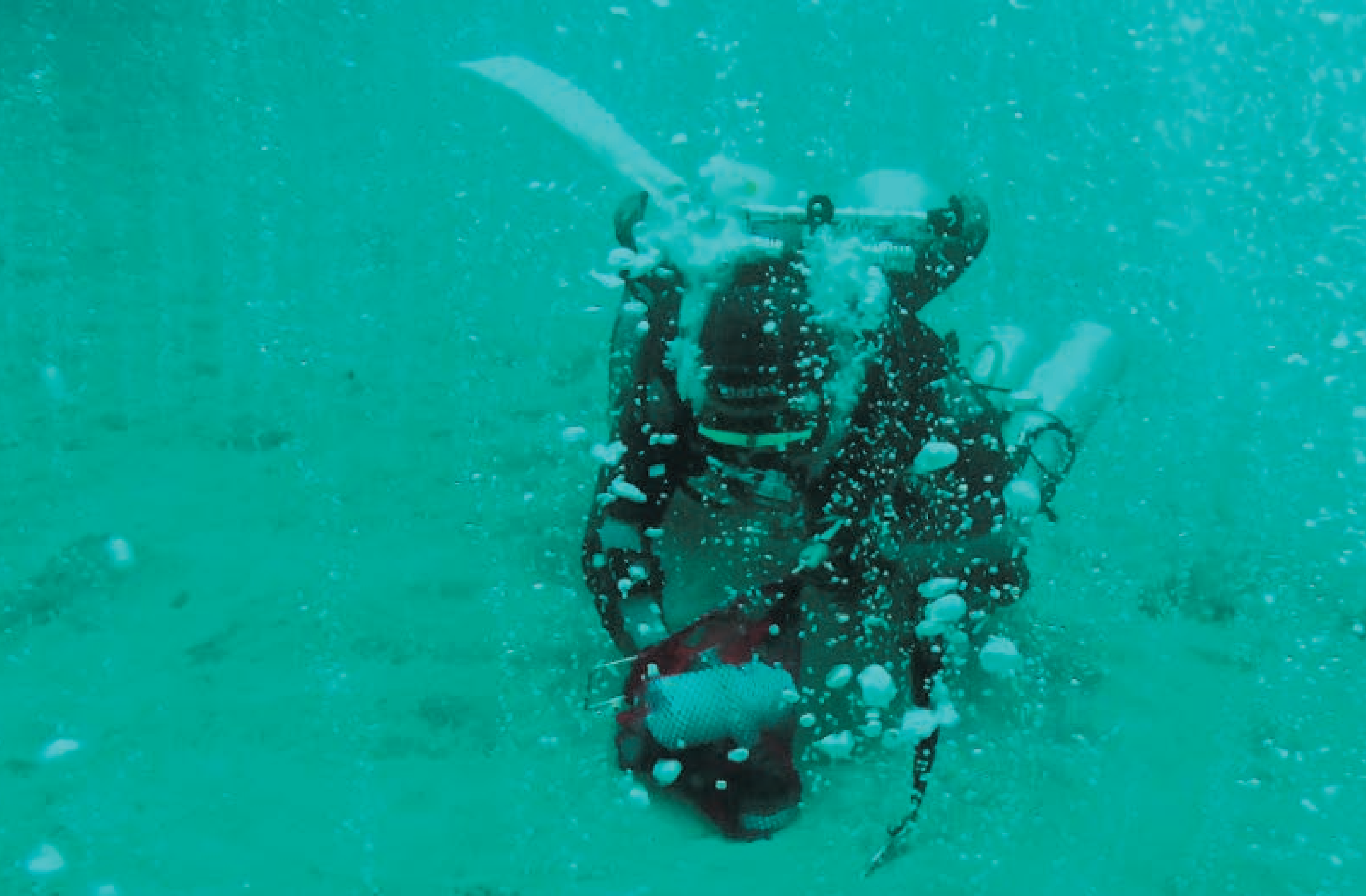

Groundwater-fed vents of bubbling gas

It's no surprise that coral reefs are in danger. As human activity adds more carbon dioxide to the atmosphere, some of it dissolves in the ocean and leaves the water more acidic and less hospitable. Scientists aren't as sure how natural submarine groundwater discharge—the underground flow from land out to sea—is affecting coral reefs and the coastal ecosystems they support. Bayani Cardenas from the University of Texas at Austin and a few colleagues suspected that the coast of the reef-rich Calumpan Peninsula that juts off the Philippine island of Luzon would have submarine groundwater discharge, so they collected seawater samples there for three years. The groundwater-fed hydrothermal springs that they discovered, pictured here, belch out so much CO_2 that the local concentration is as high as 95 000 ppm; the highest previously reported level, found in Italy in 2008, was 60 000 ppm.

The researchers followed the flow of groundwater by analyzing the geochemistry of the samples, including their pH and the amount of radon-222. The latter can be picked up by groundwater moving past igneous and metamorphic rocks where it's the product of the radioactive decay of radium-226. (Its natural occurrence explains why home basements are routinely checked for Rn accumulation.) Cardenas and his colleagues found substantial ^{222}Rn activity in the groundwater measured from wells and in seawater samples that mixed with the groundwater when it discharged into the ocean on the southeastern coast of the peninsula. That's where Cardenas and his colleagues found less robust coral reefs amidst a collection of hydrothermal vents spewing out almost entirely CO_2 from volcanoes in the region. The pH around those vents measured 6.65; in the nearby open ocean, it's 8.11. (M. B. Cardenas et al., *Geophys. Res. Lett.* **47**, e2019GL085730, 2020. Photo by Bayani Cardenas, courtesy of the University of Texas at Austin Jackson School of Geosciences.) —AL

TO SUBMIT CANDIDATE IMAGES FOR BACK SCATTER VISIT https://contact.physicstoday.org.